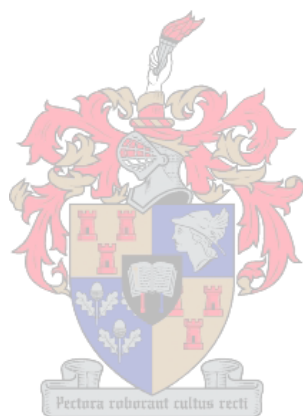


Advanced analytical methods for the analysis of complex polymers prepared by RAFT and RITP

by

Trevor Gavin Wright



*Dissertation presented in partial fulfilment of the requirements for the degree of **Doctor of Philosophy (Polymer Science)***

at the

University of Stellenbosch

Supervisor: Prof. Harald Pasch

Faculty of Science

Department of Chemistry and Polymer Science

Tas&C 2015

DECLARATION

By submitting this thesis electronically, I declare that the entirety of the work contained therein is my own, original work, that I am the sole author thereof (save to the extent explicitly otherwise stated), that reproduction and publication thereof by Stellenbosch University will not infringe any third party rights and that I have not previously in its entirety or in part submitted it for obtaining any qualification.

.....

Trevor Gavin Wright

February 2015

ABSTRACT

Synthetic polymers are complex compounds that have multiple distributions with regard to molar mass, chemical composition, functionality and molecular architecture. Therefore, the molecular complexity of these compounds can only be analysed using a combination of analytical techniques.

Well-defined complex polymers can be prepared by different types of living radical polymerisation, including reversible addition–fragmentation chain transfer polymerisation (RAFT) and reverse iodine transfer polymerisation (RITP). Using these techniques, several different homopolymers and copolymers have been prepared. However, there is still space for some more extended research.

Many different types of multifunctional RAFT agents have been reported in literature. A tetrafunctional RAFT agent was prepared in our laboratory and used for the first time in the polymerisation of styrene. The polymerisation reaction was followed using *in situ* ^1H nuclear magnetic resonance (NMR) and the molar masses of the resultant polymers were determined using size exclusion chromatography (SEC). The molar masses of the star-shaped polystyrenes (PS) were found to be less than the theoretical molar masses. This was due to the fact that SEC was calibrated with linear PS standards, while the samples under investigation are branched. Linear and branched polymers have different hydrodynamic volumes at similar molar masses. In order to prove that the star-shaped polymers were in fact four-armed, the samples were cleaved by aminolysis to yield the linear PS arms. The molar masses of the arms were in agreement with the theoretical arm molar masses based in the four-armed structure.

RITP is a relatively new living radical polymerisation technique. Various monomers have been prepared using RITP, including acrylates, methacrylates and styrene. The polymers formed using this technique have been characterised by techniques such as SEC, NMR and mass spectrometry (MS). However, very little advanced characterisation work has been done on polymers synthesised *via* RITP.

Polystyrene-block-poly(*n*-butyl acrylate) (PS-*b*-PBA) block copolymers were prepared *via* RITP and the microstructure analysed by *in situ* NMR and other advanced analytical techniques. The chromatograms from gradient HPLC of the PS-*b*-PBA block copolymers showed a separation based on chemical composition. The preparation of deuterated polymers *via* RITP has not been reported in literature.

Hydrogenous-polystyrene-block-deuterated-polystyrene (hPS-*b*-dPS) was synthesised *via* RITP and analysed using liquid chromatography at critical conditions. An isotopic separation was achieved when critical conditions were established for hydrogenous PS (h-PS). A separation of the block copolymer from the first block was also achieved under chromatographic conditions where the block copolymer eluted in SEC mode while the first block eluted in LAC mode. The separation according to the block structure was confirmed by two-dimensional liquid chromatography.

OPSOMMING

Sintetiese polimere is komplekse verbindings wat meervoudige verspreidings ten opsigte van molêre massa, chemiese samestelling, funksionaliteit en molekulêre argitektuur. Daarom kan die molekulêre kompleksiteit van hierdie verbindings net ontleed word met behulp van 'n kombinasie van analitiese tegnieke.

Goed-gedefinieerde komplekse polimere kan voorberei word deur verskillende soorte lewende radikaal polimerisasie, insluitend omkeerbare addisie-fragmentasie kettingoordrag polimerisasie (OAFO) en omgekeerde jodium oordrag polimerisasie (OJOP). Met behulp van hierdie tegnieke, was verskeie homopolimere en kopolimeer opgestel. Maar daar is nog plek vir nog uitgebreide navorsing.

Baie verskillende tipes multifunksionele OAFO agente is aangemeld in die letterkunde. Ons het 'n nuwe vier-armige OAFO agent in ons laboratorium voorberei en dit was vir die eerste keer in die polimerisasie van stireen gebruik. Die polimerisasie reaksie is gevolg met behulp van *in situ* ^1H kernmagnetieseresonans (KMR) en die molêre massas van die gevolglike polimere was bepaal deur grootte-uitsluitings chromatografie (SEC). Die molêre massas van die ster-polistireen (PS) is bevind as minder as teoretiese molêre massas. Dit is omdat SEC instrumente gekalibreer word met lineêre PS standaarde, terwyl die monsters wat tans ondersoek word vertakte polimere is. Lineêre en vertakte polimere het verskillende hidrodinamiese volumes by soortgelyke molêre massas. Ten einde te bewys dat die ster polimere in werklikheid vier-armig is, is die monsters gesny deur 'n aminolisasiereaksie om die lineêre PS arms te lewer. Die molêre massas van die arms was ooreenkomstig met die teoretiese arm molêre massas gebaseer op die vier-armige struktuur.

OJOP is 'n relatiewe nuuts lewende radikaal polimerisasie tegniek. Verskeie monomere is opgestel deur OJOP, insluitend akrilate, metakrilate en stireen. Die polimere wat gevorm is deur middel van die tegniek is al gekenmerk deur tegnieke soos SEC, KMR en massaspektrometrie (MS). Tog is daar baie min gevorderde karakterisering werk gedoen oor polimere gesintetiseer deur middel van OJOP. Polistireen-blok-poli(n-butylacrylaat) (PS-*b*-PBA) blokkopolimere was voorberei deur middel van OJOP en die mikrostruktuur ontleed met behulp van gevorderde analitiese tegnieke. Die chromatogramme van gradiënt HPLC van die PS-*b*-PBA blokkopolimere het 'n skeiding ondergaan gebaseer op die chemiese samestelling.

Die voorbereiding van gedeutereerde polimere deur middel van OJOP word nie in die letterkunde gevind nie. Gehidrogeneerde-polistireen-blok-gedeutereerde-polistireen (hPS-*b*-dPS) is gesintetiseer deur middel van OJOP en ontleed met behulp van vloeistofchromatografie onder kritiese kondisies. 'n Isotopiese skeiding was bereik wanneer kritiese kondisies gestig is vir gehidrogeneerde PS (h-PS). 'n Skeiding van die blok kopolimeer van die eerste blok was ook bereik onder chromatografiese omstandighede waar die blok kopolimeer elueer in SEC terwyl die eerste blok elueer in LAC. Die skeiding volgens die blok struktuur was bevestig deur twee-dimensionele vloeistofchromatografie.

ACKNOWLEDGEMENTS

I would like to express my gratitude to the following individuals and institutions for their support and assistance throughout my studies:

Prof. Harald Pasch for his guidance, advice and support

Dr. Nadine Pretorius for all the SEC analyses

Elsa Malherbe for her assistance in NMR analyses

Dr. Khumo Maiko for all her patience and assistance with my HPLC analyses

The members of the Pasch research group (past and present): Douglas, Eddson, Kerissa, Wolfgang, Anthony, Phiri, Sadiq, Carlo, Guillaume, Helen, Khumo, Nyasha, Nadine, Zanelle, Ashwell, Lebohang, Maggie and Pritish

The financial assistance of the National Research Foundation (NRF) and the University of Stellenbosch towards this research

TABLE OF CONTENTS

		Page
DECLARATION		i
ABSTRACT		ii
OPSOMMING		iv
ACKNOWLEDGEMENTS		vi
TABLE OF CONTENTS.....		vii
LIST OF FIGURES.....		xi
LIST OF SCHEMES.....		xv
LIST OF TABLES		xvi
GLOSSARY OF TERMS.....		xvii
LIST OF SYMBOLS.....		xx
1	INTRODUCTION AND OBJECTIVES	1
1.1	Introduction	1
1.2	Objectives	2
1.3	Layout of dissertation	3
References.....		4
2	LITERATURE REVIEW	6
2.1	Conventional radical polymerisation.....	6
2.2	Living radical polymerisation	9
2.2.1	<i>Reversible deactivation/activation mechanism</i>	<i>10</i>
2.2.2	<i>Reversible degenerative chain transfer</i>	<i>11</i>
2.2.3	<i>Radical addition-fragmentation chain-transfer polymerisation</i>	<i>11</i>
2.2.3.1	<i>Introduction</i>	<i>11</i>

2.2.3.2	<i>Mechanism of RAFT polymerisation</i>	12
2.2.3.3	<i>RAFT star polymerisation</i>	13
2.2.4	<i>Iodine transfer polymerisation</i>	15
2.2.4.1	<i>Introduction</i>	15
2.2.4.2	<i>Mechanism of ITP</i>	15
2.2.5	<i>Reverse iodine transfer polymerisation</i>	16
2.2.5.1	<i>Introduction</i>	16
2.2.5.2	<i>Mechanism of RITP</i>	17
2.3	Characterisation of complex polymers	18
2.3.1	<i>High-performance liquid chromatography of polymers</i>	19
2.3.1.1	<i>Size exclusion mode</i>	21
2.3.1.2	<i>Liquid adsorption mode</i>	22
2.3.1.3	<i>Critical conditions mode</i>	23
2.3.2	<i>Two-dimensional liquid chromatography</i>	24
	References	26
3	Z-STAR RAFT POLYMERISATION OF STYRENE	31
3.1	<i>Introduction</i>	31
3.2	<i>Experimental section</i>	32
3.2.1	<i>Chemicals</i>	32
3.2.2	<i>Polymerisation of styrene</i>	32
3.2.3	<i>Aminolysis to cleave star-shaped polymer arms</i>	33
3.3	<i>Characterisation of polymers</i>	33
3.3.1	<i>SEC analysis</i>	33
3.3.2	<i>NMR analysis</i>	33
3.4	<i>Results and discussion</i>	34
3.4.1	<i>Polymerisation of styrene</i>	34
3.4.2	<i>In situ ¹H NMR of the polymerisation of styrene</i>	40

3.4.3	<i>Aminolysis to cleave star-shaped polymer arms</i>	43
3.5	Conclusions	47
	References	48
4	SYNTHESIS OF POLYSTYRENE-B-POLY-(N-BUTYL ACRYLATE) BLOCK COPOLYMERS BY REVERSE IODINE TRANSFER POLYMERISATION	50
4.1	Introduction	50
4.2	Experimental section.....	51
4.2.1	<i>Chemicals</i>	51
4.2.2	<i>Homopolymerisation of styrene and n-butyl acrylate</i>	51
4.2.3	<i>Block copolymerisation of polystyrene-b-poly(n-butyl acrylate)</i>	52
4.3	Characterisation of polymers	53
4.3.1	<i>SEC analysis</i>	53
4.3.2	<i>NMR analysis</i>	53
4.3.3	<i>HPLC analysis</i>	53
4.3.4	<i>Two-dimensional liquid chromatography</i>	53
4.4	Results and discussion	54
4.4.1	<i>Homopolymerisation of styrene</i>	54
4.4.2	<i>Characterisation of polystyrene</i>	55
4.4.3	<i>Homopolymerisation of n-butyl acrylate</i>	59
4.4.4	<i>Characterisation of poly(n-butyl acrylate)</i>	60
4.4.5	<i>Synthesis of polystyrene-b-poly(n-butyl acrylate) block copolymers</i>	63
4.4.6	<i>Characterisation of polystyrene-b-poly(n-butyl acrylate) block copolymers</i>	64
4.4.7	<i>Analysis of PS-b-PBA block copolymers by HPLC</i>	70
4.4.7.1	<i>Separation of PS-b-PBA block copolymers using gradient elution HPLC</i>	70
4.4.7.2	<i>Two-dimensional liquid chromatography of PS-b-PBA</i>	73
4.5	Conclusions	75

References.....	76
5 SYNTHESIS OF DEUTERATED POLYSTYRENE AND BLOCK COPOLYMERS BY RITP	78
5.1 Introduction	78
5.2 Experimental section.....	79
5.2.1 <i>Chemicals</i>	79
5.2.2 <i>Homopolymerisation of styrene and styrene-d₈</i>	79
5.2.3 <i>Block copolymerisation of styrene and styrene-d₈</i>	80
5.3 Characterisation of polymers	81
5.3.1 <i>SEC analysis</i>	81
5.3.2 <i>NMR analysis</i>	81
5.3.3 <i>HPLC analysis</i>	81
5.3.4 <i>Two-dimensional liquid chromatography</i>	82
5.4 Results and discussion	82
5.4.1 <i>Homopolymerisation of styrene</i>	82
5.4.2 <i>Homopolymerisation of styrene-d₈</i>	84
5.4.3 <i>Synthesis of hPS-b-dPS block copolymers</i>	87
5.4.4 <i>Characterisation of hPS-b-dPS block copolymers</i>	87
5.4.5 <i>Analysis of hPS-b-dPS block copolymers by HPLC</i>	89
5.4.5.1 <i>Separation of hPS-b-dPS at critical conditions of h-PS</i>	89
5.4.5.2 <i>Two-dimensional liquid chromatography of hPS-b-dPS</i>	93
5.5 Conclusions	95
References.....	96
6 SUMMARY, CONCLUSIONS AND FUTURE WORK.....	98
6.1 Summary and conclusions.....	98
6.2 Future work.....	100
References.....	102

LIST OF FIGURES

Figure 2.1: Fundamental chemical structure of a RAFT agent.....	12
Figure 2.2: RAFT agent that follows the Z-star RAFT polymerisation mechanism. ..	14
Figure 2.3: RAFT agents that follow the R-star RAFT polymerisation mechanism...	14
Figure 2.4: Schematic representation of the three modes of separation in HPLC. ⁷⁶	21
Figure 2.5: Schematic representation of a typical setup for 2D-LC.	24
Figure 3.1: Chemical structure of the tetrafunctional RAFT agent used in this work.	31
Figure 3.2: Typical ¹ H NMR spectrum in CDCl ₃ of a crude sample of star-shaped PS (run 2a) synthesised at 70 °C for 24 hours.	35
Figure 3.3: Evolution of the molar mass <i>versus</i> conversion for star-shaped PS (run 4a).....	38
Figure 3.4: Molar mass distributions from SEC (RI traces) of the star-shaped PS at various monomer conversions (run 4a).	38
Figure 3.5: Molar mass distributions from SEC (UV traces) of the star-shaped PS taken at (a) = 540 min. and (b) = 1440 min.....	39
Figure 3.6: Method for following arm growth initiation of styrene-d ₈ using ¹ H NMR..	40
Figure 3.7: The ¹ H NMR spectrum of the starting reagents in styrene-d ₈ prior to polymerisation.	41
Figure 3.8: ¹ H NMR spectra in styrene-d ₈ , showing the increasing proton signal intensity at 2.5 ppm corresponding to the incorporation of the tetrafunctional RAFT agent into the polymer.....	42
Figure 3.9: ¹ H NMR spectra in styrene-d ₈ , showing the evolution of the H _α proton signal from the tetrafunctional RAFT agent.	43
Figure 3.10: Molar mass distributions from SEC (UV traces) of the star-shaped PS before (a) and after (b) aminolysis.....	44

Figure 3.11: The ^1H NMR spectra in CDCl_3 of a star-shaped PS sample before (a) and after (b) aminolysis.	45
Figure 4.1: Typical ^1H NMR spectrum in CDCl_3 of a crude sample of PS (run 1a Table 4.1) prepared <i>via</i> RITP for 24 hours at 70 °C.	56
Figure 4.2: Plot of conversion <i>versus</i> time for PS (run 1b Table 4.1) synthesised <i>via</i> RITP at 70 °C for 24 hours.	58
Figure 4.3: Plot of M_n <i>versus</i> conversion for PS (run 2 Table 4.1) synthesised <i>via</i> RITP at 70 °C for 24 hours: (■) = $M_{n, \text{calc}}$ and (●) = $M_{n, \text{SEC}}$	58
Figure 4.4: Molar mass distributions from SEC (RI traces) of PS (run 4 and 5 Table 4.1) synthesised <i>via</i> RITP for 24 hours at 70 °C.	59
Figure 4.5: Typical ^1H NMR spectrum in CDCl_3 of a crude sample of PBA (run 1 Table 4.2) synthesised <i>via</i> RITP for 24 hours at 70 °C.	61
Figure 4.6: Plot of conversion <i>versus</i> time for PBA (run 2b Table 4.2) synthesised <i>via</i> RITP at 70 °C for 24 hours.	62
Figure 4.7: Plot of M_n <i>versus</i> conversion for PBA (run 2a Table 4.2) synthesised <i>via</i> RITP at 70 °C for 24 hours: (■) = $M_{n, \text{calc}}$ and (●) = $M_{n, \text{SEC}}$	62
Figure 4.8: Molar mass distributions from SEC (RI traces) of PBA (run 3 and 4 Table 4.2) synthesised <i>via</i> RITP for 24 hours at 70 °C.	63
Figure 4.9: Typical ^1H NMR spectrum in CDCl_3 of PS- <i>b</i> -PBA (run 2) synthesised <i>via</i> RITP for 24 hours at 70 °C.	65
Figure 4.10: Enlarged portion (4.2–4.9 ppm) of the <i>in situ</i> ^1H NMR spectra of PS- <i>b</i> -PBA (run 1 Table 4.3) synthesised <i>via</i> RITP for 24 hours at 70 °C.	68
Figure 4.11: Plot of $M_{n, \text{calc}}$ <i>versus</i> conversion for the block copolymerisation of PS- <i>b</i> -PBA (run 1 Table 4.3) ($M_{n, \text{SEC}}$ of PS-I = 1600 $\text{g}\cdot\text{mol}^{-1}$, \mathcal{D} = 1.67 and $M_{n, \text{SEC}}$ of PS- <i>b</i> -PBA = 2900 $\text{g}\cdot\text{mol}^{-1}$, \mathcal{D} = 1.46).	68
Figure 4.12: Molar mass distributions from SEC (RI and UV) of PS-I (run 4 Table 4.3) and PS- <i>b</i> -PBA (run 4 Table 4.3) synthesised <i>via</i> RITP for 24 hours at 70 °C.	69

Figure 4.13: Gradient elution profile used to separate PS- <i>b</i> -PBA block copolymer (run 3 Table 4.3); stationary phase: Nucleosil silica 300 Å – 5 µm, mobile phase: heptane/(DCM+1.2%methanol).....	71
Figure 4.14: HPLC chromatogram of PS and PBA homopolymers respectively (Table 4.5); stationary phase: Nucleosil silica 300 Å – 5 µm, mobile phase: heptane/(DCM+1.2%methanol).....	72
Figure 4.15: Gradient HPLC chromatogram of a PS- <i>b</i> -PBA block copolymer (run 3 Table 4.3); stationary phase: Nucleosil silica 300 Å – 5 µm, mobile phase: heptane/(DCM+1.2%methanol).....	72
Figure 4.16: Contour plot (linear scale) of the two-dimensional separation of PS- <i>b</i> -PBA (run 3 Table 4.3) using a heptane/(DCM+1.2% methanol) gradient.....	74
Figure 4.17: Contour plot (logarithmic scale) of the two-dimensional separation of PS- <i>b</i> -PBA (run 3 Table 4.3) using a heptane/(DCM+1.2% methanol) gradient.....	74
Figure 5.1: Molar mass distributions from SEC (RI traces) of h-PS (run 3, 5 and 6 Table 5.1) synthesised <i>via</i> RITP at 70 °C for 24 hours.	83
Figure 5.2: Molar mass distributions from SEC (RI traces) of d-PS (run 2, 3 and 4) synthesised <i>via</i> RITP at 70 °C for 24 hours.	85
Figure 5.3: Evolution of the A–I transfer agent for the polymerisation of h-PS (●) and d-PS (●) at 70 °C for 24 hours.....	86
Figure 5.4: Evolution of the AIBN concentration h-PS (●) and d-PS (●) during polymerisation at 70 °C for 24 hours.	86
Figure 5.5: Molar mass distributions from SEC (RI and UV) of h-PS precursor and hPS- <i>b</i> -dPS block copolymer (run 2 Table 5.3) synthesised <i>via</i> RITP for 24 hours at 70 °C.....	88
Figure 5.6: Critical diagram of molar mass <i>versus</i> retention volume for h-PS synthesised <i>via</i> RITP; stationary phase: Phenomenex C ₁₈ 300 Å – 5 µm; mobile phase: THF/ACN; (■) = 55:45 (SEC), (●) = 50:50 (LCCC) and (▲) = 48:52 (LAC) (v/v).....	90

Figure 5.7: Plot of molar mass <i>versus</i> retention volume for h-PS and d-PS samples prepared <i>via</i> RITP at the critical conditions of h-PS; stationary phase: Phenomenex C ₁₈ 300 Å – 5 µm; mobile phase: THF/ACN 50:50; (■) = d-PS (SEC) and (●) = h-PS (LCCC) (v/v).....	91
Figure 5.8: Superimposed chromatograms of the hPS- <i>b</i> -dPS copolymers (solid lines) and the h-PS precursor at the critical conditions of h-PS; stationary phase: Phenomenex C ₁₈ 300 Å 5 µm; mobile phase: THF/ACN (50:50). Run 1 (red) and run 2 (blue) from Table 5.3.	91
Figure 5.9: Plot of molar mass <i>versus</i> retention volume for h-PS and d-PS samples prepared <i>via</i> RITP at the LAC conditions of h-PS and SEC conditions of d-PS ; stationary phase: Phenomenex C ₁₈ 300 Å – 5 µm; mobile phase: THF/ACN (48:52); (■) = d-PS (SEC) and (●) = h-PS (LCCC).....	92
Figure 5.10: HPLC chromatogram of the hPS- <i>b</i> -dPS block copolymer (run 3 Table 5.3) at 46 °C and THF/ACN (48:52) (v/v); stationary phase: Phenomenex C ₁₈ 300 Å 5 µm.....	93
Figure 5.11: Contour plot of the two-dimensional separation of the hPS- <i>b</i> -dPS block copolymer (run 3) measured at a THF/ACN composition of 48:52 (v/v) and column oven temperature of 46 °C.	94

LIST OF SCHEMES

Scheme 2.1: The three fundamental stages of conventional free radical polymerisation.....	6
Scheme 2.2: The general mechanism of reversible deactivation/activation in LRP..	10
Scheme 2.3: The general mechanism of degenerative chain transfer in LRP.....	11
Scheme 2.4: The fundamental mechanism of RAFT polymerisation.....	13
Scheme 2.5: A basic representation of the mechanism of ITP.....	16
Scheme 2.6: A basic representation of the two stages in the mechanism of RITP...	17
Scheme 2.7: Reversible formation of 1,2-diiodoethyl benzene.	18
Scheme 3.1: Schematic representation of the Z-star RAFT polymerisation mechanism controlled by the tetrafunctional RAFT agent.....	34
Scheme 3.2: Cleavage of the star-shaped polymer arms when treated with an amine.	43
Scheme 4.1: Basic representation of the homopolymerisation of styrene <i>via</i> RITP..	54
Scheme 4.2: Basic representation of the homopolymerisation of n-butyl acrylate <i>via</i> RITP.....	59
Scheme 4.3: Basic representation of the block copolymerisation of PS- <i>b</i> -PBA <i>via</i> RITP.....	64
Scheme 4.4: Degradation of PS-I macro-initiator during block copolymerisation.....	67
Scheme 5.1: Typical anionic polymerisation of d-PS.	78
Scheme 5.2: Basic representation of the homopolymerisation of styrene-d ₈ by RITP.	84
Scheme 5.3: Simplified schematic of the copolymerisation of h-PS with styrene-d ₈ <i>via</i> RITP.....	87

LIST OF TABLES

Table 2.1: The four main types of copolymers.....	7
Table 2.2: Examples of Z-group and R-group species of thiocarbonylthio RAFT agents. ³³	12
Table 3.1: Results of star-shaped PS synthesised for 24 hours at 70 °C.....	37
Table 3.2: Molar mass data for star-shaped PS before and after aminolysis.	46
Table 4.1: Results of styrene polymerisation <i>via</i> RITP for 24 hours at 70 °C.....	57
Table 4.2: Results of n-butyl acrylate polymerised <i>via</i> RITP for 24 hours at 70 °C. .	60
Table 4.3: Results of block copolymerisation of PS- <i>b</i> -PBA <i>via</i> RITP at 70 °C for 24 hours.....	65
Table 4.4: Comparison of the weight percentages of the monomer units incorporated into the block copolymers prepared <i>via</i> RITP.	67
Table 4.5: Polymers synthesised <i>via</i> RITP that were used in the HPLC study.....	70
Table 5.1: Results of styrene homopolymerisation <i>via</i> RITP for 24 hours at 70 °C. .	83
Table 5.2: Results of styrene-d ₈ homopolymerisation <i>via</i> RITP for 24 hours at 70 °C.	85
Table 5.3: Results of hPS- <i>b</i> -dPS polymerisation <i>via</i> RITP for 24 hours at 70 °C.....	88
Table 5.4: Molar masses of the h-PS and d-PS samples used in the HPLC analyses.	89

GLOSSARY OF TERMS

2D-LC	: two-dimensional liquid chromatography
ACN	: acetonitrile
AIBN	: 2,2'-azobis(isobutyronitrile)
ATRP	: atom transfer radical polymerisation
BPO	: benzoyl peroxide
CCD	: chemical composition distribution
CDCl ₃	: deuterated chloroform
C ₆ D ₆	: deuterated benzene
C ₈ D ₈	: deuterated styrene
CRP	: conventional radical polymerisation
CTA	: chain transfer agent
DCM	: dichloromethane
d-PS	: deuterated polystyrene
DT	: degenerative chain transfer
ELSD	: evaporative light scattering detector
ESI-MS	: electrospray ionisation mass spectrometry
FTD	: functionality type distribution
HPLC	: high-performance liquid chromatography
h-PS	: hydrogenated polystyrene
hPS- <i>b</i> -dPS	: hydrogenous polystyrene- <i>block</i> -deuterated polystyrene
IR	: infra-red

ITP	: iodine transfer polymerisation
LAC	: liquid adsorption chromatography
LC	: liquid chromatography
LCCC	: liquid chromatography at critical conditions
LDPE	: low density polyethylene
LRP	: living radical polymerisation
MAD	: molecular architecture distribution
MALDI-ToF	: matrix-assisted laser desorption/ionisation time-of-flight
MMA	: methyl methacrylate
MMD	: molar mass distribution
MS	: mass spectrometry
NMP	: nitroxide-mediated polymerisation
NMR	: nuclear magnetic resonance
PBA	: poly(n-butyl acrylate)
PRE	: persistent radical effect
PS	: polystyrene
PS- <i>b</i> -PBA	: polystyrene- <i>block</i> -poly(n-butyl acrylate)
PS-I	: iodinated polystyrene (macro-initiator)
PVC	: polyvinyl chloride
RAFT	: reversible addition fragmentation chain transfer
RPLC	: reversed phase liquid chromatography
RI	: refractive index

GLOSSARY OF TERMS

RITP	: reverse iodine transfer polymerisation
SDV	: styrene-divinylbenzene
SEC	: size exclusion chromatography
THF	: tetrahydrofuran
UHP	: ultra high purity
UV	: ultraviolet

LIST OF SYMBOLS

δ	: chemical shift
D	: dispersity
ΔG	: change in Gibbs free energy
ΔH	: change in enthalpy
ΔS	: change in entropy
ε	: energy of interaction
ε_c	: critical energy of adsorption
f	: initiator efficiency
F^{iodine}	: iodine functionality
\int	: integral
k_a	: activation rate constant
K_d	: distribution coefficient
k_d	: deactivation rate constant
k_{ex}	: chain transfer rate constant
k_{ij}	: rate constant addition of monomer j to monomer i
K_{LAC}	: distribution coefficient for ideal LAC separation
k_p	: cross-propagation rate constant
K_{SEC}	: distribution coefficient for ideal SEC separation
$[M]$: monomer concentration
M_n	: number average molecular weight
R	: gas constant

LIST OF SYMBOLS

r_i	: reactivity ratio of monomer i
δ	: chemical shift
T	: absolute temperature
V_i	: interstitial volume
V_p	: pore volume
V_R	: retention volume
V_{stat}	: volume of the stationary phase
X	: conversion

1 INTRODUCTION AND OBJECTIVES

1.1 Introduction

Living radical polymerisation (LRP) is an attractive technique for preparing polymers in a controlled manner. LRP techniques include atom transfer radical polymerisation (ATRP),¹ nitroxide-mediated polymerisation (NMP),² reversible addition-fragmentation chain transfer polymerisation (RAFT),³ iodine transfer polymerisation (ITP)⁴ and most recently reverse iodine transfer polymerisation (RITP).⁵⁻⁷ The most effective LRP techniques are reportedly NMP, ATRP and RAFT.⁸

The key moiety in RAFT agents is a thiocarbonylthio group (S=C=S). Attached to the thiocarbonylthio moiety is a Z-group (stabilising group) and an R-group (reinitiating/leaving group). Many different types of multifunctional RAFT agents have been reported in literature.⁹⁻¹² Star RAFT polymerisations can follow one of two pathways. A R-star RAFT agent follows a mechanism where the RAFT agent is attached *via* a reinitiating R-group. Alternatively, a Z-star RAFT agent follows a mechanism where the RAFT agent is attached to the core *via* a stabilising Z-group.¹³

Techniques such as RAFT require preparation of a RAFT agent prior to use in a polymerisation reaction. RITP, on the other hand, is a relatively simple technique that only requires monomer, initiator and molecular iodine. This combination of reagents is attractive, as molecular iodine is quite cheap and readily available. In RITP, CTAs are formed *in situ* by the reaction between initiator radicals and molecular iodine and there is no need to prepare or buy transfer agents. The formation of these CTAs has been studied before and the resultant polymers have been characterised by techniques such as size exclusion chromatography (SEC), nuclear magnetic resonance spectroscopy (NMR) and mass spectrometry (MS). However, synthetic polymers are complex materials that exhibit multiple distributions of their molecular parameters including molar mass distribution (MMD), chemical composition distribution (CCD), functionality type distribution (FTD) and distribution in molecular architecture (MAD).¹⁴

The molecular complexity of synthetic polymers can only be analysed by a combination of analytical techniques such as ultraviolet-visible spectroscopy (UV),¹⁵ infra-red (IR),¹⁶ NMR,^{17,18} MS¹⁹ and liquid chromatography (LC).^{20,21}

High-performance liquid chromatography (HPLC) can be tuned to be selective towards molar mass, chemical composition or functionality. To date, very little HPLC work has been done on polymers synthesised by RITP.²²

Various polymers have been prepared using RITP, including monomers such as acrylates,⁶ methacrylates⁵ and styrene.^{7,23} Deuterated monomers are generally quite expensive, yet deuterated compounds do have some useful applications.

Applications for deuterated compounds are found in pharmacology,²⁴⁻²⁹ tracing biodegradation in water³⁰ and in nuclear fusion experiments.^{31,32} The preparation of deuterated polystyrene (d-PS) using living anionic polymerisation^{33,34} and RAFT³⁵ has been reported in literature. To the best of our knowledge, preparation of deuterated polymers *via* RITP has not been reported in literature.

1.2 Objectives

The objectives of this project were to:

- i synthesise PS using a tetrafunctional RAFT agent
 - confirm that the tetrafunctional RAFT agent forms PS of the desired topology
 - trace the evolution of the tetrafunctional RAFT agent during polymerisation of styrene
 - determine the molar mass of the polymer after aminolysis
- ii synthesise PS, PBA and PS-*b*-PBA block copolymers using RITP
 - evaluate the control of the homopolymerisations of styrene and n-butyl acrylate
 - investigate the livingness of PS through end group analysis
 - characterise the PS-*b*-PBA block copolymers using ¹H NMR, SEC and HPLC
- iii synthesise h-PS, d-PS and hPS-*b*-dPS block copolymers using RITP
 - characterise d-PS using *in situ* ¹H NMR and SEC
 - compare the results of h-PS and d-PS
 - characterise the hPS-*b*-dPS block copolymers using SEC and HPLC

1.3 Layout of dissertation

In Chapter 1, a brief introduction to the project and objectives for the work are given.

An overview of the history and background to this work is presented in Chapter 2. The literature review focuses on controlled radical polymerisation techniques, particularly RAFT and iodine mediated polymerisation. Some background on HPLC is also given.

In Chapter 3, the Z-star RAFT polymerisation of styrene is investigated. *In situ* ^1H NMR was used to trace the evolution of the tetrafunctional RAFT agent during polymerisation. The resultant polymers were characterised using SEC and ^1H NMR.

Chapter 4 describes the synthesis of PS, PBA and PS-*b*-PBA block copolymers *via* RITP. The homopolymers (PS and PBA) were characterised by SEC and ^1H NMR. The block copolymers were investigated using a combination of ^1H NMR, SEC, gradient HPLC and 2D-LC.

Chapter 5 describes the synthesis of h-PS, d-PS and hPS-*b*-dPS block copolymers *via* RITP. H-PS and d-PS were characterised by SEC and *in situ* ^1H NMR was used to compare the kinetics of each system. The block copolymers were analysed using SEC, HPLC at critical conditions and 2D-LC.

Lastly, Chapter 6 is a summary of the results from this work and some recommendations for future work are made.

References

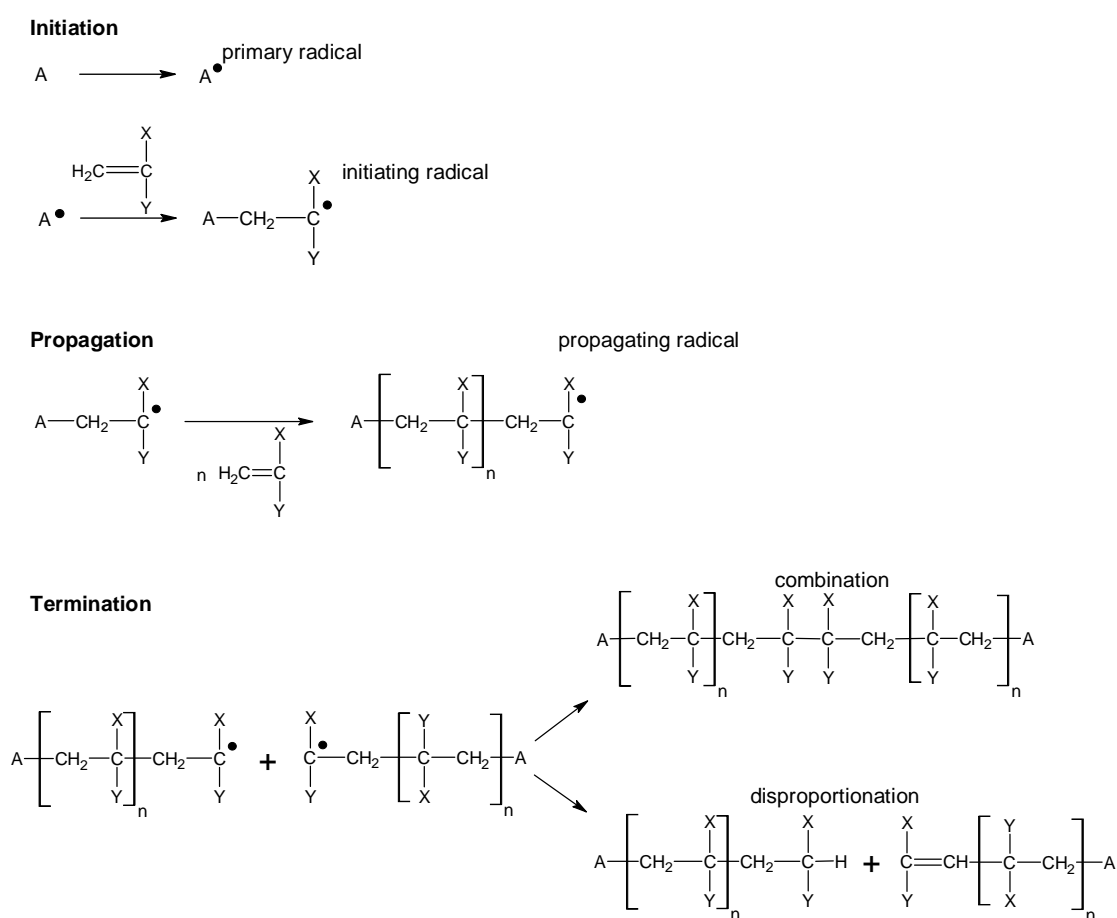
- 1 Matyjaszewski, K.; Xia, J. *Chemical Reviews* 2001, 101, 2921–2990.
- 2 Hawker, C. J.; Bosman, A. W.; Harth, E. *Chemical Reviews* 2001, 101, 3661–3688.
- 3 Moad, G.; Rizzardo, E.; Thang, S. H. *Australian Journal of Chemistry* 2005, 58, 379–410.
- 4 Tatemoto, M. *Kobunshi Ronbunshu* 1992, 49, 765–783.
- 5 Boyer, C.; Lacroix-Desmazes, P.; Robin, J.-J.; Boutevin, B. *Macromolecules* 2006, 39, 4044–4053.
- 6 Lacroix-Desmazes, P.; Severac, R.; Boutevin, B. *Macromolecules* 2005, 38, 6299–6309.
- 7 Tonnar, J.; Severac, R.; Lacroix-Desmazes, P.; Boutevin, B. *Polymer Preprints* 2008, 49, 68–69.
- 8 Matyjaszewski, K.; Davis, T. P. *Handbook of Radical Polymerization*; Wiley-Interscience: Canada 2002, 361–406.
- 9 Boyer, C.; Stenzel, M. H.; Davis, T. P. *Journal of Polymer Science: Part A: Polymer Chemistry* 2010, 49, 551–595.
- 10 Hart-Smith, G.; Chaffey-Millar, H.; Barner-Kowollik, C. *Macromolecules* 2008, 41, 3023–3041.
- 11 Mayadunne, R. T. A.; Jeffery, J.; Moad, G.; Rizzardo, E. *Macromolecules* 2003, 36, 1505–1513.
- 12 Moad, G.; Mayadunne, R. T. A.; Rizzardo, E.; Skidmore, M.; Thang, S. H. *Macromolecular Symposia* 2003, 192, 1–12.
- 13 Johnston-Hall, G.; Monteiro, M. J. *Journal of Polymer Science: Part A: Polymer Chemistry* 2008, 46, 3155–3173.
- 14 Pasch, H. *Advances in Polymer Science* 1999, 150, 1–66.
- 15 Garcia-Rubio, L. H.; Mehta, J. *ACS Symposium Series* 1986, 313, 202–218.
- 16 Koenig, J. L. *Spectroscopy of Polymers*, 2nd Ed.; Elsevier Science, New York 1999.
- 17 Bevington, J. C.; Huckerby, T. N. *European Polymer Journal* 2006, 42, 1433–1436.
- 18 Kitayama, T.; Hatada, K. *NMR Spectroscopy of Polymers*, Springer Laboratory 2004.
- 19 Hanton, S. D. *Chemical Reviews* 2001, 101, 527–570.
- 20 Murgasova, R.; Hercules, D. M. *Analytical and Bioanalytical Chemistry* 2002, 373, 481–489.
- 21 Pasch, H. *Polymer Chemistry* 2013, 4, 2628–2650.
- 22 Greesh, N.; Sanderson, R.; Hartmann, P. *Journal of Applied Polymer Science* 2012, 126, 1773–1783.

-
- 23 Wright, T.; Chirowodza, H.; Pasch, H. *Macromolecules* 2012, 45, 2995–3003.
- 24 Baker, M. T.; Ronnenberg, W. C.; Ruzicka, J. A.; Chiang, C. K.; Tinker, J. H. *Drug Metabolism & Disposition* 1993, 21, 1170–1171.
- 25 Costanzo, L. D.; Moulin, M.; Haertlein, M.; Meilleur, F.; Christianson, D. W. *Archives of Biochemistry and Biophysics* 2007, 465, 82–89.
- 26 Modutlwa, N.; Maegawa, T.; Monguchi, Y.; Sajiki, H. *Journal of Labelled Compounds and Radiopharmaceuticals* 2010, 53, 686–692.
- 27 Nelson, S. D.; Trager, W. F. *Drug Metabolism & Disposition* 2003, 31, 1481–1497.
- 28 Pons, G.; Rey, E. *Pediatrics* 1999, 104, 633–639.
- 29 Sharma, R.; Strelevitz, T. J.; Gao, H.; Clark, A. J.; Schildknecht, K.; Obach, R. S.; Ripp, S. L.; Spracklin, D. K.; Tremaine, L. M.; Vaz, A. D. N. *Drug Metabolism & Disposition* 2012, 40, 625–634.
- 30 Thierrin, J.; Davis, G. B.; Barber, C. *Groundwater* 1995, 33, 469–475.
- 31 Gillich, D. J.; Kovanen, A.; Danon, Y. *Journal of Nuclear Materials* 2010, 405, 181–185.
- 32 Lin, Z.; Yongjian, T.; Chifeng, Z.; Xuan, L.; Houqiong, Z. *Nuclear Instruments and Methods in Physics Research Section A: Accelerators, Spectrometers, Detectors and Associated Equipment* 2002, 480, 242–245.
- 33 Sinha, P.; Harding, G. W.; Maiko, K.; Hiller, W.; Pasch, H. *Journal of Chromatography A* 2012, 1265, 95–104.
- 34 Wang, X.; Xu, Z.; Wan, Y.; Huang, T.; Pispas, S.; Mays, J. W.; Wu, C. *Macromolecules* 1997, 30, 7202–7205.
- 35 Boschmann, D.; Mänz, M.; Pöppler, A.-C.; Sörensen, N.; Vana, P. *Journal of Polymer Science: Part A: Polymer Chemistry* 2008, 46, 7280–7286.

2 LITERATURE REVIEW

2.1 Conventional radical polymerisation

There are three primary stages in conventional radical polymerisation (CRP), namely initiation, propagation and termination (Scheme 2.1). During the initiation stage, the initiator (A) undergoes either thermo- or photolysis to form a primary radical (A[•]). Typical initiators include 2,2'-azobis(isobutyronitrile) (AIBN) and benzoyl peroxide (BPO). These primary radicals then add to the monomer to form propagating radicals.



Scheme 2.1: The three fundamental stages of conventional free radical polymerisation.

Chain growth is terminated by way of bimolecular reactions in two possible ways. The first type of termination occurs when two growing chains combine with one another (combination) and the second type of termination occurs when two different products are formed (disproportionation).

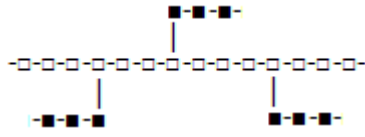
Chain growth can also be terminated by transfer reactions. Chain transfer results in termination of a particular chain with another radical still being present. Concurrently, defect structures are formed when initiating radicals are transferred to the monomer, impurities and solvent.¹

CRP is an appealing polymerisation technique due to its robust nature. CRP can be performed in bulk monomer, in solution and in dispersed media (emulsions). The temperature range of this polymerisation technique is also quite broad, from -100 °C to more than 200 °C. Industrially, CRP is used on a large scale and accounts for approximately 50% of all commercial polymers. Examples of some synthetic polymers produced commercially *via* CRP include low density polyethylene (LDPE), poly(vinyl chloride) (PVC), polystyrene (PS) and polyacrylates.²⁻⁴

The most significant drawbacks of CRP include the inability to prepare well-defined homopolymers or copolymers with respect to chain architecture, end group functionality and molar mass. This poor control is attributed to the propagating chains short lifespan (~1 s), which is too short to accommodate any sort of architectural manipulation.²

Several types of copolymers are possible, with each type differing by the manner in which the monomer units are arranged. There are four main types of copolymers, as described in Table 2.1.

Table 2.1: The four main types of copolymers.

Type of copolymer	Structure	Description
Alternating	-□-■-□-■-□-■-□-■-□-■-□-■-	Alternation of different monomer units
Block	-□-□-□-□-□-□-■-■-■-■-■-■-	two or more homopolymer units
Graft		polymer backbone contains branches of monomer units different to that of the backbone
Random	-□-□-■-□-■-□-■-■-□-■-□-■-	no particular monomer unit arrangement

The description of a binary copolymerisation reaction involving two monomers is described most conveniently using the “terminal model”. In this model, several assumptions are made to describe the copolymerisation as simply as possible.

The first assumption is that the addition of the second monomer can occur in only four ways (Equations 2.1–2.4):



where $P_1 \bullet$ and $P_2 \bullet$ are the propagating species, M_1 and M_2 are the monomers added to the propagating species, and k_{11} , k_{12} , k_{21} and k_{22} are the rate constants of monomer addition.

The second assumption in the model is that the rate of monomer consumption is not affected by the initiation and termination stages of the reaction (Equations 2.5 and 2.6):

$$-\frac{d[M_1]}{dt} = k_{11}[P_1 \bullet][M_1] + k_{21}[P_2 \bullet][M_1] \quad (2.5)$$

$$-\frac{d[M_2]}{dt} = k_{12}[P_1 \bullet][M_2] + k_{22}[P_2 \bullet][M_2] \quad (2.6)$$

Equations 2.5 and 2.6 can be rewritten as a ratio (Equation 2.7):

$$\frac{d[M_1]}{d[M_2]} = \frac{k_{11}[P_1 \bullet][M_1] + k_{21}[P_2 \bullet][M_1]}{k_{12}[P_1 \bullet][M_2] + k_{22}[P_2 \bullet][M_2]} \quad (2.7)$$

Finally, it is assumed that the concentrations of the two propagating species are in a steady state (Equation 2.8):

$$k_{12}[P_1 \bullet][M_2] = k_{21}[P_2 \bullet][M_1] \quad (2.8)$$

Since $P_1 \bullet$ and $P_2 \bullet$ are assumed to be in a steady state, Equation 2.7 can be rewritten to give the Mayo-Lewis equation (Equation 2.9):

$$\frac{d[M_1]}{d[M_2]} = \frac{[M_1]}{[M_2]} \left(\frac{r_1[M_1] + [M_2]}{[M_1] + r_2[M_2]} \right) \quad (2.9)$$

where r_1 and r_2 are the reactivity ratios of the monomers (Equations 2.10 and 2.11).

$$r_1 = \frac{k_{11}}{k_{12}} \quad (2.10)$$

$$r_2 = \frac{k_{22}}{k_{21}} \quad (2.11)$$

The type of copolymerisation reaction that takes place can be drawn from Equation 2.9:

- when $r_1 = r_2 \gg 1$, the reactivity ratios of the two monomers are so exceedingly high that they prefer to react with themselves, thus leading to the formation of two separate homopolymers
- when $r_1 = r_2 > 1$, M_1 homopolymerisation is preferable, but M_2 is capable of cross-linking and therefore block copolymers are formed (the same is true for M_2)
- when $r_1 = r_2 \sim 1$, the monomers react readily with M_1 or M_2 and therefore random copolymers are formed
- when $r_1 = r_2 \sim 0$, the monomers are incapable of a homopolymerisation reaction, thus an alternating copolymer is formed

The ideal case would occur if $r_1 r_2 = 1$, since the two propagating species would demonstrate the same preference for adding one or the other of the two monomers. In reality, however, copolymers tend to fall into a category somewhere between the ideal case and an alternating copolymer.⁵⁻⁷

2.2 Living radical polymerisation

The drawbacks associated with CRP were overcome when living radical polymerisation (LRP) was developed. In this context, the term “living” refers to the ability of a polymer to grow with negligible amounts of chain termination.² Living anionic polymerisation was discovered by Michael Szwarc.⁴ The technique eliminates irreversible chain transfer and irreversible termination reactions from growing chains, thus allowing chains to grow simultaneously.^{8,9} Owing to the fact that the initiation is fast and there is little to no termination, the quantity of dead chains is usually limited to less than 10%.² In this context, the term “dead” describes a polymer chain that can not propagate any further due to its chain ends being terminated.

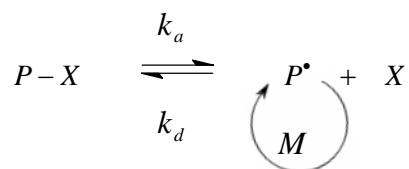
For a polymerisation system to be classified as living, the following list of criteria should be considered, as compiled by Quirk and Lee:¹⁰

- polymerisation advances until complete monomer consumption and may proceed with the addition of more monomer
- molar mass increases linearly with conversion
- concentration of the active species remains constant
- polymerisations yield narrow molar mass distributions
- block copolymers can be prepared by adding a second batch of monomer
- end group functionality is retained

The living nature of LRP polymers allows for the formation of block copolymers with various properties.¹¹⁻¹⁴ Although LRP was initially performed in an academic environment, it was used in industry soon after its inception to produce well-defined block copolymers.¹⁵ The fundamental feature of LRP is the dynamic equilibrium that exists between the propagating radicals and the dormant species.^{16,17} These radicals can either be part of a reversible deactivation/activation mechanism (Scheme 2.2) or a reversible degenerative chain transfer (DT) mechanism (Scheme 2.3).

2.2.1 Reversible deactivation/activation mechanism

A reversible deactivation/activation mechanism (Scheme 2.2) involves a propagating radical (P^{\bullet}) that reacts with a stable free radical (X), resulting in the formation of a dormant chain ($P-X$). This effect is known as the persistent radical effect (PRE). In essence, the initiator undergoes homolysis to generate a stable (persistent) free radical.^{16,18} Examples of CRP techniques that follow reversible deactivation/activation mechanism include nitroxide-mediated polymerisation (NMP) and atom transfer radical polymerisation (ATRP). The stable radicals in NMP are alkoxyamines^{13,19}, while the stable radicals in ATRP are alkyl halides or organometallics.²⁰⁻²⁵

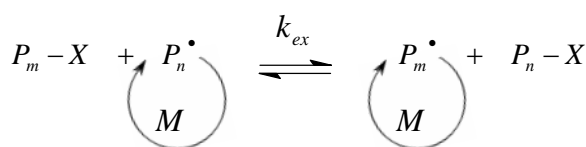


Scheme 2.2: The general mechanism of reversible deactivation/activation in LRP.

2.2.2 Reversible degenerative chain transfer

A DT mechanism (Scheme 2.3) occurs when a chain transfer agent (CTA) (R-X) reacts with a propagating radical (P[•]) to form a dormant chain (P-X). This reaction leaves a chain carrier (R[•]) that can reinitiate polymerisation. There is a constant exchange between the propagating radical and either the CTA or the dormant species. Polymerisation techniques that are governed by a DT mechanism include radical addition-fragmentation chain-transfer polymerisation (RAFT), iodine transfer polymerisation (ITP) and more recently reverse iodine transfer polymerisation (RITP).

In RAFT polymerisation, the CTAs are thiocarbonylthio derived compounds,²⁶ while ITP involves the use of alkyl iodide compounds.^{27,28} In RITP, there are no CTAs at the beginning of the reaction, as the CTAs are generated from the reaction between molecular iodine and initiator radicals.²⁹



Scheme 2.3: The general mechanism of degenerative chain transfer in LRP.

2.2.3 Radical addition-fragmentation chain-transfer polymerisation

2.2.3.1 Introduction

The RAFT polymerisation technique was first discovered by Chiefari *et al.* in 1998 and is a very flexible technique with regards to reaction conditions.³⁰ Indeed, the flexibility of the RAFT process is comparable to the robust nature of FRP. Like FRP, RAFT polymerisation can also be performed in bulk monomer, in solution and in dispersed media. In addition, the fact that RAFT can be performed in a wide range of temperatures and with most monomers makes it an extremely useful technique. RAFT polymerisation is exceptional at providing control over molar mass, molar mass distribution and chain end functionality.^{31,32} Figure 2.1 shows the fundamental chemical structure of RAFT agents, with the key chemical moiety being the thiocarbonylthio group (S=C-S). The Z-group is the stabilising group and the R-group is the reinitiating/leaving group.

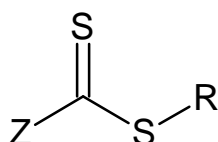


Figure 2.1: Fundamental chemical structure of a RAFT agent.

Based on their Z-group, RAFT agents can be categorised into four classes: (1) dithioesters (Z-group is an aryl or alkyl), (2) dithiocarbamates (Z-group is a substituted nitrogen), (3) dithiocarbonates/xanthates (Z-group is a substituted oxygen), and (4) trithiocarbonates (Z-group is a substituted sulphur). Some examples of the Z-groups and R-groups of thiocarbonylthio RAFT agents are shown in Table 2.2.³³

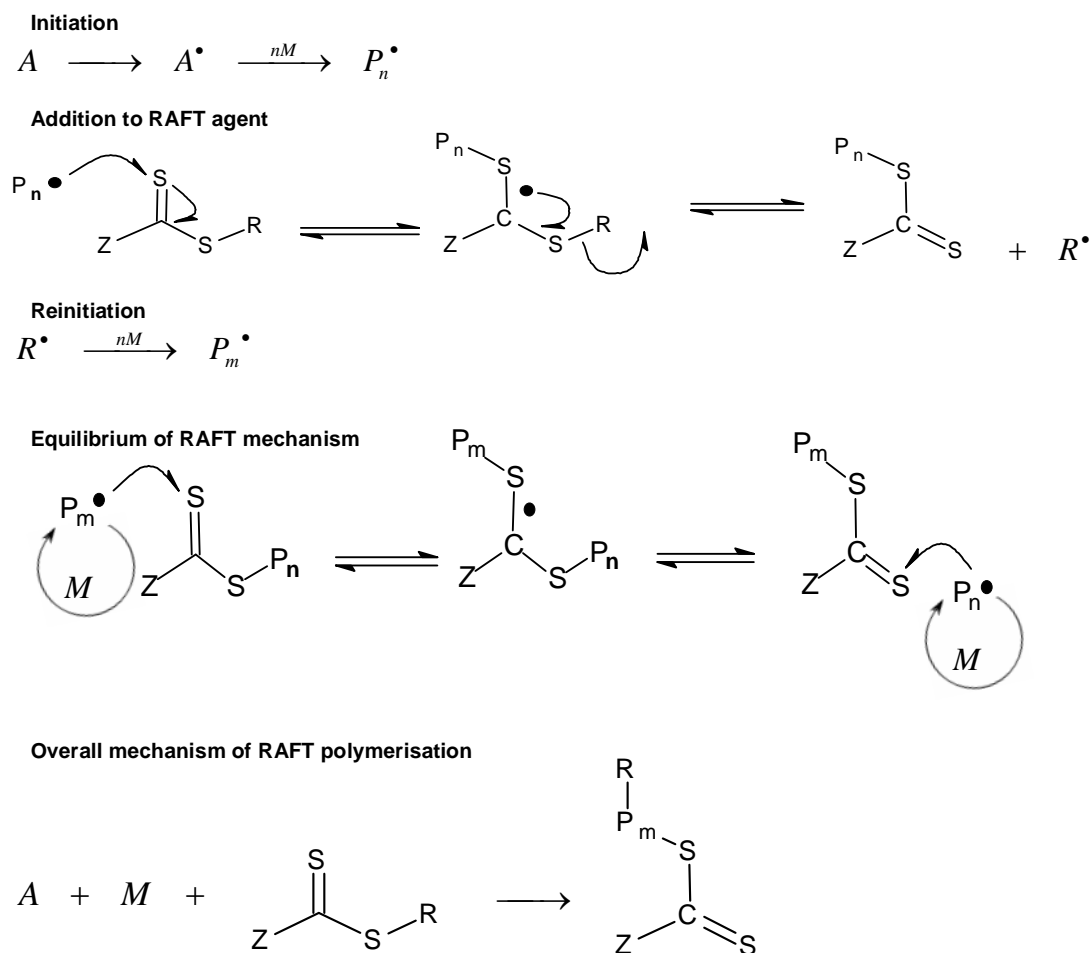
Table 2.2: Examples of Z-group and R-group species of thiocarbonylthio RAFT agents.³³

Class	Z-group	R-group
Dithioester	CH ₃	CH ₂ CN
Dithiocarbamate	NEt ₂	C(CH ₃)(CN)CH ₂ CH ₂ COOH
Dithiocarbonate (a.k.a. xanthate)	OEt	C(CH ₃) ₂ Ph
Trithiocarbonate	SCH ₃	C(CH ₃) ₂ CN

2.2.3.2 Mechanism of RAFT polymerisation

RAFT polymerisation is governed by a DT mechanism where there are three main stages; initiation, propagation and reinitiation. The fundamental mechanism of RAFT polymerisation is shown in Scheme 2.4. The initiation step in RAFT polymerisation is analogous to the initiation step in CRP, where the initiator (A) is decomposed thermally to form a primary initiator-derived radical (A[•]). The primary radical is then added to the monomer (M) to form an initiating radical (P_n[•]). After several monomer additions to the initiating radical, a propagating radical is formed which adds to the thiocarbonylthio compound to form an intermediate radical. The intermediate radical undergoes fragmentation, resulting in the R-group being released (R[•]). At this stage, the R-group reinitiates polymerisation by reacting with the monomer and forming a new propagating radical (P_m[•]). As long as unreacted monomer is present, there is equilibrium between the active propagating radicals (P_n[•] and P_m[•]) and the dormant thiocarbonylthio end-capped polymeric compound.

This equilibrium allows the active species to propagate, and is the basis for the control over molecular mass and narrow dispersity.³³



Scheme 2.4: The fundamental mechanism of RAFT polymerisation.

2.2.3.3 RAFT star polymerisation

A RAFT star is compound that contains several arms containing a thiocarbonylthio moiety. Several examples of different types of multifunctional RAFT agents can be found in literature.^{32,34-36} Star RAFT agents can be designed to follow one of two approaches, namely a Z-star or R-star.³⁷

A RAFT agent designed to follow the Z-star RAFT polymerisation mechanism is shown in Figure 2.2. With such a RAFT agent, the polymer arms grow whilst being detached from the core. Therefore, the core is dormant as a result of this detachment and few radical-radical couplings may produce linear polymers in small quantities.

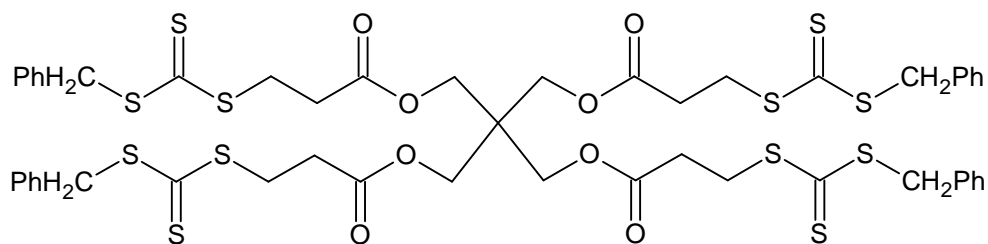


Figure 2.2: RAFT agent that follows the Z-star RAFT polymerisation mechanism.

The presence of linear polymer formed during synthesis of a star polymer can be detected through size exclusion chromatography (SEC). In the SEC chromatogram, the linear polymer yields a peak with about half the molar mass of the star polymer peak.³³ Regardless of the approach taken by the RAFT agent, the star polymers still exhibit good molar mass control with low dispersity.^{26,36,38} RAFT agents designed to follow the R-star RAFT polymerisation mechanism are shown in Figure 2.3.^{36,38}

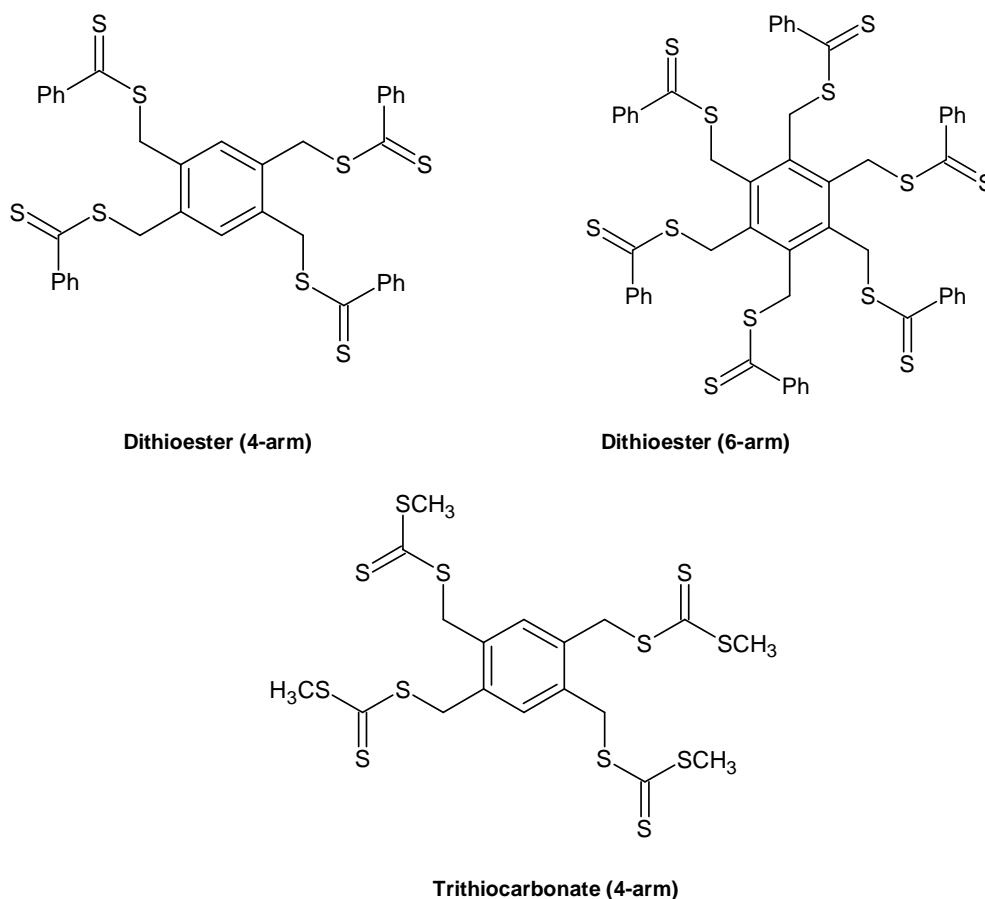


Figure 2.3: RAFT agents that follow the R-star RAFT polymerisation mechanism.

These multifunctional dithioester and trithiocarbonate RAFT agents cause the polymer arms to grow away from the core whilst remaining attached. A drawback associated with these RAFT agents is that the propagating chains are attached to the core. This attachment leads to termination coupling reactions of radicals and the subsequent formation of a few star-star coupled compounds. Evidence of these coupled compounds can also be detected in SEC, where the coupled compounds give rise to peaks with twice the molar mass of the star polymer peak.^{26,36}

2.2.4 Iodine transfer polymerisation

2.2.4.1 Introduction

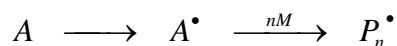
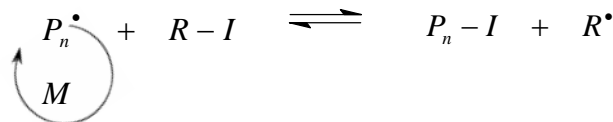
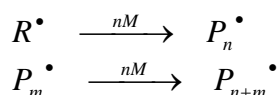
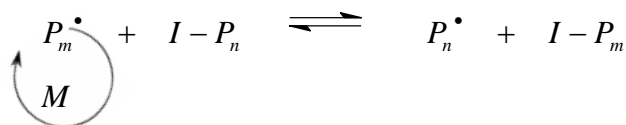
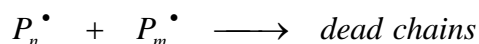
In the late 1970s, Tatemoto *et al.*³⁹ developed a living radical polymerisation technique they called iodine transfer polymerisation (ITP). This polymerisation technique involves the use of iodinated CTAs (R-I) which can either be fluorinated or non-fluorinated.^{27,28} Iodinated CTAs can be prepared in three ways:

- addition of H-X (X Cl, Br or I) to monomers²⁷
- addition of iodine monochloride (ICl) to fluoroalkenes^{40,41}
- nucleophilic substitution^{42,43}

The chemical structure of the CTA is typically such that it imitates the structure of the propagating radical. For an iodinated CTA to be efficient, the C-I bond has to be labile enough to facilitate the transfer of the iodine atom to the propagating radical.²⁷ In addition to this, the structure of the R-group should be able to stabilise the resulting radical, either by inductive or resonance effects.⁴²

2.2.4.2 Mechanism of ITP

The mechanism of ITP is shown in Scheme 2.5. When heated, the initiator (A) is decomposed to form initiator-derived radicals (A[•]). These radicals then attach to monomer (M) to form propagating radicals (P_n[•]). When iodine from the CTA (R-I) is expelled, it attaches to the propagating radicals, resulting in a polymer alkyl iodide (P_n-I) and a new initiating radical (R[•]). At this stage, propagation can occur either by R[•] attaching to monomer or by P_n[•] attaching to monomer. The degenerative transfer reaction takes place because the propagating species (P_n[•] and P_m[•]) are structurally similar.⁴²

Initiation**Chain transfer****Propagation****Degenerative transfer****Termination****Scheme 2.5: A basic representation of the mechanism of ITP.**

ITP can be performed on a wide variety of monomers, including vinyl acetate,⁴² styrene⁴⁴ and acrylates.⁴⁵ ITP can also be used to synthesise block copolymers in a controlled manner. Interestingly, Gaynor *et al.*²⁷ observed that ITP of methyl methacrylate (MMA), when using 1-phenyl-ethyl iodide as a CTA, could not be controlled. The lack of control was evident from the fact that molar mass did not increase with conversion. Another drawback to ITP is that the iodinated transfer agents are susceptible to degradation when exposed to ultraviolet (UV) light or a heat source and the transfer agents often decompose in storage.⁴⁶

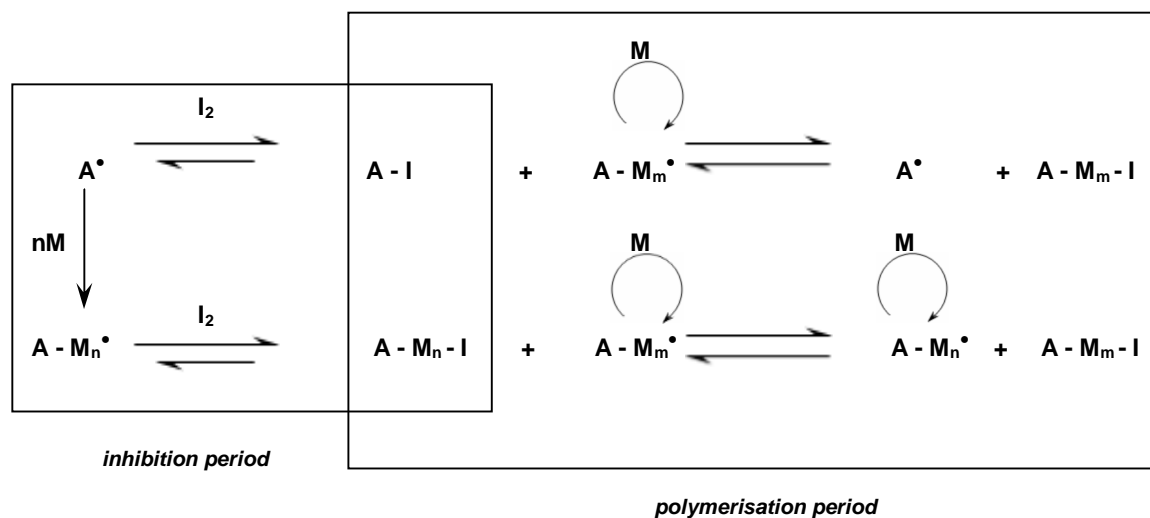
2.2.5 Reverse iodine transfer polymerisation**2.2.5.1 Introduction**

Reverse iodine transfer polymerisation (RITP) was developed by Lacroix-Desmazes *et al.* around the year 2005.²⁹ It was developed mainly in an attempt to overcome some of the drawbacks of ITP, particularly the inability to control the synthesis of poly(methyl methacrylate).

RITP is distinguished from ITP in that CTAs are generated *in situ*, rather than being added to the reaction mixture. The technique is relatively simple and only requires an initiator (usually AIBN), iodine and monomer. Furthermore, RITP can be performed in solution^{29,47}, emulsion⁴⁸⁻⁵¹ or in mini-emulsion.^{52,53}

2.2.5.2 Mechanism of RITP

Mechanistically, RITP is split into two distinct periods. A basic representation of the mechanism of RITP is shown in Scheme 2.6, illustrating that there is an inhibition period and a polymerisation period.

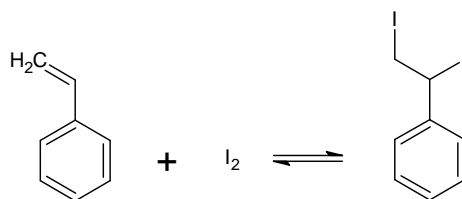


Scheme 2.6: A basic representation of the two stages in the mechanism of RITP.

During the inhibition period, CTAs are generated *in situ*. These CTAs are formed when the reaction mixture is heated and the initiator decomposes to form initiator-derived radicals (A^\bullet). The radicals then react with molecular iodine (I_2) to form alkyl iodide CTAs ($A-I$). The initiator-derived radical can also react with $A-M_n^\bullet$ to form iodine end-capped telomer CTAs ($A-M_n-I$), where A is the initiator fragment, M is a monomer unit, n is the mean number degree of polymerisation and I is an iodine atom.

During the inhibition period it is also possible for iodine to react with the double bond of a monomer species and form a 1,2-disubstituted olefin. As long as the reaction takes place in the absence of UV light, this reaction is reversible.^{54,55}

In the case of styrene, which has a complex chemistry when reacted with iodine, the double bond reacts with iodine to form 1,2-diiodoethyl benzene (Scheme 2.7). This reaction has some significance in styrene polymerisation, as the initiator-derived radicals compete with styrene for free iodine that is required to form iodinated CTAs. Competition for free iodine results in an inhibition period that is shorter than predicted. Fortunately, the reaction between iodine and styrene is reversible and iodine is liberated from 1,2-diiodoethyl benzene throughout the polymerisation period, resulting in controlled molar mass and dispersity of polymers.⁵⁶



Scheme 2.7: Reversible formation of 1,2-diiodoethyl benzene.

The inhibition period concludes when all iodine has been consumed. In a qualitative sense, this is visible by the disappearance of the typical dark violet colour of iodine in solution resulting in the mixture being colourless. Once all the iodine has reacted to form CTAs, a period of polymerisation ensues that is governed by a DT mechanism.^{29,47,57}

2.3 Characterisation of complex polymers

At the end of any polymerisation procedure, there is inevitably a heterogeneous mixture of compounds. In this regard, polymers and copolymers alike are considered complex molecules. Their complexity extends to the fact that they can be described according multiple distributions, including a chemical composition distribution (CCD), molecular architecture distribution (MAD), functionality type distribution (FTD) and molar mass distribution (MMD).⁵⁸

Several spectroscopic and spectrometric techniques exist that can be used to characterise polymers according to their end group functionality as well as determine the types of monomer present. Such techniques include:

- ultraviolet-visible spectroscopy (UV)⁵⁹
- infra-red spectroscopy (IR)^{60,61}

- nuclear magnetic resonance spectroscopy (NMR)⁶¹⁻⁶⁷
- electrospray ionisation mass spectrometry (ESI-MS)⁶⁸
- matrix-assisted laser desorption/ionisation time-of-flight mass spectrometry (MALDI-ToF)^{68,69}

The limitations of these spectroscopic techniques are that they can not be used to determine the end group functionality of high molar mass polymers, due to the low concentration of end groups. Also, the abovementioned techniques do not provide any information on molar mass distribution.

SEC is the most commonly used chromatographic technique for separation of molecules according to molecular size. A limitation of SEC is that it cannot distinguish a mixture of polymers with different end group functionalities, as the chromatogram corresponds to the sum of the distributions of the different molecules.⁵⁸ Therefore, when using SEC, either the molar mass or the chemical composition should be known.

Alternatively, complex polymers can be fractionated into homogeneous components and then analysed for molar mass using a technique known as high-performance liquid chromatography (HPLC). Using HPLC, it is possible to combine a separation technique with a spectroscopic technique or to hyphenate two separation techniques. The combination of a separation technique with a spectroscopic technique allows for a qualitative and quantitative analysis of the chemical composition. Hyphenation of two separation techniques is particularly beneficial as it provides information on chemical composition as well as molar mass distribution. Therefore, in order to obtain a complete understanding of complex molecules, it is necessary to use at least two characterisation techniques.^{58,70-74}

2.3.1 High-performance liquid chromatography of polymers

HPLC is an analytical technique used to separate compounds so that they may be quantified individually. When an analyte is run through a liquid chromatographic system, it is distributed between the mobile and the stationary phase.

The retention volume (V_R) of the analyte is expressed by Equation 2.12

$$V_R = V_i + V_p K_d \quad (2.12)$$

where V_i is the interstitial volume of the column, V_p is the pore volume of stationary phase and K_d is the distribution coefficient.

K_d is defined as the ratio of the concentration of the analyte in the mobile and stationary phase. The distribution coefficient relates to ΔG by Equation 2.13

$$\Delta G = \Delta H - T\Delta S = -RT \ln K_d \quad (2.13)$$

where ΔH is the change in enthalpy, ΔS is the change in entropy and T is the absolute temperature of the system.

Therefore, an alternative expression for K_d is given by Equation 2.14.

$$K_d = \exp\left(\frac{\Delta S}{R} - \frac{\Delta H}{RT}\right) \quad (2.14)$$

The influence of these parameters on ΔG is listed below:

- ΔH is due to an analyte interacting with the surface of the stationary phase
- ΔS is attributed to the inability of an analyte to engage in all possible conformations due to confinement in the pores of the stationary phase

In general, the distribution coefficient is given by Equation 2.15

$$K_d = K_{SEC} K_{LAC} \quad (2.15)$$

where K_{SEC} is related to entropic effects, while K_{LAC} relates to enthalpic effects. The mode of separation is therefore determined by the extent of the entropic and enthalpic effects.

When performing HPLC, there are three modes in which analytes can be separated. The three modes of separation are size exclusion chromatography (SEC), liquid chromatography at critical conditions (LCCC) and liquid adsorption chromatography (LAC). A schematic representation of the three modes of separation is shown in Figure 2.4.⁷⁵⁻⁷⁷

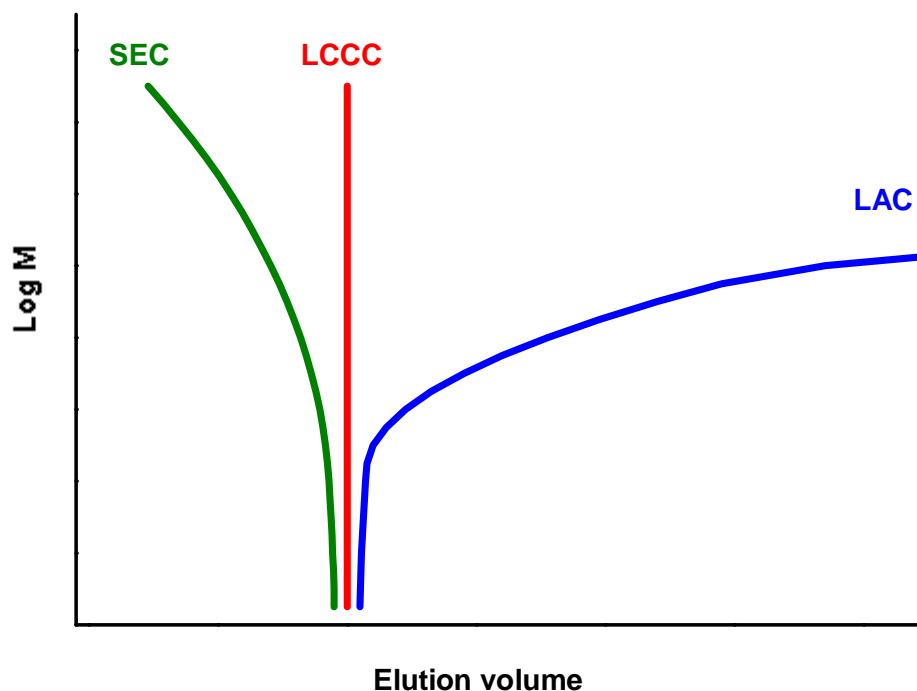


Figure 2.4: Schematic representation of the three modes of separation in HPLC.⁷⁶

2.3.1.1 Size exclusion mode

In size exclusion chromatography, analytes are separated with respect to their hydrodynamic volume. The amount of analyte that interacts with the stationary phase is dependant on the size of the molecule relative to the pore size of the stationary phase. In ideal SEC, the separation is governed by changes in conformation (ΔS) due to penetration of the macromolecules into the pores of the stationary phase and therefore there is no change in enthalpy ($\Delta H = 0$). The expression for the distribution coefficient for ideal SEC (K_{SEC}) is given by Equation 2.16

$$K_{SEC} = \exp\left(\frac{\Delta S}{R}\right) \quad (2.16)$$

The range of values for K_{SEC} lies between 0 and 1, as explained below:

- if $K_{SEC} = 0$, the analytes are too large to enter the pores of the stationary phase
- if $K_{SEC} = 1$, the analytes are able to access all of the pore volume without any change in conformation (separation threshold)

The retention volume for ideal SEC is given by Equation 2.17

$$V_R = V_i + V_p K_{SEC} \quad (2.17)$$

In real SEC, however, there are adsorptive interactions between the analytes and the stationary phase, and therefore the enthalpic interactions must be considered. This means that the retention volume is influenced by K_{SEC} and K_{LAC} .

To summarise, the smaller a molecule, the longer it is retained in the stationary phase due to their ability to penetrate the pores of the stationary phase. Smaller molecules are thus retained by the stationary phase and are eluted later than larger molecules.⁶⁹

2.3.1.2 Liquid adsorption mode

In liquid adsorption chromatography, the separation is governed by the adsorption of analytes to the stationary phase. In ideal LAC, there is no change in conformation of analytes ($\Delta S = 0$) and therefore, the process is governed by changes in enthalpy (ΔH). The distribution coefficient for ideal LAC is shown in Equation 2.18.

$$K_{LAC} = \exp\left(-\frac{\Delta H}{RT}\right) \quad (2.18)$$

The retention volume of the analyte is dependant on the pore size of the stationary phase and therefore two scenarios are possible. If the pores are too small for an analyte to penetrate ($K_{SEC} = 0$), separation occurs on the outer surface of the stationary phase. In this case, the retention volume is a function of the interstitial volume and the volume of the stationary phase (V_{stat}), as shown in Equation 2.19.

$$V_R = V_i + V_{stat} K_{LAC} \quad (2.19)$$

If the pores are sufficiently large for an analyte to penetrate ($K_{SEC} = 1$), the pore volume becomes relevant to the retention volume, as shown in Equation 2.20.

$$V_R = V_i + V_p + V_{stat} K_{LAC} \quad (2.20)$$

In real LAC, however, a small amount of pores are accessible to analytes and hence changes in conformation may occur.

The retention volume in real LAC is therefore a function of enthalpic interactions at the surface of the stationary phase, enthalpic interactions in the pores of the stationary phase and entropic interactions due to pore size (Equation 2.21).

$$V_R = V_i + V_p (K_{SEC} K_{LAC}) + V_{stat} K_{LAC} \quad (2.21)$$

Due to the enthalpic interaction of analytes with the stationary phase, the retention volume increases as the molar mass of the analyte molecule increases.

2.3.1.3 Critical conditions mode

In the case where entropic interactions are greater than enthalpic interactions ($T\Delta S > \Delta H$), a separation in size exclusion mode is observed. Conversely, when the enthalpic interactions are greater than the entropic interactions ($\Delta H > T\Delta S$), a separation in liquid adsorption mode is observed. Both separation modes are affected by molecule size as well as pore size of the stationary phase and therefore there is the need to define an energy of interaction (ε). This energy of interaction is a function of the stationary phase, the chemical composition of the monomer unit of the polymer, the mobile phase composition and the temperature.

According to the theory of adsorption at porous adsorbents, there is a critical energy of adsorption (ε_c) that corresponds to the energy where an analyte adsorbs to a stationary phase. Consequently, if $\varepsilon > \varepsilon_c$, the analyte is adsorbed, while if $\varepsilon < \varepsilon_c$, the analyte remains unadsorbed. When $\varepsilon = \varepsilon_c$, there is a transition from SEC to LAC.

This point of transition is known as the critical point of adsorption. A chromatographic separation at this critical point is known as liquid chromatography at critical conditions (LCCC). At the critical point of adsorption, there is a balance between adsorption and entropy losses ($T\Delta S = \Delta H$). As a result, the Gibbs free energy is constant ($\Delta G = 0$) and $K_d = 1$, regardless of the molar mass of the polymer or the pore size of the stationary phase.⁷⁸⁻⁸⁰

The critical point of adsorption is extremely sensitive towards any changes in mobile phase composition or temperature, as there is quite a narrow range between size exclusion and adsorption modes. Despite the sensitivity of this separation mode, liquid chromatography at critical conditions remains a widely used chromatographic technique to characterise complex polymers.⁸¹⁻⁸³

2.3.2 Two-dimensional liquid chromatography

As mentioned earlier, complex polymers are heterogeneous compounds with distributions according to chemical composition, functionality and molar mass. In order to obtain a more comprehensive understanding of these polymers, it can be useful to analyse them using two-dimensional liquid chromatography (2D-LC). A schematic of a typical 2D-LC setup is shown in Figure 2.5.

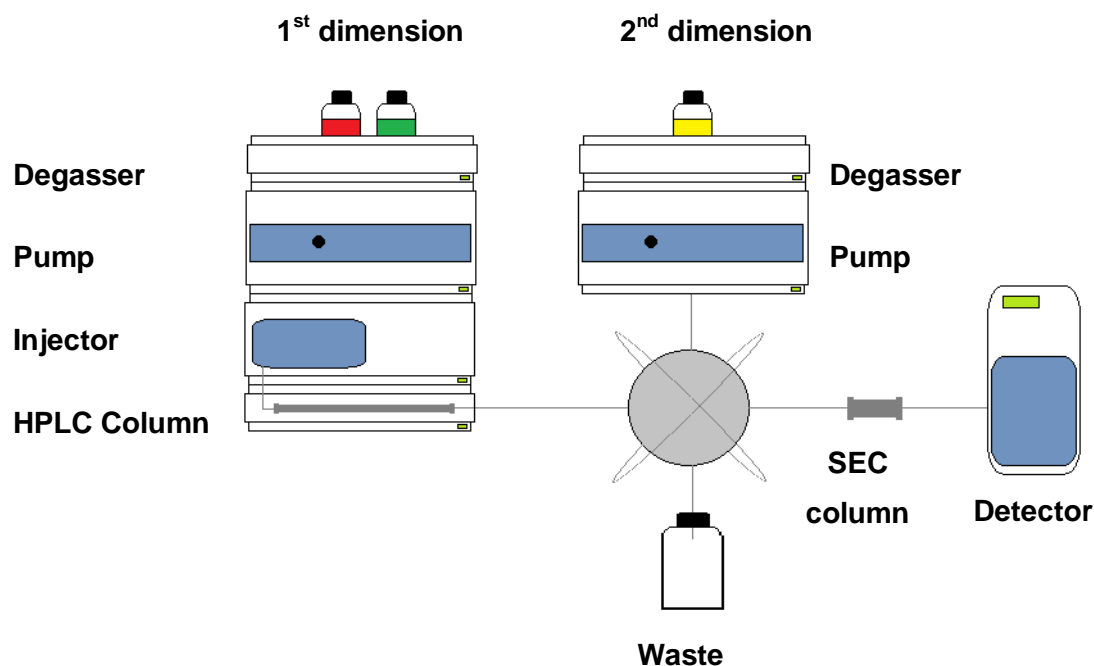


Figure 2.5: Schematic representation of a typical setup for 2D-LC.

Two different columns are required in a 2D-LC setup, namely an HPLC column for the first dimension and a SEC column for the second dimension. The coupling of these two dimensions is facilitated by an eight (or ten) port transfer valve equipped with two storage loops.

Throughout the analysis, fractions from the first dimension are collected in one of the storage loops, while a previously collected fraction in the second loop is analysed in the second dimension. Separation in the first dimension is with respect to chemical composition or functionality. In the second dimension, molecules are separated according to molar mass.⁸⁴⁻⁹⁰

There are two primary coupling systems that are used for 2D-LC. The first system is the coupling of gradient HPLC in the first dimension with SEC in the second dimension.⁹¹⁻⁹⁴ The second system involves coupling LCCC in the first dimension with SEC in the second dimension.⁹⁵⁻⁹⁷ Theoretically, there are several other ways to set up a 2D-LC system, however, some systems are easier and more practical to use than others.⁸⁶

References

- 1 Moad, G.; Solomon, D. H. *The Chemistry of Radical Polymerization*, 2nd ed.; Elsevier: Oxford, U.K. 2006, 1–9.
- 2 Braunecker, W. A.; Matyjaszewski, K. *Progress in Polymer Science* 2007, 32, 93–146.
- 3 Matyjaszewski, K.; Davis, T. P. *Handbook of Radical Polymerization*; Wiley-Interscience: Canada 2002, 361–406.
- 4 Szwarc, M. *Nature* 1956, 178, 1168–1169.
- 5 Billmeyer, F. W. *Textbook of Polymer Science*, John Wiley and Sons: New York 1970.
- 6 Mayo, F. R.; Lewis, F. M. *Journal of the American Chemical Society* 1944, 66, 1594–1601.
- 7 Moad, G.; Solomon, D. H. *The Chemistry of Radical Polymerization*, 2nd ed.; Elsevier: Oxford, U.K. 2006, 333–412.
- 8 Moad, G.; Solomon, D. H. *The Chemistry of Radical Polymerization*, 2nd ed.; Elsevier: Oxford, U.K. 2006, 450–585.
- 9 Penczek, S. *Journal of Polymer Science Part A: Polymer Chemistry* 2002, 40, 1665–1676.
- 10 Quirk, R. P.; Lee, B. *Polymer International* 1992, 27, 359–367.
- 11 David, G.; Boyer, C.; Tonnar, J.; Ameduri, B.; Lacroix-Desmazes, P.; Boutevin, B. *Chemical Reviews* 2006, 106, 3936–3962.
- 12 Davis, K. A.; Matyjaszewski, K. *Macromolecules* 2000, 33, 4039–4047.
- 13 Hawker, C. J.; Bosman, A. W.; Harth, E. *Chemical Reviews* 2001, 101, 3661–3688.
- 14 Moad, G.; Rizzardo, E.; Thang, S. H. *Australian Journal of Chemistry* 2006, 59, 669–692.
- 15 Holden, G.; Kricheldorf, H. R.; Quirk, R. P. *Thermoplastic elastomers*, 3rd ed.: Munich, Hanser 2004.
- 16 Goto, A.; Fukuda, T. *Progress in Polymer Science* 2004, 29, 329–385.
- 17 Grezta, D.; Mardare, D.; Matyjaszewski, K. *Macromolecules* 1994, 27, 638–644.
- 18 Fischer, H. *Chemical Reviews* 2001, 101, 3581–3610.
- 19 Georges, M. K.; Veregin, R. P. N.; Kazmaier, P. M.; Hamer, G. K. *Macromolecules* 1993, 26, 2987–2988.
- 20 Matyjaszewski, K.; Xia, J. *Chemical Reviews* 2001, 101, 2921–2990.
- 21 Wang, J.-S.; Matyjaszewski, K. *Journal of the American Chemical Society* 1995, 117, 5614–5615.

-
- 22 Wang, J.-S.; Matyjaszewski, K. *Macromolecules* 1995, 28, 7901–7910.
 - 23 Wang, J.-S.; Matyjaszewski, K. *Macromolecules* 1995, 28, 7572–7573.
 - 24 Kamigaito, M.; Ando, T.; Sawamoto, M. *Chemical Reviews* 2001, 101, 3689–3746.
 - 25 Patten, T. E.; Matyjaszewski, K. *Advanced Materials* 1998, 10, 901–915.
 - 26 Rizzardo, E.; Chiefari, J.; Mayadunne, R. T. A.; Moad, G.; Thang, S. H. *ACS Symposium Series* 2000, 768, 278–296.
 - 27 Gaynor, S. G.; Wang, J.-S.; Matyjaszewski, K. *Macromolecules* 1995, 28, 8051–8056.
 - 28 Gaynor, S. G. W., J. S.; Matyjaszewski, K. *Polymer Preprints* 1995, 36, 467–468.
 - 29 Lacroix-Desmazes, P.; Severac, R.; Boutevin, B. *Macromolecules* 2005, 38, 6299–6309.
 - 30 Chiefari, J.; Chong, Y. K.; Ercole, F.; Krstina, J.; Jeffery, J.; Le, T. P. T.; Mayadunne, R. T. A.; Meijs, G. F.; Moad, C. L.; Moad, G.; Rizzardo, E.; Thang, S. H. *Macromolecules* 1998, 31, 5559–5562.
 - 31 Moad, G.; Chong, Y. K.; Postma, A.; Rizzardo, E.; Thang, S. H. *Polymer* 2005, 46, 8458–8468.
 - 32 Moad, G.; Mayadunne, R. T. A.; Rizzardo, E.; Skidmore, M.; Thang, S. H. *Macromolecular Symposia* 2003, 192, 1–12.
 - 33 Matyjaszewski, K.; Davis, T. P. *Handbook of Radical Polymerization*; Wiley-Interscience: Canada 2002, 361–406.
 - 34 Boyer, C.; Stenzel, M. H.; Davis, T. P. *Journal of Polymer Science: Part A: Polymer Chemistry* 2010, 49, 551–595.
 - 35 Hart-Smith, G.; Chaffey-Millar, H.; Barner-Kowollik, C. *Macromolecules* 2008, 41, 3023–3041.
 - 36 Mayadunne, R. T. A.; Jeffery, J.; Moad, G.; Rizzardo, E. *Macromolecules* 2003, 36, 1505–1513.
 - 37 Johnston-Hall, G.; Monteiro, M. J. *Journal of Polymer Science: Part A: Polymer Chemistry* 2008, 46, 3155–3173.
 - 38 Chong, Y. K.; Le, T. P.; Moad, G.; Rizzardo, E.; Thang, S. H. *Macromolecules* 1999, 32, 2071–2074.
 - 39 Tatemoto, M. *Kobunshi Ronbunshu* 1992, 49, 765–783.
 - 40 Améduri, B.; Boutevin, B.; Kostov, G. K.; Petrova, P. *Journal of Fluorine Chemistry* 1995, 74, 261–267.
 - 41 Hauptschein, M.; Braid, M.; Fainberg, A. H. *Journal of the American Chemical Society* 1961, 83, 2495–2500.
 - 42 Iovu, M. C.; Matyjaszewski, K. *Macromolecules* 2003, 36, 9346–9354.

-
- 43 Teodorescu, M. *European Polymer Journal* 2001, 37, 1417–1422.
- 44 Lansalot, M.; Farcet, C.; Charleux, B.; Vairon, J.-P. *Macromolecules* 1999, 32, 7354–7360.
- 45 Farcet, C.; Lansalot, M.; Pirri, R.; Vairon, J. P.; Charleux, B. *Macromolecular Rapid Communications* 2000, 21, 921–926.
- 46 Barson, C. A.; Hunt, B. J. *Polymer* 1996, 37, 5699–5702.
- 47 Boyer, C.; Lacroix-Desmazes, P.; Robin, J.-J.; Boutevin, B. *Macromolecules* 2006, 39, 4044–4053.
- 48 Shin, H. C.; Oh, H. G.; Lee, K.; Lee, B. H.; Choe, S. *Polymer* 2009, 50, 4299–4307.
- 49 Tonnar, J.; Lacroix-Desmazes, P.; Boutevin, B. *Polymer Preprints* 2005, 46, 280–281.
- 50 Tonnar, J.; Lacroix-Desmazes, P.; Boutevin, B. *Macromolecular Rapid Communications* 2006, 27, 1733–1738.
- 51 Lacroix-Desmazes, P.; Tonnar, J.; Boutevin, B. *Macromolecular Symposia* 2007, 248, 150–157.
- 52 Pouget, E.; Tonnar, J.; Eloy, C.; Lacroix-Desmazes, P.; Boutevin, B. *Macromolecules* 2006, 39, 6009–6016.
- 53 Tonnar, J.; Lacroix-Desmazes, P.; Boutevin, B. *Macromolecules* 2007, 40, 186–190.
- 54 Fraenkel, G.; Bartlett, P. D. *Journal of the American Chemical Society* 1959, 81, 5582–5590.
- 55 Trifan, D. S.; Bartlett, P. D. *Journal of the American Chemical Society* 1959, 81, 5573–5581.
- 56 Wright, T.; Chirowodza, H.; Pasch, H. *Macromolecules* 2012, 45, 2995–3003.
- 57 Tonnar, J.; Severac, R.; Lacroix-Desmazes, P.; Boutevin, B. *Polymer Preprints* 2008, 49, 68–69.
- 58 Pasch, H. *Advances in Polymer Science* 1999, 150, 1–66.
- 59 Garcia-Rubio, L. H.; Mehta, J. *ACS Symposium Series* 1986, 313, 202–218.
- 60 Buback, M.; Huckestein, B.; Kuchta, F.-D.; Russell, G. T.; Schmid, E. *Macromolecular Chemistry and Physics* 1994, 195, 2117–2140.
- 61 Koenig, J. L. *Spectroscopy of Polymers*, 2nd Ed.; Elsevier Science, New York 1999.
- 62 Starnes, W. H.; Plitz, I. M.; Schilling, F. C.; Villacorta, G. M.; Park, G. S.; Saremi, A. H. *Macromolecules* 1984, 17, 2507–2512.
- 63 Carduner, K. R.; Carter, R. O.; Zinbo, M.; Gerlock, J. L.; Bauer, D. R. *Macromolecules* 1988, 21, 1598–1603.
- 64 Meijs, G. F.; Morton, T. C.; Rizzardo, E.; Thang, S. H. *Macromolecules* 1991, 24, 3689–3695.
- 65 Meijs, G. F.; Rizzardo, E.; Thang, S. H. *Macromolecules* 1988, 21, 3122–3124.

-
- 66 Bevington, J. C.; Huckerby, T. N. *European Polymer Journal* 2006, 42, 1433–1436.
- 67 Kitayama, T.; Hatada, K. *NMR Spectroscopy of Polymers*, Springer Laboratory 2004.
- 68 Hanton, S. D. *Chemical Reviews* 2001, 101, 527–570.
- 69 Nielen, M. W. F. *Mass Spectrometry Reviews* 1999, 18, 309–344.
- 70 Albrecht, A.; Brüll, R.; Macko, T.; Sinha, P.; Pasch, H. *Macromolecular Chemistry and Physics* 2008, 209, 1909–1919.
- 71 Falkenhagen, J.; Much, H.; Stauf, W.; Müller, A. H. E. *Macromolecules* 2000, 33, 3687–3693.
- 72 Mortensen, K.; Gasser, U.; Gürsel, S. A.; Scherer, G. G. *Journal of Polymer Science: Part B* 2008, 46, 1660–1668.
- 73 Murgasova, R.; Hercules, D. M. *Analytical and Bioanalytical Chemistry* 2002, 373, 481–489.
- 74 Suggs, L. J.; Payne, R. G.; Yaszemski, M. J.; Alemany, L. B.; Mikos, A. G. *Macromolecules* 1997, 30, 4318–4323.
- 75 Glöckner, G. *Gradient HPLC of copolymers and chromatographic cross-fractionation*, Springer, Berlin Heidelberg New York 1991.
- 76 Pasch, H.; Trathnigg, B. *HPLC of Polymers*, Springer-Verlag Berlin Heidelberg 2013.
- 77 Striegel, A. M.; Yau, W. W.; Kirkland, J. J.; Bly, D. D. *Modern Size-exclusion Liquid Chromatography*, 2nd ed.; John Wiley and sons Inc: New Jersey 2009.
- 78 Gorshkov, A. V.; Much, H.; Becker, H.; Pasch, H.; Evreinov, V. V.; Entelis, S. G. *Journal of Chromatography A* 1990, 523, 91–102.
- 79 Philipsen, H. J. A. *Journal of Chromatography A* 1996, 727, 13–25.
- 80 Skvortsov, A. M.; Gorbunov, A. A. *Polymer Science U.S.S.R.* 1979, 21, 371–380.
- 81 Berek, D. *Macromolecular Chemistry and Physics* 2008, 209, 695–706.
- 82 Macko, T.; Hunkeler, D. *Advances in Polymer Science* 2003, 163, 62–136.
- 83 Malik, M. I.; Pasch, H. *Progress in Polymer Science* 2014, 39, 87–123.
- 84 Adrian, J.; Esser, E.; Hellmann, G.; Pasch, H. *Polymer* 2000, 41, 2439–2449.
- 85 Dugo, P.; Herrero, M.; Kumm, T.; Giuffrida, D.; Dugo, G.; Mondello, L. *Journal of Chromatography A* 2008, 1189, 196–206.
- 86 Kilz, P. *Chromatographia* 2004, 59, 3–14.
- 87 Malerod, H.; Lundanes, E.; Greibrokk, T. *Analytical Methods* 2010, 2, 110–122.
- 88 Potts, L. W.; Stoll, D. R.; Li, X.; Carr, P. W. *Journal of Chromatography A* 2010, 1217, 5700–5709.
- 89 Stoll, D. R.; Li, X.; Wang, X.; Carr, P. W.; Porter, S. E. G.; Rutan, S. C. *Journal of Chromatography A* 2007, 1168, 3–43.
- 90 Svec, F. *The Chemical Educator* 1997, 2, 1–8.

-
- 91 Gao, H.; Louche, G.; Sumerlin, B. S.; Jahed, N.; Golas, P.; Matyjaszewski, K. *Macromolecules* 2005, 38, 8979–8982.
- 92 Jiang, X.; Horst, A. v. d.; Lima, V.; Schoenmakers, P. J. *Journal of Chromatography A* 2005, 1076, 51–61.
- 93 Raust, J.-A.; Brüll, A.; Moire, C.; Farcet, C.; Pasch, H. *Journal of Chromatography A* 2008, 1203, 207–216.
- 94 Siewing, A.; Lahn, B.; Braun, D.; Pasch, H. *Journal of Polymer Science Part A: Polymer Chemistry* 2003, 41, 3143–3148.
- 95 Gao, H.; Min, K.; Matyjaszewski, K. *Macromolecular Chemistry and Physics* 2006, 207, 1709–1717.
- 96 Graef, S. M.; Zyl, A. J. P. V.; Sanderson, R. D.; Klumperman, B.; Pasch, H. *Journal of Applied Polymer Science* 2003, 88, 2530–2538.
- 97 Sinha, P.; Harding, G. W.; Maiko, K.; Hiller, W.; Pasch, H. *Journal of Chromatography A* 2012, 1265, 95–104.

3 Z-STAR RAFT POLYMERISATION OF STYRENE

3.1 Introduction

This chapter describes the polymerisation of styrene using a tetrafunctional RAFT agent. The main objectives of this study were to analyse the star-shaped polymer using ^1H NMR and SEC in order to elucidate the molecular heterogeneity of the polymer.

Many different types of multifunctional RAFT agents have been reported in literature.¹⁻⁴ As mentioned in Section 2.2.3.3, star RAFT polymerisation can follow one of two approaches. In the R-star RAFT polymerisation mechanism, the RAFT agent is attached *via* a reinitiating R-group. Alternatively, the Z-star RAFT polymerisation mechanism involves a RAFT agent that is attached to the core *via* a stabilising Z-group.⁵ In order to synthesise homogeneous star polymers *via* RAFT polymerisation, it is best to use a star RAFT agent that contains a stabilising Z-group at the core.⁶⁻⁹ The main advantage of using a Z-star RAFT agent is that there are no star-star couplings or linear by-products, which do form when using a RAFT agent that follows the R-star RAFT polymerisation mechanism.^{3,4,9-11}

In this work we make use of a tetrafunctional RAFT, tetrabenzyl(1,3-dithietane-2,2,4,4-tetrayl)tetracarbanotrithioate,¹² whose Z-group constitutes the core and the R-group is a benzyl moiety (Figure 3.1).

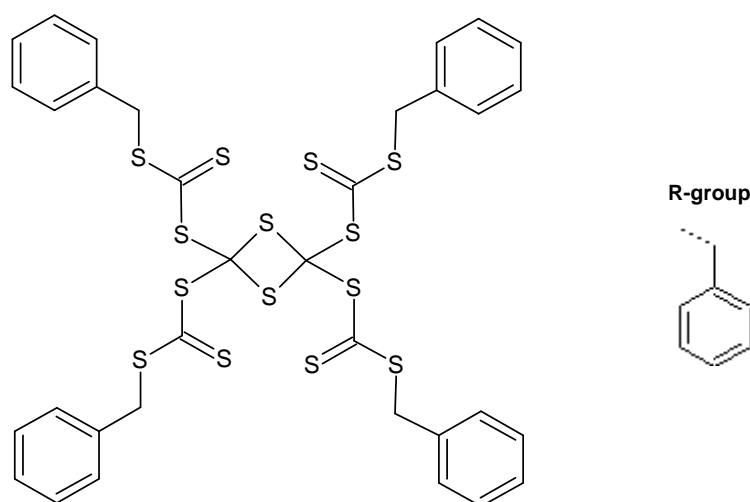


Figure 3.1: Chemical structure of the tetrafunctional RAFT agent used in this work.

3.2 Experimental section

3.2.1 Chemicals

Styrene ($\geq 99\%$, Sigma-Aldrich) was washed three times with an aqueous solution of 0.3 M sodium hydroxide and washed an additional three times with distilled de-ionised water. Thereafter, the styrene monomer was dried using anhydrous magnesium sulphate overnight. The dried monomer was distilled under reduced pressure and stored in a refrigerator at $-5\text{ }^{\circ}\text{C}$. Azobis(isobutyronitrile) (AIBN, Riedel de Haën) was recrystallised from methanol, dried under vacuum and stored in a refrigerator at $-5\text{ }^{\circ}\text{C}$. Deuterated styrene (styrene- d_8 , Sigma-Aldrich 98%) was passed through a column of alumina to remove inhibitor. Deuterated chloroform (CDCl_3 , Sigma-Aldrich 99%) and carbon disulphide (LabChem) were used as received. The tetrafunctional RAFT agent was synthesised according to reference 12. The yellow solid was washed several times with pentane and washed twice with water. The yellow solid was dried at $50\text{ }^{\circ}\text{C}$ and crystallised from carbon disulfide.

^1H NMR (400 MHz, CDCl_3): δ (ppm) 7.40–7.25 (20H, m, Ar), 4.51 (8H, s, CH_2)

^{13}C NMR (100 MHz, CDCl_3): δ (ppm) 218.00 (C=S), 133.71, 129.16, 128.59, 127.76 (Ar), 72.58 (quaternary C), 41.21 (CH_2)

3.2.2 Polymerisation of styrene

In a typical polymerisation reaction (run 1a, Table 3.1), styrene (5.00 g, 4.80×10^{-2} mol), AIBN (2.1 mg, 1.28×10^{-5} mol), RAFT agent (0.232 g, 2.62×10^{-5} mol) and a magnetic stirrer were added to a Schlenk flask. The flask was degassed three times with successive freeze-pump-thaw cycles and then backfilled with UHP argon gas. The flask was immersed in an oil bath that was preheated to $70\text{ }^{\circ}\text{C}$ and the polymerisation was carried out with magnetic stirring for 24 hours. The polymerisation was stopped after 24 hours and the Schlenk flask placed in a container of ice. The polymer was dissolved in THF, precipitated from cold methanol and left overnight to dry in a vacuum.

The polymerisation of styrene was also studied *via in situ* ^1H NMR at $70\text{ }^{\circ}\text{C}$ using styrene- d_8 instead of hydrogenous styrene. The ^1H NMR spectra were recorded on a Varian Unity INOVA 400 MHz spectrometer, with a pulse width of $3\text{ }\mu\text{s}$ (40°) and a 4 second acquisition time.

A reference spectrum of the sample was recorded at 25 °C. Thereafter, the magnet was heated to 70 °C and left to stabilise for 30 minutes. Once the temperature was stable, the NMR tube was inserted into the magnet and the sample was shimmed. The first spectrum was recorded 3 – 4 minutes after the sample had been shimmed. Thereafter, spectra (15 scans) were recorded every 15 minutes for 24 hours. All NMR data was processed using ACD Labs 10.0 ¹H NMR processor[®]. All spectra were phased automatically whilst baseline correction and integration were performed manually.

3.2.3 Aminolysis to cleave star-shaped polymer arms

In a typical aminolysis procedure, 0.2 g of star-shaped polystyrene was dissolved in 5 mL of THF. The Schlenk flask was degassed by three successive freeze-pump-thaw cycles and backfilled with UHP argon gas. A gastight syringe was used to add 0.5 mL of propylamine to the flask and the mixture was left to stir overnight. The resulting polymer was precipitated from methanol and dried in a vacuum oven overnight.

3.3 Characterisation of polymers

3.3.1 SEC analysis

An SEC instrument equipped with a Waters 717plus Autosampler, Waters 600E system controller and a Waters 610 fluid unit were used to perform SEC analyses. A Waters 2414 differential refractometer was used for detection. Two PLgel 5 µm Mixed-C columns and a PLgel 5 µm guard column were used. The oven temperature was maintained at 30 °C and 100 µL of 2mg/mL sample was injected into the column. THF (HPLC grade, BHT stabilised) was used as the eluent for the analyses at a flow rate of 1mL/min. Narrow polystyrene standards with molar masses ranging from 800–2 x 10⁶ g/mol were used to calibrate the instrument. Data obtained from SEC is reported as polystyrene equivalents.

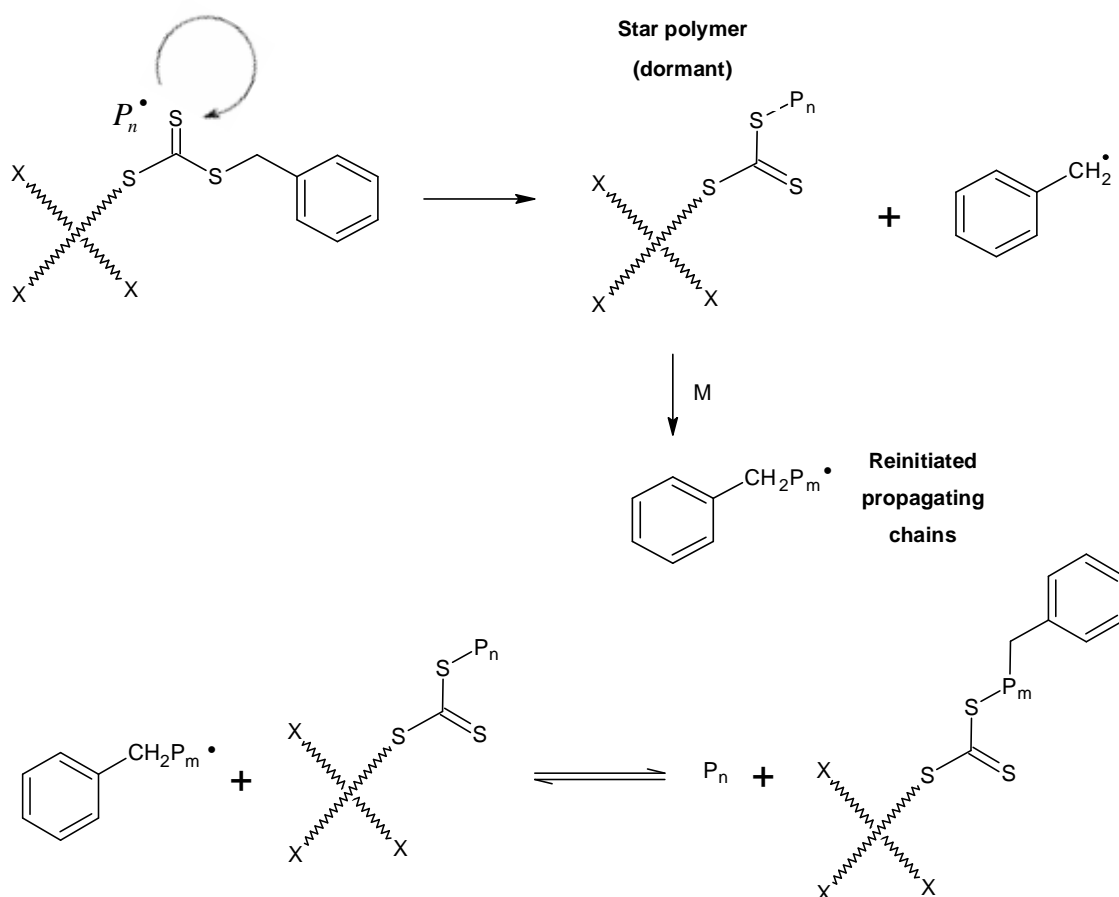
3.3.2 NMR analysis

¹H NMR spectra were recorded on a Varian Unity INOVA 400 MHz spectrometer. Deuterated chloroform (CDCl₃) was used to analyse polymer samples at ambient temperature, whereas the *in situ* ¹H NMR experiments were run in deuterated styrene (C₈D₈).

3.4 Results and discussion

3.4.1 Polymerisation of styrene

The tetrafunctional RAFT agent used in this study follows the Z-star RAFT polymerisation mechanism (Scheme 3.1), where propagating radicals grow away from the core. In this mechanism, the RAFT agent is fragmented, resulting in the formation of a benzyl radical that is detached from the core. When monomer is added to the benzyl radicals, they can reinitiate polymerisation away from the core, thus resulting in linear propagating chains. There is equilibrium between the linear propagating chains and the arms of the star polymer. This equilibrium makes it possible for the propagation of the star polymer arms to occur in a controlled manner.³



Scheme 3.1: Schematic representation of the Z-star RAFT polymerisation mechanism controlled by the tetrafunctional RAFT agent.

The polymerisation reactions in this study were carried out at 70 °C for 24 hours. After 24 hours, the reaction was stopped by placing the Schlenk flask on ice. After each reaction was stopped, a small amount of crude sample was extracted for analysis by ^1H NMR (Figure 3.2). Thereafter, the remaining crude polymer from each reaction was precipitated from cold methanol.

The signal attributed to the vinylic protons of residual styrene (**a** and **b** in Figure 3.2) are observed at 5.2 – 5.8 ppm. The methine proton of residual styrene (**c** in Figure 3.2) is seen at 6.7 ppm. A signal at 4.5 ppm corresponds to the methine proton (**d** in Figure 3.2) adjacent to the thiocarbonylthio moiety. The signal at 1.7–2.4 ppm is attributed to the CH protons (**e** in Figure 3.2) of the polymer backbone. The CH_2 protons (**f** in Figure 3.2) that correspond to the polymer backbone are observed at 1.3–1.6 ppm. A signal attributed to the CH_2 protons of the benzyl end group could not be observed, as the signal was overlapped by the broad polymer signal (**e** in Figure 3.2). Boschmann *et al.*¹⁶ used deuterated styrene to follow the evolution of this CH_2 signal, using *in situ* ^1H NMR. This will be discussed later in this chapter.

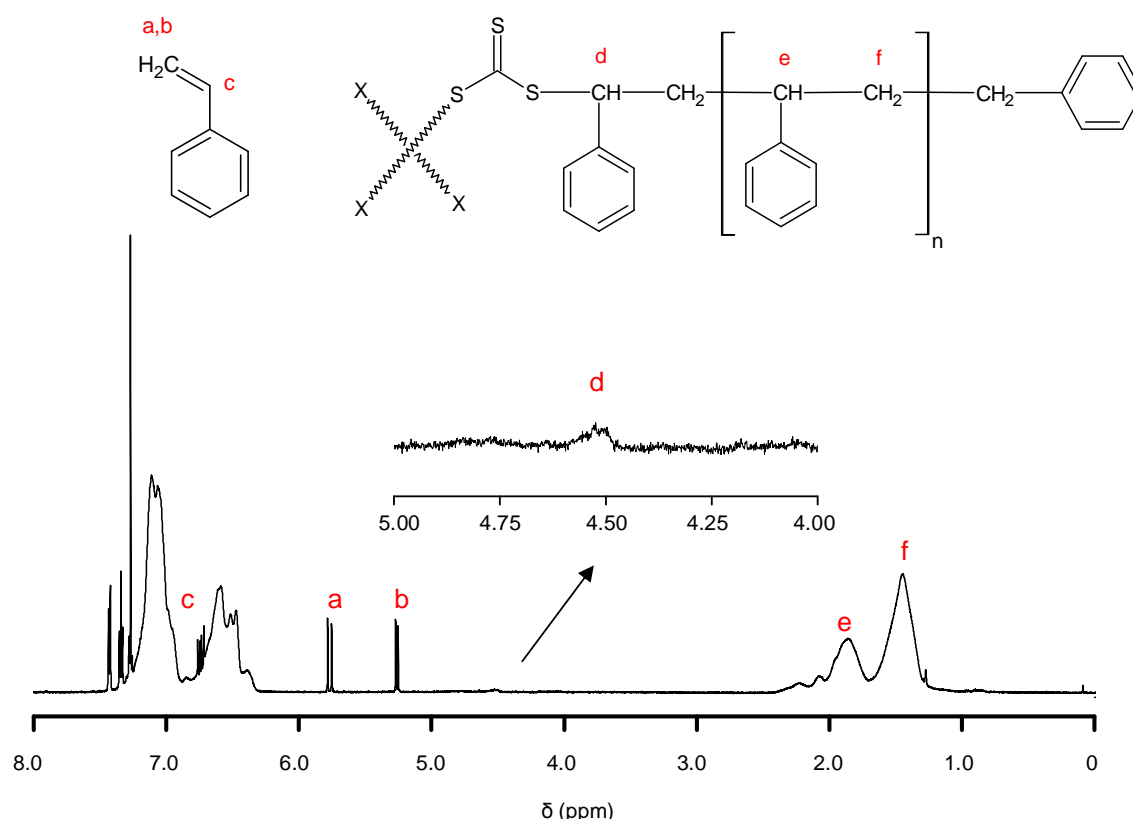


Figure 3.2: Typical ^1H NMR spectrum in CDCl_3 of a crude sample of star-shaped PS (run 2a) synthesised at 70 °C for 24 hours.

Analysing the crude sample by ^1H NMR is useful for the determination of monomer conversion using Equation 3.1

$$X = \left(1 - \frac{\int \text{CH}_2}{\int \text{C}_6\text{H}_5} \right) \times 100 \quad (3.1)$$

where $\int \text{CH}_2$ is the integral of the vinylic protons of residual styrene (5.2 – 5.8 ppm) and $\int \text{C}_6\text{H}_5$ is the integral of the aromatic protons of PS. Once the monomer conversion has been calculated, the theoretical molar mass can then be estimated using Equation 3.2¹³

$$M_{n, calc} = \frac{X \times c_M^0 \times M_{mon}}{c_{RAFT}^0 + c_I^0 \times d \times f(1 - e^{-k_d t})} + M_{RAFT} \quad (3.2)$$

where X is the monomer conversion, c_M^0 is the initial monomer concentration, M_{mon} is the molar mass of the monomer, c_{RAFT}^0 is the initial concentration of the RAFT agent, c_I^0 is the initial concentration of the initiator, d is the number of chains generated in the termination process (~ 1 for styrene), k_d is the initiator decomposition rate coefficient ($k_d = 3.71 \times 10^{-5}$ for AIBN) and f is the initiator efficiency ($f \sim 1$). Schaeffgen *et al.*¹⁴ suggested a way in which to estimate the dispersity of a star polymer, according to Equation 3.3

$$\frac{M_w}{M_n} = 1 + \frac{1}{r} \quad (3.3)$$

where r is the number of arms in the star polymer. Therefore, the dispersities of the resultant polymers in this work should theoretically be close to 1.25 if four polymer arms are formed. The results for the styrene polymerisation reactions are shown in Table 3.1. The monomer conversion after 24 hours at 70 °C is typically about between 35–40%. This is consistent with what has been reported in literature when using star RAFT agents containing a benzyl leaving group. The low monomer conversion after 24 hours is due to the benzyl radical having relatively high energy, resulting in an inefficient pre-equilibrium. The rate of fragmentation of the initial intermediate radical is slowed by the benzyl radical, while a back-transfer during pre-equilibrium is sped up.¹⁵ As a result of this inefficient pre-equilibrium, the initiation of arm growth is slow.^{9,13,16}

Fröhlich *et al.*^{17,18} reported that the addition reaction in Z-star RAFT polymerisation is ten times slower than the addition reaction for linear RAFT polymerisation. The slow addition reaction does not, however, prevent the RAFT reaction from occurring.^{6,7,13}

Table 3.1: Results of star-shaped PS synthesised for 24 hours at 70 °C.

Run	[M]/[RAFT]/[AIBN] ^a	Conv (%) ^b	M _{n, calc} (g.mol ⁻¹) ^c	M _{n, SEC} (g.mol ⁻¹) ^d	Đ
1a	2425/3/1	41	34300	11200	1.22
2a	3800/5/1	34	14300	6100	1.28
3a	3800/5/1	34	21100	10000	1.24
4a	3800/5/1	38	32000	10300	1.27

^a Represented as molar ratios

^b Determined by ¹H NMR of crude sample in CDCl₃ by $X = (1 - ([CH_2]/[C_6H_5])) \times 100$ where $[CH_2]$ is the integral of the vinylic protons of residual styrene at 5.2 – 5.8 ppm, and $[C_6H_5]$ is the integral of the aromatic protons PS.

^c Calculated by $M_{n, calc} = (X \times c_M^0 \times M_{mon} / c_{RAFT}^0 + c_I^0 \times d \times f(1 - e^{-k_d t})) + M_{RAFT}$

^d Calibrated using PS standards.

The dispersities reported in Table 3.1 are relatively low, but still higher than for systems that have an efficient pre-equilibrium.¹⁹ Nevertheless, the dispersities for the star-shaped PS are in good agreement with the approximation using Equation 3.3. Typical of a living system, the molar mass increases linearly with conversion (Figure 3.3). It is clear from Figure 3.3 that there is a discrepancy between the theoretical molar masses and the molar masses determined by SEC.

The theoretical molar mass is determined using Equation 3.2, which assumes that the polymer under investigation is linear. Star-shaped polymers fall under the category of branched polymers, and therefore have a lower hydrodynamic volume relative to a linear polymer of similar molar mass.¹³ Since linear PS standards are used to calibrate SEC instruments, the molar mass of the star-shaped polymers is lower than the theoretical molar mass.

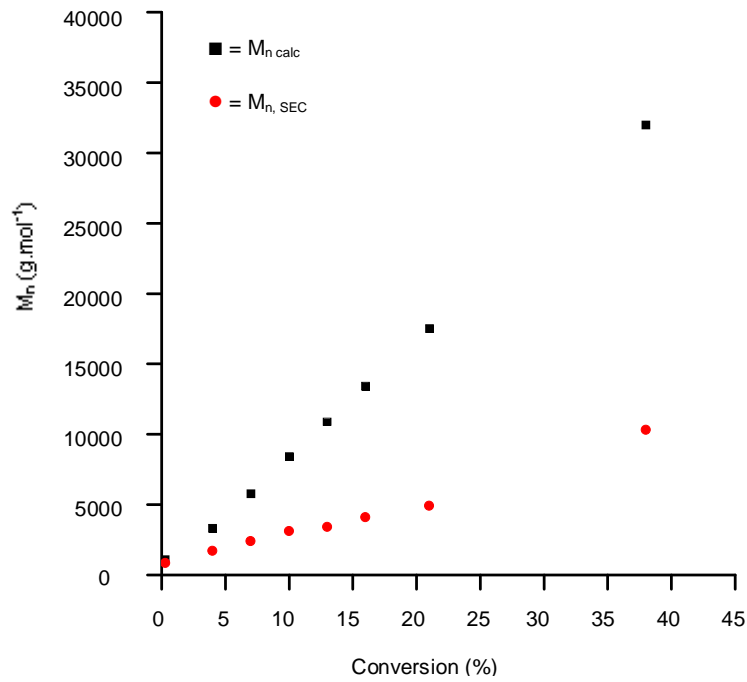


Figure 3.3: Evolution of the molar mass *versus* conversion for star-shaped PS (run 4a).

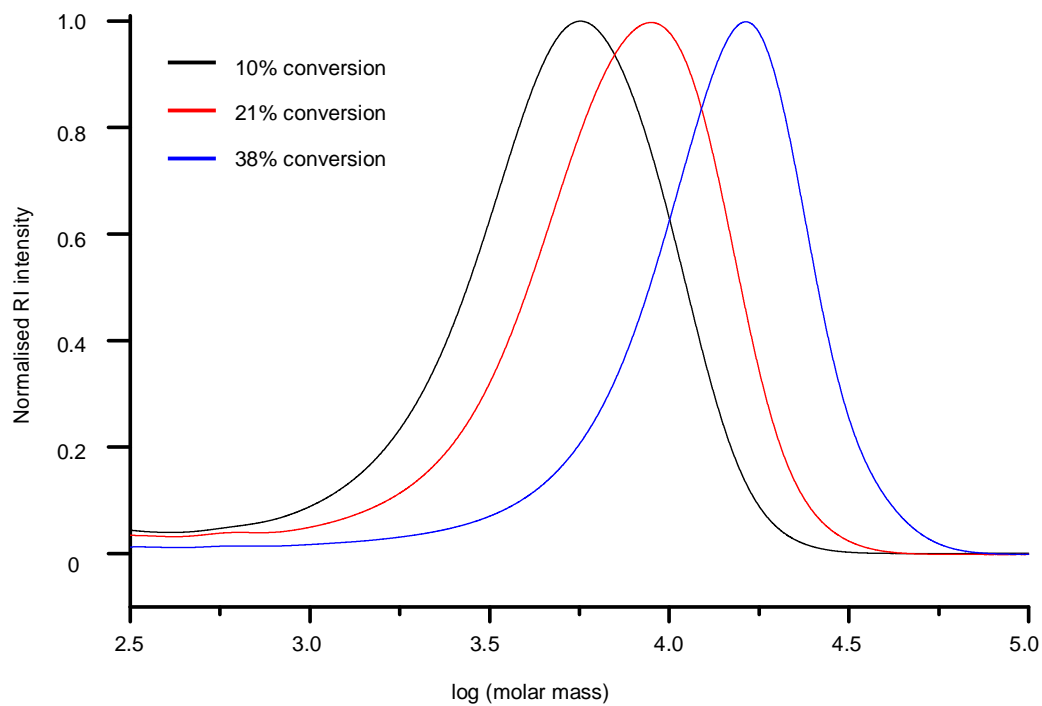


Figure 3.4: Molar mass distributions from SEC (RI traces) of the star-shaped PS at various monomer conversions (run 4a).

Figure 3.4 shows the molar mass distributions from SEC (RI traces) of the star-shaped PS, where extractions were taken to follow the monomer conversion over time. The molar mass distributions are unimodal with lower molar mass tailing. Mayadunne *et al.*³ reported similar results for a Z-star RAFT agent, where lower molar mass tailing was attributed to continuous termination of linear propagating radicals.

An overlay of the molar mass distributions from SEC (UV traces) at 254 nm and 320 nm is shown in Figure 3.5. The two samples compared in these molar mass distributions are from those of a sample extraction after 540 minutes (Figure 3.5 a) and a sample extraction of the final polymer at 1440 minutes (Figure 3.5 b). The incorporation of the thiocarbonylthio moiety from the tetrafunctional RAFT agent into the polymer can be selectively detected using a UV wavelength between 300–330 nm. At this UV wavelength, the thiocarbonylthio moiety absorbs strongly.^{7,20} The disappearance of the small hump in the 320 nm trace after 1440 minutes indicates that the thiocarbonylthio moiety had been incorporated into the polymer.

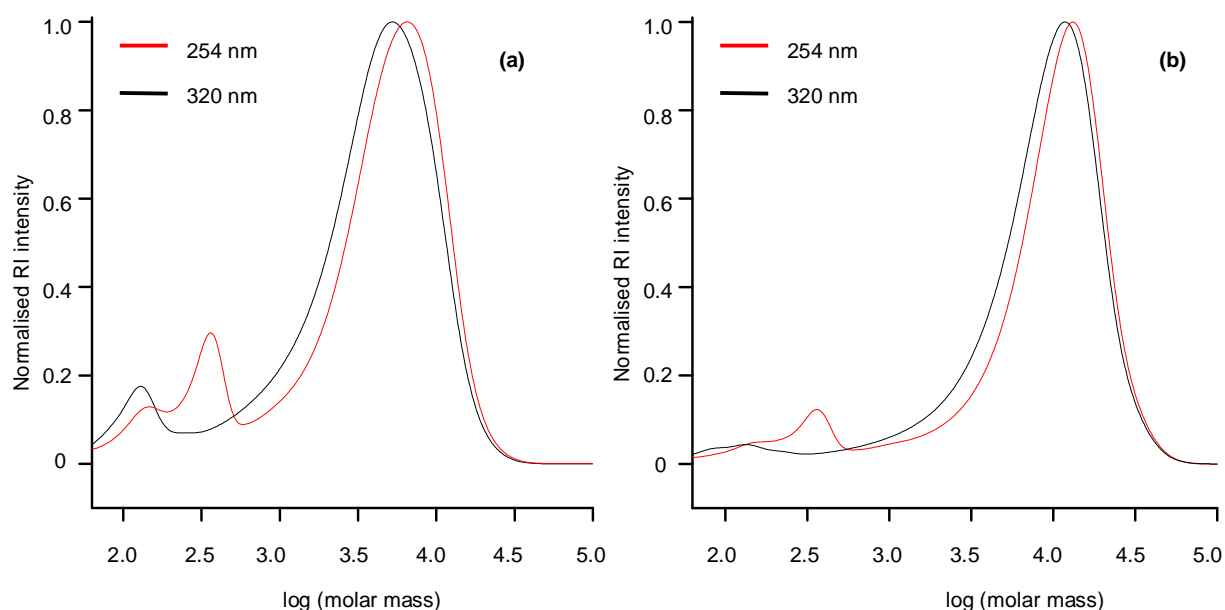


Figure 3.5: Molar mass distributions from SEC (UV traces) of the star-shaped PS taken at (a) = 540 min. and (b) = 1440 min.

3.4.2 *In situ* ^1H NMR of the polymerisation of styrene

In a study done by Boschmann *et al.*,¹⁶ styrene polymerisation was followed that used two types of hexafunctional trithiocarbonate RAFT agent following the Z-star RAFT polymerisation mechanism. They found that, beyond 30% monomer conversion, the hexafunctional RAFT agent carrying a phenylethyl R-group could form well-defined star-shaped polymers with six arms. However, in the case of the hexafunctional RAFT agent carrying a benzyl R-group, it was observed that the number of arms would only increase gradually, barely forming the expected six arms. This was attributed to the benzyl group slowing down the initiation of arm growth.

The number of arms in a star-shaped polymer can not be detected if monomer conversion is lower than 30%. Therefore, it was useful to observe arm growth through kinetic ^1H NMR. To follow the arm growth initiation, styrene- d_8 was used with the tetrafunctional RAFT agent instead of regular styrene. By using deuterated styrene, the arm growth could be followed by the change in the chemical shift of H_α (Figure 3.6).¹⁶ Any changes that occur to the tetrafunctional RAFT agent could be observed more easily using deuterated styrene because styrene- d_8 is 98% deuterated and hence, 2% undeuterated styrene could be observed.

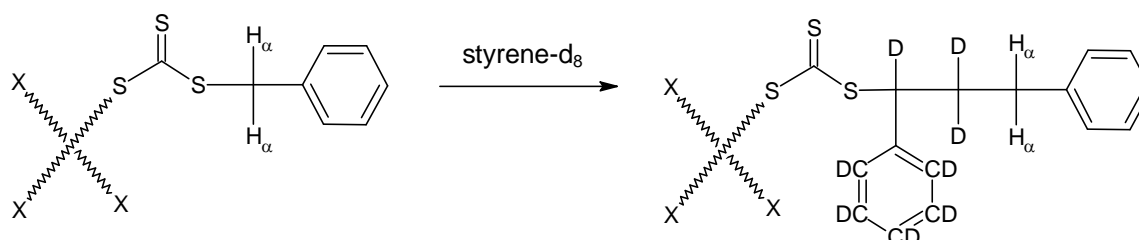


Figure 3.6: Method for following arm growth initiation of styrene- d_8 using ^1H NMR.

Analogous to the study done by Boschmann *et al.*, we performed an *in situ* study using our tetrafunctional RAFT agent in a solution of styrene- d_8 . Once the reaction mixture was degassed and ready for *in situ* ^1H NMR, a spectrum was recorded at 25 °C to observe the proton signals prior to polymerisation (Figure 3.7). The signal of the vinyl protons (**a** and **b** in Figure 3.7) of styrene can be seen at 5.00–5.70 ppm. The signal of the methine proton of styrene (**c** in Figure 3.7) appears at 6.50–6.60 ppm. All aromatic proton signals (benzene- d_6 , styrene and RAFT agent) overlap one another in the region of 6.90–7.30 ppm. A singlet is observed at 4.18 ppm corresponding to vinyl protons (H_α in Figure 3.7) of the RAFT agent.

This chemical shift is, of course, different to the value reported when the RAFT agent was analysed in CDCl_3 (4.51 ppm). The signal for the methyl protons of AIBN can be seen at 1.20 ppm.

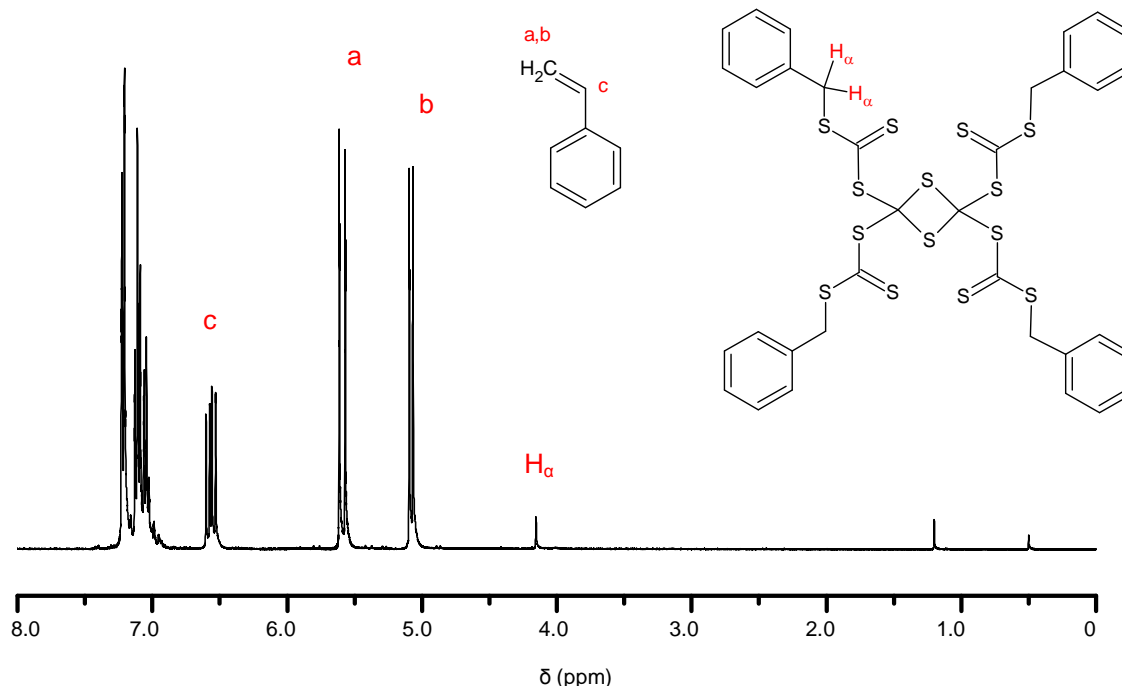


Figure 3.7: The ^1H NMR spectrum of the starting reagents in styrene-d_8 prior to polymerisation.

The NMR tube is then removed and the magnet heated to 70°C . Once the temperature of the magnet is stable at 70°C , the sample is inserted into the magnet and the reaction proceeds. At this stage of the reaction, the R-group detaches from the core and becomes a terminal group of the growing polymer arm. This departure of the R-group leaves the core of the RAFT agent with no protons to be detected by ^1H NMR. Therefore, the only proton signals that can be traced in relation to arm growth are the vinyl protons of the R-group. The CH_2 proton signal for the benzyl R-group is at 4.18 ppm prior to polymerisation (Figure 3.7), and shifts to 4.24 ppm when reaction proceeds at 70°C . Figure 3.8 shows the evolution of a new signal at 2.51 ppm with increasing monomer conversion. This signal is attributed to the incorporation of the H_α protons into the deuterated polymer, thus becoming a terminal group.

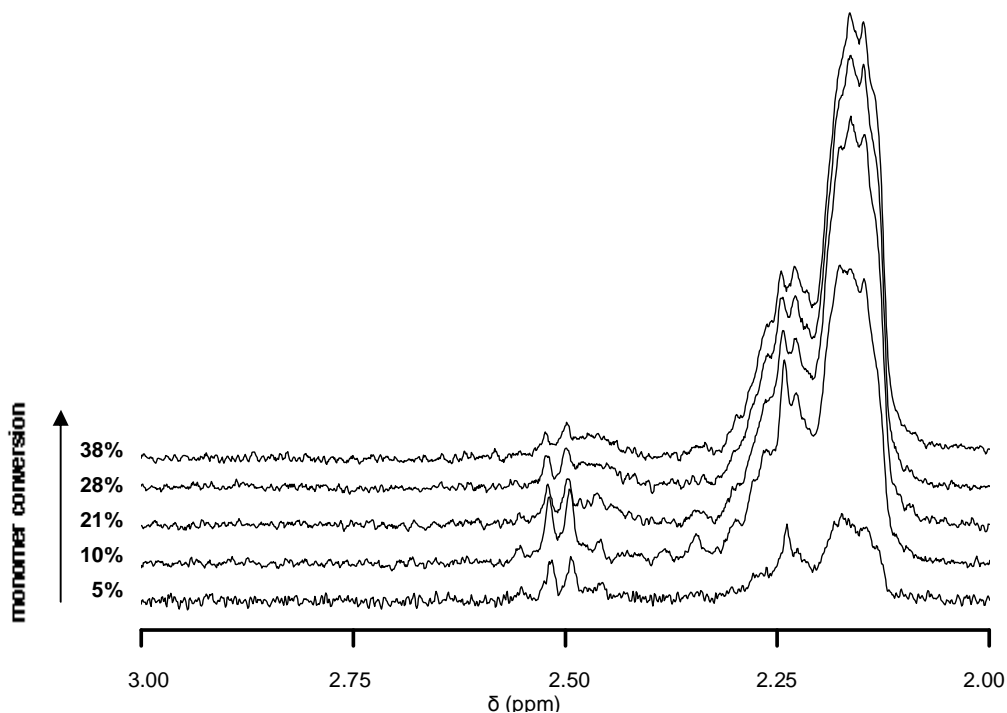


Figure 3.8: ¹H NMR spectra in styrene-d₈, showing the increasing proton signal intensity at 2.5 ppm corresponding to the incorporation of the tetrafunctional RAFT agent into the polymer.

The signal at 2.51 ppm is gradually engulfed by the overlapping polymer proton signal that broadens as monomer conversion increases. The increase in intensity of the broad signals between 2.00–2.51 ppm is indicative that the polymer chains are growing.

Concurrently, one would expect to see a reduction in the signal intensity for the proton signal of H_α (the vinyl protons from the RAFT agent) at 4.24 ppm. A decrease in the signal intensity at 4.24 ppm would correspond to the situation where initiation of arm growth has occurred. Indeed, Figure 3.9 shows clearly that there is a decrease in the signal intensity for the H_α proton signal at 4.24 ppm as monomer conversion increases. The signal for the methine proton adjacent to the thiocarbonylthio moiety in the star-shaped polymer (**d** in Figure 3.2) is seen at ~4.15 ppm and increases with monomer conversion.

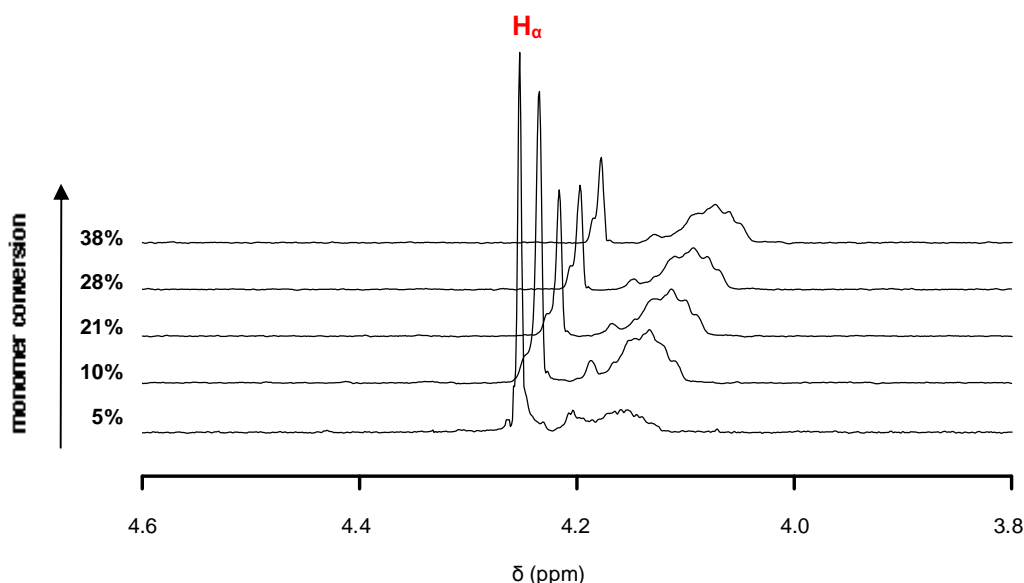
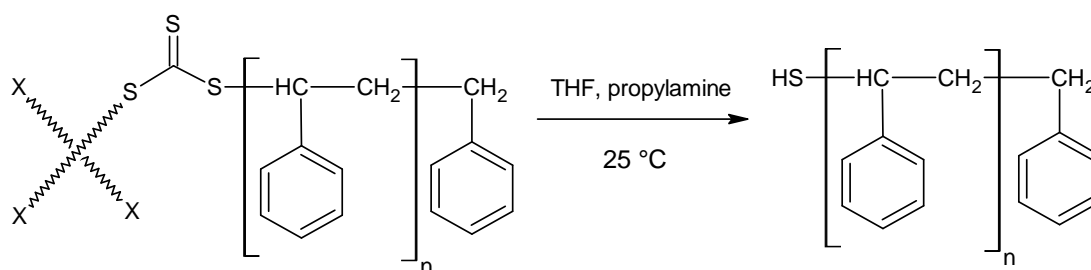


Figure 3.9: ^1H NMR spectra in styrene- d_8 , showing the evolution of the H_α proton signal from the tetrafunctional RAFT agent.

3.4.3 Aminolysis to cleave star-shaped polymer arms

In general, linear PS standards of various molar masses are used when calibrating an SEC instrument. Star-shaped PS has a lower hydrodynamic volume relative to the linear PS standards. Therefore, in order to determine the molar mass of the star-shaped polymers more precisely, the arms need to be cleaved using a strong nucleophile (Scheme 3.2).^{7,20,21} Propylamine was used to cleave the arms of the star-shaped PS and the resultant linear polymer was characterised using SEC and ^1H NMR.



Scheme 3.2: Cleavage of the star-shaped polymer arms when treated with an amine.

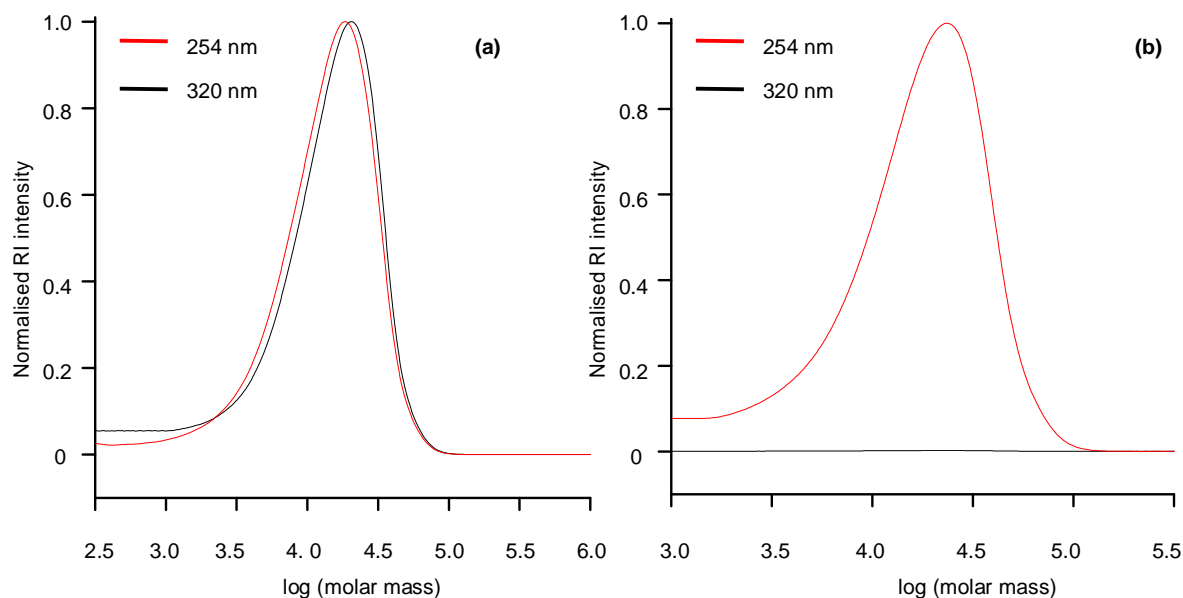


Figure 3.10: Molar mass distributions from SEC (UV traces) of the star-shaped PS before (a) and after (b) aminolysis.

As mentioned earlier in this chapter, the thiocarbonylthio moiety absorbs strongly at a UV wavelength of 300–330 nm. Therefore, there should be no UV absorbance present at 320 nm for the polymer after the aminolysis reaction. The molar mass distributions from SEC (UV traces) in Figure 3.10 clearly show that the thiocarbonylthio has been removed, implying that the arms were cleaved during aminolysis. Also, the ^1H NMR spectra (Figure 3.11) show clearly that the methine proton adjacent to the thiocarbonylthio moiety (a) is no longer present after aminolysis (b).

Another more qualitative way of determining whether aminolysis is successful is through a visual comparison of the colour of the polymers. In general, RAFT polymers are coloured, whereas a polymer treated for end group removal is colourless.²⁰ In our case, the star-shaped PS was yellow in colour prior to aminolysis, but changed to a white precipitate after treatment with propylamine.

From the changes observed in SEC, ^1H NMR and colour, we could assume that the arms of the star-shaped polymer had been cleaved and that these arms were linear. With this assumption taken into consideration, the molar mass of the cleaved PS arms could be calculated using Equation 3.4

$$M_{n, calc linear} = (M_{n, cleaved} \times 4) + M_{n, core} \quad (3.4)$$

where $M_{n, core}$ is the molar mass of the core of the RAFT agent ($393 \text{ g}\cdot\text{mol}^{-1}$). A comparison between the molar mass of the polymer before and after aminolysis is shown in Table 3.2.

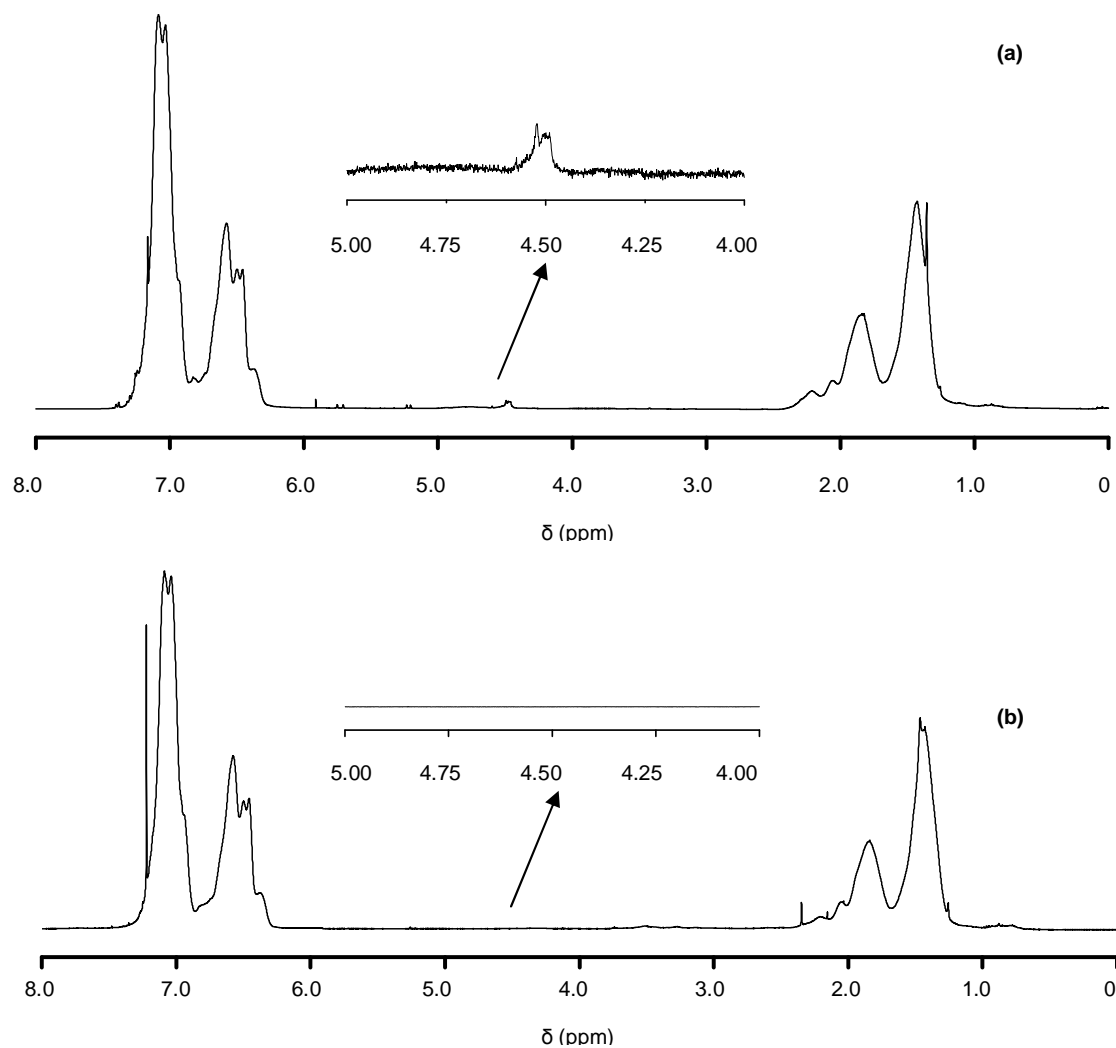


Figure 3.11: The ^1H NMR spectra in CDCl_3 of a star-shaped PS sample before (a) and after (b) aminolysis.

According to the results shown in Table 3.2, the molar mass of the cleaved arms was lower than that of their star-shaped polymer counterpart. When multiplying the molar mass of the cleaved arms by four (Equation 3.4), $M_{n, calc}$ after aminolysis is in reasonable agreement with $M_{n, calc}$ before aminolysis.

Table 3.2: Molar mass data for star-shaped PS before and after aminolysis.

Before aminolysis					After aminolysis			
Run	Conv (%) ^a	M _{n, SEC} (g.mol ⁻¹) ^b	M _{n, calc} (g.mol ⁻¹) ^c	<i>D</i>	Run	M _{n, SEC} (g.mol ⁻¹) ^b	M _{n, calc linear} (g.mol ⁻¹) ^d	<i>D</i>
1a	41	11200	34300	1.22	1b	7600	30800	1.55
2a	34	6100	14300	1.28	2b	3400	14000	1.46
3a	34	10000	21100	1.24	3b	5800	23700	1.36
4a	38	10300	32000	1.27	4b	6900	28100	1.32

^a Determined by ¹H NMR of crude sample in CDCl₃ by conversion = (1 - ([CH₂]/[C₆H₅])) x 100 where [CH₂] is the integral of the vinylic protons of residual styrene at 5.2 – 5.8 ppm, and [C₆H₅] is the integral of the aromatic protons PS.

^b Calibrated using PS standards.

^c Calculated by $M_{n, calc} = (X \times c_M^0 \times M_{mon} / c_{RAFT}^0 + c_I^0 \times d \times f(1 - e^{-k_d t})) + M_{RAFT}$

^d Calculated by $M_{n, calc linear} = (M_{n, cleaved} \times 4) + M_{n, core}$

The agreement between M_{n, calc} and M_{n, calc linear} is an indication that four arms were formed during the polymerisation reaction. Despite the dispersity of the cleaved arms being higher than their star-shaped counterpart, the dispersity is still relatively narrow. This relatively narrow dispersity of the cleaved arms indicates that the arms have all grown to have similar molar masses.

3.5 Conclusions

A tetrafunctional RAFT agent with benzyl leaving groups was used to synthesise star-shaped polystyrene. The polymerisation of styrene at 70 °C with this Z-star RAFT agent yielded monomer conversions between 35–40% after 24 hours. This relatively low monomer conversion is attributed to the ineffective pre-equilibrium of a Z-star RAFT agent containing a benzyl leaving group. Molar masses determined by SEC were lower than theoretical molar masses. The difference in molar masses is due to the fact that SEC is calibrated using linear PS standards, which have higher hydrodynamic volumes relative to star-shaped polymers of similar molar masses. Arm growth was followed by *in situ* ^1H NMR by using deuterated styrene instead of hydrogenous styrene. The formation of a proton signal at 2.5 ppm was indicative that the hydrogenous vinyl protons of the RAFT agent became a terminal group in the deuterated star-shaped polymer. Concurrently, there was a decrease in the proton signal intensity of H_α (the vinyl protons from the RAFT agent) at 4.2 ppm. The molar mass of the star polymer was determined more precisely by cleaving the arms using an amine. In the molar mass distributions from SEC (UV traces) of the cleaved polymer, there was no absorbance at 320 nm, a wavelength where thiocarbonylthio groups typically absorb. In the ^1H NMR of the cleaved polymer, there was no proton signal for a methine proton adjacent to the thiocarbonylthio moiety. Finally, the molar mass of the cleaved polystyrene, multiplied by four, was found to be in good agreement with the theoretical molar mass determined prior to aminolysis, indicating that the star-shaped polymer contained four arms.

References

- 1 Boyer, C.; Stenzel, M. H.; Davis, T. P. *Journal of Polymer Science: Part A: Polymer Chemistry* 2010, 49, 551–595.
- 2 Hart-Smith, G.; Chaffey-Millar, H.; Barner-Kowollik, C. *Macromolecules* 2008, 41, 3023–3041.
- 3 Mayadunne, R. T. A.; Jeffery, J.; Moad, G.; Rizzardo, E. *Macromolecules* 2003, 36, 1505–1513.
- 4 Moad, G.; Mayadunne, R. T. A.; Rizzardo, E.; Skidmore, M.; Thang, S. H. *Macromolecular Symposia* 2003, 192, 1–12.
- 5 Johnston-Hall, G.; Monteiro, M. J. *Journal of Polymer Science: Part A: Polymer Chemistry* 2008, 46, 3155–3173.
- 6 Boschmann, D.; Vana, P. *Polymer Bulletin* 2005, 53, 231–242.
- 7 Boschmann, D.; Vana, P. *Macromolecules* 2007, 40, 2683–2693.
- 8 Darcos, V.; Duréault, A.; Taton, D.; Gnanou, Y.; Marchand, P.; Caminade, A.-M.; Majoral, J.-P.; Destarac, M.; Leising, F. *Chemical Communications* 2004, 2110–2111.
- 9 Stenzel, M. H.; Davis, T. P. *Journal of Polymer Science Part A: Polymer Chemistry* 2002, 40, 4498–4512.
- 10 Chaffey-Millar, H.; Stenzel, M. H.; Davis, T. P.; Coote, M. L.; Barner-Kowollik, C. *Macromolecules* 2006, 39, 6406–6419.
- 11 Stenzel-Rosenbaum, M.; Davis, T. P.; Chen, V.; Fane, A. G. *Journal of Polymer Science Part A: Polymer Chemistry* 2001, 39, 2777–2783.
- 12 Weber, W.; Chirowodza, H.; Pasch, H. *Tetrahedron* 2013, 69, 2017–2021.
- 13 Boschmann, D.; Edam, R.; Schoenmakers, P. J.; Vana, P. *Polymer* 2008, 49, 5199–5208.
- 14 Schaeffgen, J. R.; Flory, P. J. *Journal of the American Chemical Society* 1948, 70, 2709–2718.
- 15 Barner-Kowollik, C.; Quinn, J. F.; Nguyen, T. L. U.; Heuts, J. P. A.; Davis, T. P. *Macromolecules* 2001, 34, 7849–7857.
- 16 Boschmann, D.; Mänz, M.; Pöppler, A.-C.; Sörensen, N.; Vana, P. *Journal of Polymer Science: Part A: Polymer Chemistry* 2008, 46, 7280–7286.
- 17 Fröhlich, M. G.; Vana, P.; Zifferer, G. *Macromolecular Theory and Simulations* 2007, 16, 610–618.
- 18 Fröhlich, M. G.; Vana, P.; Zifferer, G. *The Journal of Chemical Physics* 2007, 127, 164906.
- 19 Chong, Y. K.; Krstina, J.; Le, T. P. T.; Moad, G.; Postma, A.; Rizzardo, E.; Thang, S. H. *Macromolecules* 2003, 36, 2256–2272.

- 20 Willcock, H.; O'Reilly, R. K. *Polymer Chemistry* 2010, 1, 149–157.
- 21 Xu, J.; He, J.; Fan, D.; Wang, X.; Yang, Y. *Macromolecules* 2006, 39, 8616–8624.

4 SYNTHESIS OF POLYSTYRENE-B-POLY-(N-BUTYL ACRYLATE) BLOCK COPOLYMERS BY REVERSE IODINE TRANSFER POLYMERISATION

4.1 Introduction

RITP is a LRP method where chain transfer agents are generated *in situ*, due to the reaction between AIBN and molecular iodine. Molecular iodine inhibits polymerisation, and this inhibitory property is exploited in RITP. There is a period where AIBN and iodine react to form chain transfer agents, known as the inhibition period. Once all of the iodine has been consumed, the polymerisation can commence. The resultant polymer has a cyanoisopropyl α -chain end and an iodinated ω -chain end.

The living nature of the iodo-terminated polymer can then be used as a macro-initiator to form block copolymers. In cases where the homopolymerisation reaction yields high monomer conversion (>95%), such as acrylates,^{1,3} the crude sample is generally used without purification. However, in styrene homopolymerisation *via* RITP, the monomer conversion typically is not as high as in the case of acrylates (~60%).⁵⁻⁷ Therefore, in the case of polystyrene, the polymer needs to be purified and dried before it can be used as a macro-initiator. Several examples of block copolymers prepared using RITP can be found in literature.¹⁻⁴ Typically, these block copolymers are analysed using SEC, NMR and mass spectrometry.

The main objectives of this study were to analyse the microstructure of the block copolymers using advanced analytical methods. RITP homopolymerisation reactions of styrene and n-butyl acrylate were run at 70 °C for 24 hours. Using SEC, the molar mass and dispersity of the polymers were established. Using PS homopolymer as a macro-initiator, block copolymers of PS-*b*-PBA were prepared. This chapter describes, for the first time, the analysis of PS-*b*-PBA block copolymers prepared *via* RITP using advanced analytical methods (SEC, *in situ* ¹H NMR and HPLC).

¹H NMR of the samples was used to determine the copolymer composition, while SEC and HPLC were used to confirm the formation of block copolymers.

4.2 Experimental section

4.2.1 Chemicals

Styrene ($\geq 99\%$ Sigma-Aldrich) was washed three times with an aqueous solution of 0.3 M sodium hydroxide and then three times with distilled de-ionised water. After the monomer has been washed, a drying agent (anhydrous magnesium sulphate) is added in order to remove any residual water. The dried monomer was distilled under reduced pressure at 45 °C and stored in a refrigerator at – 5 °C. The same procedure was used to distil n-butyl acrylate ($\geq 99\%$ Sigma-Aldrich). Azobis(isobutyronitrile) (AIBN, Riedel de Haën) was recrystallised from methanol, dried under vacuum and stored in a refrigerator at – 5 °C. Deuterated chloroform (CDCl_3 , Sigma-Aldrich 99%), deuterated benzene (C_6D_6 , Sigma-Aldrich 99%) and iodine (I_2 , ACROS Organics) were used as received.

4.2.2 Homopolymerisation of styrene and n-butyl acrylate

The homopolymerisation of styrene was carried out by adding styrene (4.00 g, 3.84×10^{-2} mol), toluene (4.00g, 4.34×10^{-2} mol), AIBN (63.6 mg, 3.88×10^{-4} mol) and iodine (51.8 mg, 2.04×10^{-4} mol) into a Schlenk flask, together with a magnetic stirrer bar. The Schlenk flask was then degassed by three successive freeze-pump-thaw cycles and back filled with UHP argon gas. The flask was then submerged in silicone oil heated to 70 °C and the reaction was run for 24 hours in the dark. After the reaction had run for 24 hours, it was stopped by placing the flask on ice. Finally, the polymer was precipitated in cold methanol and left to dry overnight in a vacuum oven.

In a typical homopolymerisation reaction involving n-butyl acrylate (4.00 g, 3.12×10^{-2} mol), toluene (4.00g, 4.34×10^{-2} mol), AIBN (67.1 mg, 4.08×10^{-4} mol) and iodine (54.6 mg, 2.15×10^{-4} mol) were added to a Schlenk flask. Due to the difficulty in precipitating poly(n-butyl acrylate), the polymer was placed in a disposable aluminium tray and dried in a vacuum oven overnight. In addition to the abovementioned experiments, the homopolymerisations of styrene and n-butyl acrylate were performed using *in situ* ^1H NMR. In the case of styrene polymerisation, styrene (2.00 g, 19.2×10^{-2} mol), AIBN (31.8 mg, 1.94×10^{-4} mol) and iodine (25.9 mg, 1.02×10^{-4} mol) were mixed in a glass vial until all reagents were completely dissolved. A fraction (0.15 g) of this stock solution was then inserted into the J Young NMR tube together with 0.15 g of benzene- d_6 .

The final step in the preparation of the sample was to degas the NMR tube by three successive freeze-thaw pump cycles and then fill it with UHP argon gas. A similar procedure was used for n-butyl acrylate homopolymerisation *via in situ* ^1H NMR.

When running the *in situ* ^1H NMR, a pre-polymerisation spectrum was taken at 25 °C to use as a reference. The NMR tube was then removed from the NMR magnet and the temperature of the magnet was elevated to 70 °C. Once the temperature had stabilised, the NMR tube was inserted. On average it took between 3–4 minutes to shim the magnet at the elevated temperature and record the first spectrum. For the subsequent spectra, 15 scans were taken every 15 minutes for 24 hours with a pulse width of 3 μs (40°) and a 4 second acquisition time.

ACD Labs 10.0 ^1H NMR processor[®] was used to process the NMR data. For each spectrum that was processed, automatic phase correction was done followed by manual baseline correction and integration.

4.2.3 Block copolymerisation of polystyrene-*b*-poly(*n*-butyl acrylate)

For the block copolymerisation reaction, it was essential that the precipitated PS-I was dried completely for use as a macro-initiator, in order to exclude any residual monomer. In a typical copolymerisation reaction, PS-I (1.0 g, 2.78×10^{-5} mol) was mixed with n-butyl acrylate (1.0 g, 8.91×10^{-3} mol), AIBN (1.37 mg, 8.33×10^{-6} mol) and toluene (2.0 g, 2.17×10^{-2} mol) in a Schlenk flask. The flask was degassed by three successive freeze-pump-thaw cycles and then back filled with UHP argon gas. The flask was then submerged in silicone oil heated to 70°C and the reaction was run for 24 hours in the dark. The resultant copolymer was precipitated in cold methanol and left to dry in a vacuum oven overnight.

The block copolymerisation of PS-*b*-PBA was also followed *via in situ* ^1H NMR. In a typical block copolymerisation reaction, PS-I (1.0 g, 5.56×10^{-4} mol) was mixed with n-butyl acrylate (1.0 g, 7.80×10^{-3} mol), AIBN (41.1 mg, 2.5×10^{-4} mol) and toluene (2.0 g, 2.17×10^{-2} mol) in a Schlenk flask. ACD Labs 10.0 ^1H NMR processor[®] was used to process the NMR data. For the array of spectra, automatic phase correction was used. Manual baseline correction and integration were performed on each individual spectrum from the array.

4.3 Characterisation of polymers

4.3.1 SEC analysis

An SEC instrument equipped with a Waters 717plus Autosampler, Waters 600E system controller and a Waters 610 fluid unit were used to perform SEC analyses. A Waters 2414 differential refractometer was used for detection. Two PLgel 5 μm Mixed-C columns and a PLgel 5 μm guard column were used. The oven temperature was maintained at 30 °C and 100 μL of 2mg/mL sample was injected into the column set. THF (HPLC grade, BHT stabilised) was used as the eluent for the analyses at a flow rate of 1 mL/min. Narrow polystyrene standards with molar masses ranging from 800–2 $\times 10^6$ g.mol⁻¹ were used to calibrate the instrument. Data obtained from SEC is reported as polystyrene equivalents.

4.3.2 NMR analysis

A Varian Unity INOVA 400 MHz spectrometer was used to record all ¹H NMR spectra. Deuterated chloroform (CDCl₃) was used to dissolve polymer samples (crude and precipitated), while *in situ* ¹H NMR experiments were run in deuterated benzene (C₆D₆).

4.3.3 HPLC analysis

For the HPLC analyses performed in this study, an Agilent 1200 series (Agilent Technologies, Boblingen, Germany) comprising an auto sampler, vacuum degasser, quaternary pump, column oven, variable wavelength UV detector and Agilent 1260 infinity evaporative light scattering detector (ELSD) was used. The data was recorded and processed using WinGPC Unity (version 7). The separation was carried out using a Macherey-Nagel Nucleosil Si 300 Å column (250 x 4.6 mm) with 5 μm particle size. The column temperature was kept at 25 °C. The solvents used were heptane and DCM with 1.2% methanol (HPLC grade). Samples were prepared in DCM to have a concentration of 1 mg/mL. These samples were injected with an injection volume of 10 μL and a flow rate of 0.5 mL/min was used.

4.3.4 Two-dimensional liquid chromatography

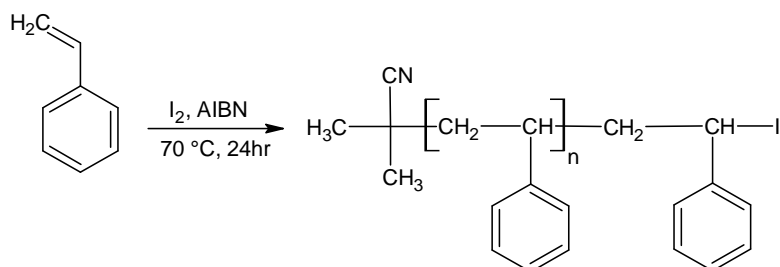
In two-dimensional liquid chromatography (2D-LC), the first dimension separated according to chemical composition on a silica column, whilst the second dimension

separated according to molar mass. Samples were prepared in DCM with a concentration of 5 mg/mL and 50 μ L was injected into the first dimension column at a flow rate of 0.02 mL/min. Sample fractions from the first dimension were injected into the second dimension column *via* an electronically controlled eight port transfer valve (VICI Valco instruments, Texas, USA) consisting of two 50 μ L storage loops. The apparatus used in the second dimension consisted of an Agilent 1200 isocratic pump and a 50 mm x 20 mm PSS Linear M 5 μ m styrene-divinylbenzene (SDV) column. THF was the solvent used for analyses in the second dimension, with a flow rate of 3 mL/min. Detection in the second dimension was done using an ELSD detector. The nebuliser temperature was set to 90 $^{\circ}$ C and nitrogen gas was used as the carrier gas in the ELSD. The data was recorded and processed using WinGPC Unity (version 7).

4.4 Results and discussion

4.4.1 Homopolymerisation of styrene

The polymerisation of styrene *via* RITP requires monomer, AIBN, molecular iodine and solvent. The resultant polymers were expected to contain an initiator derived α -chain end and an iodinated ω -chain end (Scheme 4.1).



Scheme 4.1: Basic representation of the homopolymerisation of styrene *via* RITP.

In order to synthesise a block copolymer *via* RITP, PS-I must first be prepared to use as a macro-initiator. Several styrene homopolymerisation reactions were carried out to establish the effect of molar mass and [initiator]/[iodine] ratio. At high monomer conversion, the functionality of polymers synthesised by LRP decreases.^{8,9}

It was, therefore, important to keep the conversion of PS-I relatively low in order to maintain suitable end group functionality.^{2,10} In addition to this, the ratio of [initiator]/[transfer agent] must be kept as low as possible in order to decrease the amount of dead chains.¹¹

4.4.2 Characterisation of polystyrene

The polymerisation reactions were run for 24 hours, after which the reactions were stopped by placing the Schlenk flasks on ice. A small amount of crude sample was then extracted from each reaction and analysed by ¹H NMR. Thereafter, the remaining crude samples were precipitated in cold methanol. A typical example of a ¹H NMR spectrum of a crude PS sample is shown in Figure 4.1. The signals that correspond to the cyanoisopropyl protons (**a** in Figure 4.1) that derive from the radical initiator are observed at 0.8 – 1.1 ppm.

The CH₂ protons (**b** in Figure 4.1) of the polymer backbone give rise to a signal at 1.2 – 1.5 ppm. The signal of the CH protons (**c** in Figure 4.1) of the polymer backbone is observed at 1.6 – 1.9 ppm. The signals at 6.2 – 7.4 ppm are attributed to the aromatic protons (**d** in Figure 4.1) of PS. The signal at 4.4 – 4.7 ppm corresponds to that of the methine proton (-CH-) (**e** in Figure 4.1) adjacent to the iodinated chain end. Using the ¹H NMR spectrum of a crude PS sample, it was possible to calculate the molar mass of the samples. First, the monomer conversion was calculated using Equation 4.1

$$X_{mon} = \left(1 - \frac{\int CH_2}{\int C_6H_5} \right) \times 100 \quad (4.1)$$

where $\int CH_2$ is the integral of the vinylic protons of residual styrene (5.1 – 5.7 ppm) and $\int C_6H_5$ is the integral of the aromatic protons of PS.¹² Once the conversion had been calculated, the molar mass of the polymer could be determined using Equation 4.2

$$M_{n, calc} = \frac{(m_{mon} \times X_{mon})}{(2 \times n_{iodine})} + M_{chain\ ends} \quad (4.2)$$

where m_{mon} is the mass of the monomer, X_{mon} is the monomer conversion determined from ¹H NMR, n_{iodine} is the number of moles of iodine and $M_{chain\ ends}$ is the combined molar mass of the cyanoisopropyl and iodinated chain ends (195 g.mol⁻¹).^{3,6,13}

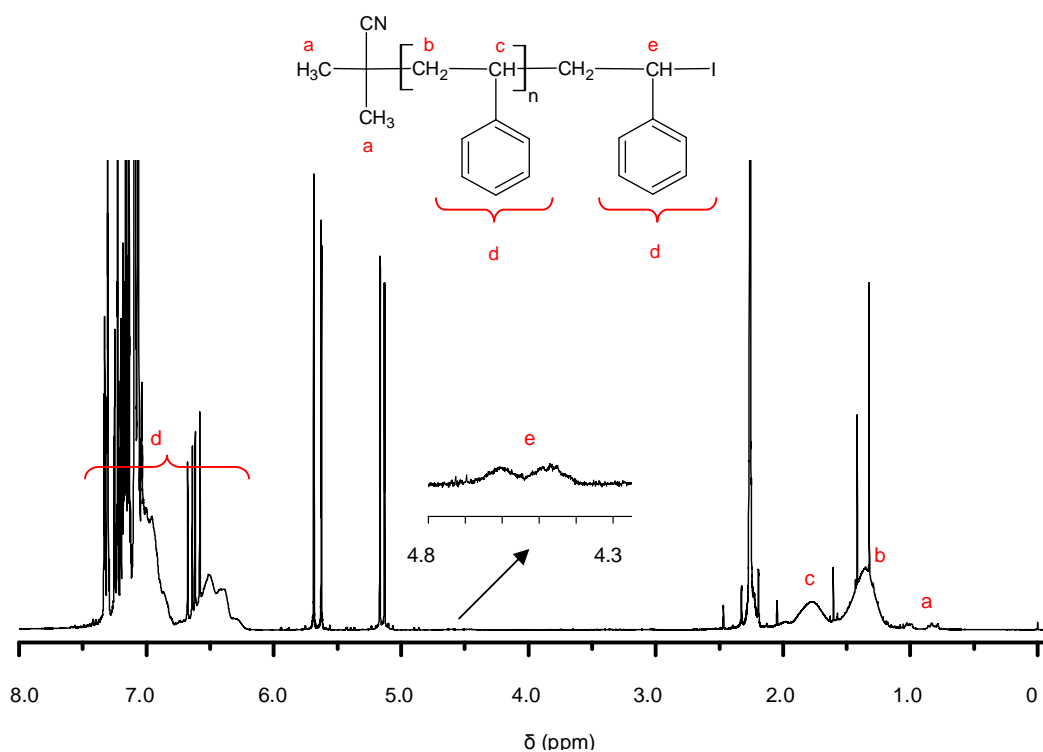


Figure 4.1: Typical ^1H NMR spectrum in CDCl_3 of a crude sample of PS (run 1a Table 4.1) prepared *via* RITP for 24 hours at 70°C .

The results obtained from the ^1H NMR data are shown in Table 4.1. From Table 4.1 it can be seen that the conversion generally only reaches about 60%. An increase in the [initiator]/[iodine] ratio leads to a slight increase in the monomer conversion as well as the dispersity. This trend of improved conversion has been reported in literature for PS synthesised by RITP.⁶ The dispersity of the polymers is in an acceptable range for PS synthesised by iodine mediated polymerisation.^{1,2,6,7,14} Figure 4.2 shows a plot of conversion *versus* time for PS (run 1b Table 4.1) synthesised *via* RITP. The plot shows the inhibition period (~ 400 minutes) where monomer conversion is insignificant.

This inhibition period is typical of RITP of styrene at 70°C .^{6,7} After the inhibition period, the polymerisation period commences. It is evident that the monomer conversion increases linearly with time up to approximately 60% monomer conversion, at which point the rate of monomer conversion drops slightly.

Table 4.1: Results of styrene polymerisation via RITP for 24 hours at 70 °C.

Run	[AIBN]/[I ₂]	M _{n, target} (g.mol ⁻¹)	Conv (%) ^a	M _{n, calc} (g.mol ⁻¹) ^b	M _{n, SEC} (g.mol ⁻¹) ^c	\bar{D}	F ^{iodine} ^d
1a	1.7	3000	58	1800	1600	1.47	89
1b*	1.7	3000	65	1900	1700	1.42	86
2	1.7	10000	63	6300	6000	1.55	89
3	1.7	30000	56	16800	16600	1.63	88
4	1.9	3000	63	1900	1800	1.51	85
5	1.9	30000	64	19200	18900	1.65	83

* Run using *in situ* ¹H NMR

^a Determined by ¹H NMR of crude sample in CDCl₃ by $X_{\text{mon}} = (1 - ([\text{CH}_2]/[\text{C}_6\text{H}_5])) \times 100$ where $[\text{CH}_2]$ is the integral of the vinylic protons of residual styrene at 5.1 – 5.7 ppm, and $[\text{C}_6\text{H}_5]$ is the integral of the aromatic protons PS.

^b Calculated by $M_{n, \text{calc}} = ((m_{\text{mon}} \times X_{\text{mon}})/(2 \times n_{\text{iodine}})) + M_{\text{chain ends}}$.

^c Calibrated using PS standards.

^d Calculated by $F^{\text{iodine}} = \int(-\text{CH}-) / (\int(-\text{C}(\text{CN})(\text{CH}_3)_2-)/6)$

A plot of M_n versus conversion, for PS (run 2 Table 4.1) synthesised via RITP, is shown in Figure 4.3. The plot shows that M_n increased linearly with conversion, which implies that the homopolymerisation proceeded in a controlled manner. The iodine functionality (F^{iodine}) of the PS-I homopolymer can be determined by using the ¹H NMR spectrum. The integrals of the cyanoisopropyl end group (**a** in Figure 4.1) and the integral of the methine proton (**e** in Figure 4.1) adjacent to the iodine end group were substituted into Equation 4.3 to calculate the functionality.^{2,5,10,13}

$$F^{\text{iodine}} = \frac{\int(-\text{CH}-)}{\int(-\text{C}(\text{CN})(\text{CH}_3)_2-)/6} \quad (4.3)$$

Table 4.1 shows that the iodine functionality of the PS-I homopolymers was typically greater than 85%. The best functionality was observed when an [initiator]/[iodine] ratio of 1.7 was used. At this [initiator]/[iodine] ratio, the iodine functionality of PS-I was sufficiently high to use it as a macro-initiator in the synthesis of PS-*b*-PBA. Molar mass distributions from SEC of two PS homopolymers (run 4 and 5 Table 4.1) are shown in Figure 4.4. The distributions are unimodal and shift towards higher molar masses, with evidence of low molar mass tailing.

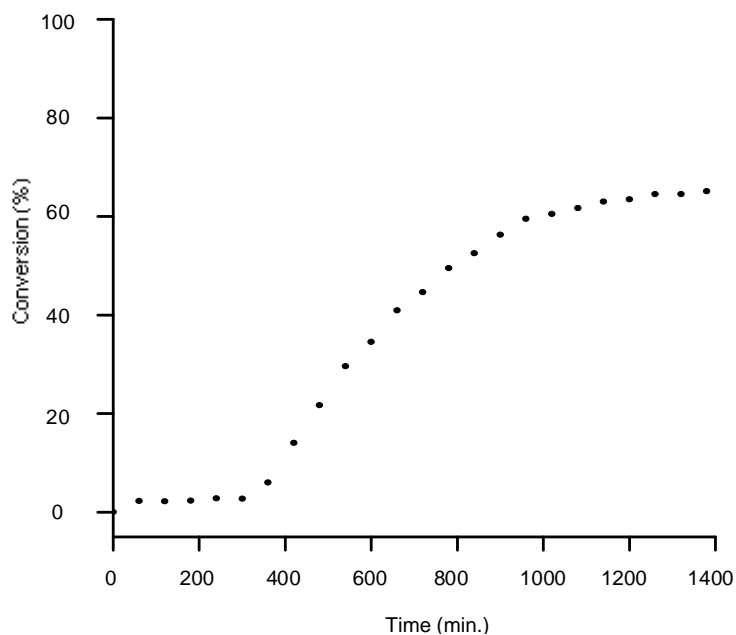


Figure 4.2: Plot of conversion *versus* time for PS (run 1b Table 4.1) synthesised *via* RITP at 70 °C for 24 hours.

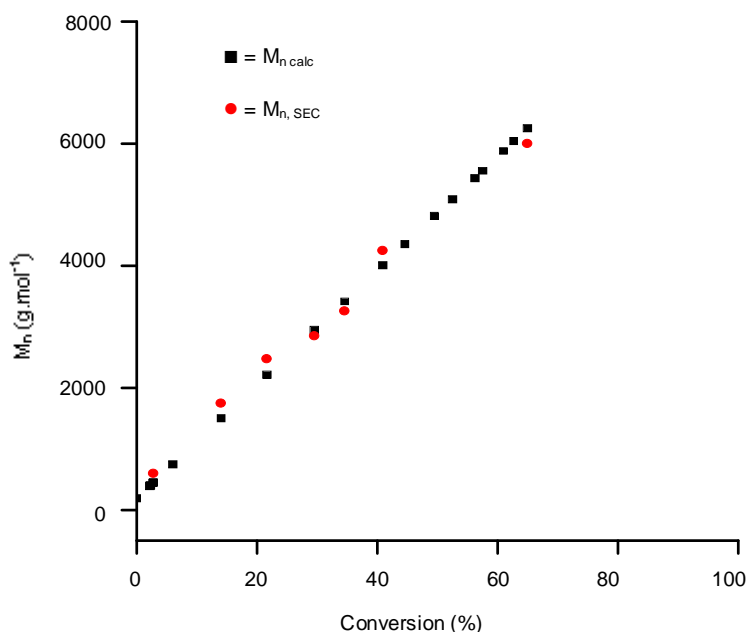


Figure 4.3: Plot of M_n *versus* conversion for PS (run 2 Table 4.1) synthesised *via* RITP at 70 °C for 24 hours: (■) = $M_{n, calc}$ and (●) = $M_{n, SEC}$.

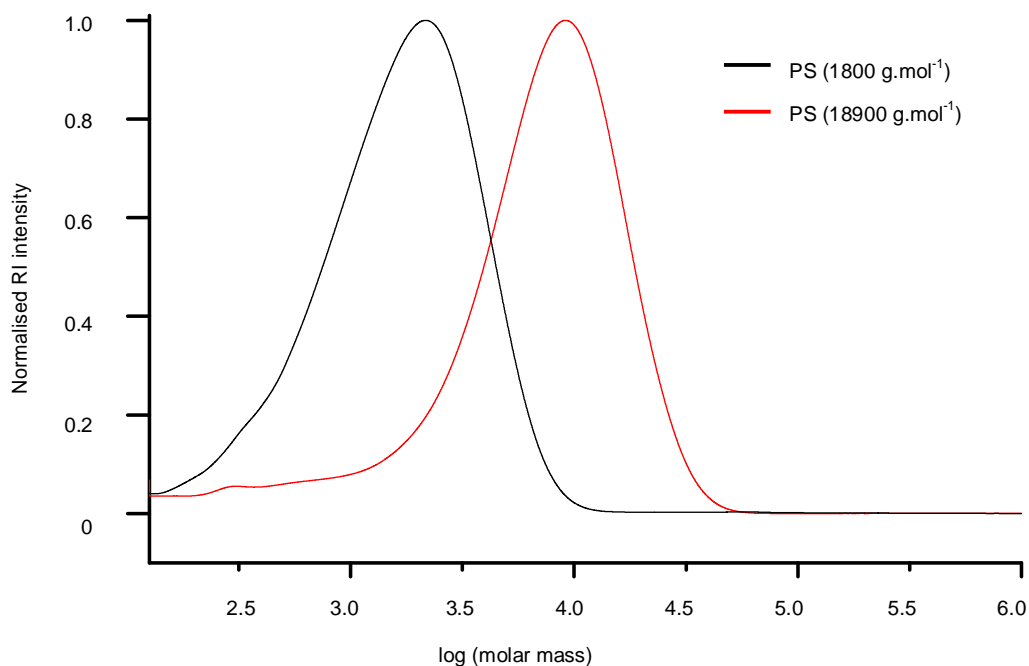
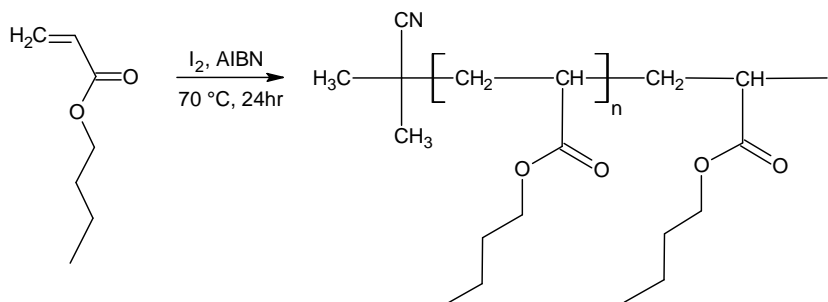


Figure 4.4: Molar mass distributions from SEC (RI traces) of PS (run 4 and 5 Table 4.1) synthesised *via* RITP for 24 hours at 70 °C.

4.4.3 Homopolymerisation of *n*-butyl acrylate

Poly (*n*-butyl acrylate) PBA was synthesised in a similar way to the method used for PS synthesis. The polymers were characterised using SEC to determine molar mass and ^1H NMR was used to determine conversion. A basic representation of the polymerisation reaction of *n*-butyl acrylate *via* RITP is shown in Scheme 4.2.



Scheme 4.2: Basic representation of the homopolymerisation of *n*-butyl acrylate *via* RITP.

4.4.4 Characterisation of poly(*n*-butyl acrylate)

A ^1H NMR spectrum of *n*-butyl acrylate polymerised by RITP is shown in Figure 4.5 below. The cyanoisopropyl signal (**a** in Figure 4.5) could not be seen in the ^1H NMR spectrum of PBA, as the signal overlapped with broad polymer signals. The signal at 0.9 ppm (**e** in Figure 4.5) corresponds to the methyl protons of the acrylate moiety. At 1.6 ppm (**b** in Figure 4.5) there is a signal that is attributed to the CH_2 protons. The signal at 1.9 ppm (**c** in Figure 4.5) corresponds to the CH protons of the polymer backbone. The CH_2 protons of the backbone give rise to a signal at 2.3 ppm (**f** in Figure 4.5). The signal at 4.0 ppm (**d** in Figure 4.5) is attributed to $-\text{O}-\text{CH}_2-$ protons. The methine proton gives rise to a signal at 4.3 ppm (**g** in Figure 4.5). As was the case with PS, ^1H NMR spectra of crude samples of PBA were used to calculate the molar masses of the samples. The conversion was calculated using Equation 4.4

$$X_{\text{mon}} = \left(1 - \frac{\int \text{CH}_2}{\int \text{CH}_3} \right) \times 100 \quad (4.4)$$

where $\int \text{CH}_2$ is the integral of the vinyl protons of residual *n*-butyl acrylate at 5.8–6.4 ppm and $\int \text{CH}_3$ is the integral of the methyl protons of the butyl acrylate moiety of the homopolymer at 0.9 ppm. Equation 4.2 was used to calculate the molar mass of the polymers. The results of these calculations are shown in Table 4.2 below.

Table 4.2: Results of *n*-butyl acrylate polymerised via RITP for 24 hours at 70 °C.

Run	[AIBN]/[I ₂]	M _{n, target} (g.mol ⁻¹)	Conv (%) ^a	M _{n, calc} (g.mol ⁻¹) ^b	M _{n, SEC} (g.mol ⁻¹) ^c	<i>D</i>
1	1.7	3000	98	2900	3400	1.95
2a	1.7	9500	97	9200	10100	1.99
2b*	1.7	9500	99	9400	10100	2.01
3	1.9	3000	98	2900	3400	1.97
4	1.9	9500	98	9300	10300	1.98

* Run using *in situ* ^1H NMR.

^a Determined by ^1H NMR of crude sample in CDCl_3 by $X_{\text{mon}} = (1 - (\int \text{CH}_2 / \int \text{CH}_3)) \times 100$ where $\int \text{CH}_2$ is the integral of the vinyl protons of residual *n*-butyl acrylate at 5.8–6.4 ppm and $\int \text{C}_6\text{H}_5$ is the integral of the methyl protons of the butyl acrylate moiety at 0.9 ppm.

^b Calculated by $M_{n, \text{calc}} = ((m_{\text{mon}} \times X_{\text{mon}}) / (2 \times n_{\text{iodine}})) + M_{\text{chain ends}}$.

^c Calibrated using PS standards.

As seen in Table 4.2, almost all monomer was consumed to form PBA. Lacroix-Desmazes *et al.*³ reported a relatively low degenerative chain transfer constant (k_{ex}) for methacrylates, which gives rise to dispersity in the region of 1.7–2.0.^{15,16} Comparably, the dispersity of the PBA samples prepared in this study was in a typical range for acrylates synthesised *via* RITP.^{1,3,17}

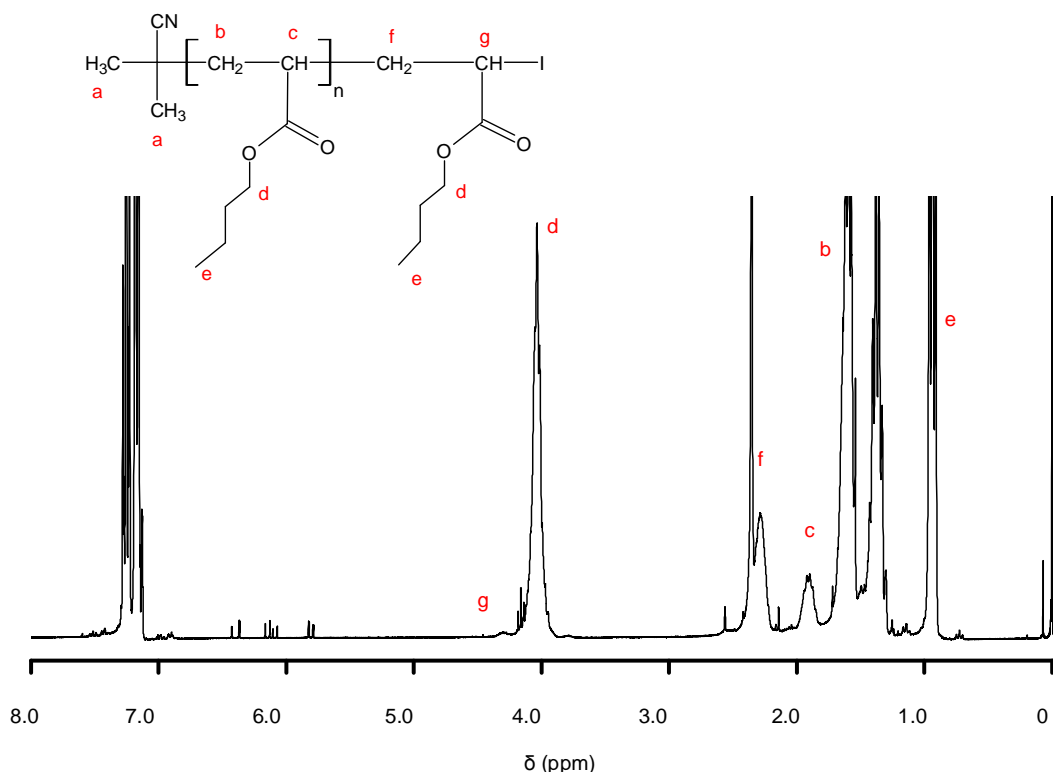


Figure 4.5: Typical ¹H NMR spectrum in CDCl₃ of a crude sample of PBA (run 1 Table 4.2) synthesised *via* RITP for 24 hours at 70 °C.

Figure 4.6 shows a plot of conversion *versus* time for PBA synthesised *via* RITP. The plot shows the inhibition period that is customary to RITP. Unlike PS, the inhibition period of n-butyl acrylate was quite lengthy (~900 minutes). However, once the polymerisation had commenced, the polymerisation went to near completion fairly rapidly (~350 minutes). Typical of a LRP technique, a linear increase of M_n with conversion (Figure 4.7) shows that the homopolymerisation of n-butyl acrylate was controlled. The slightly higher $M_{n,SEC}$ molar masses seen in Figure 4.7 were most likely due to the fact that the SEC instrument was calibrated using PS standards.

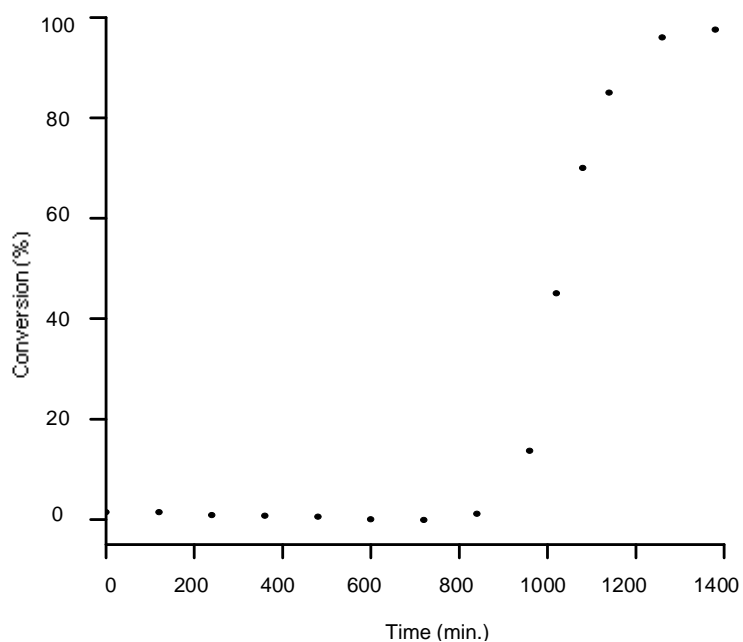


Figure 4.6: Plot of conversion versus time for PBA (run 2b Table 4.2) synthesised via RITP at 70 °C for 24 hours.

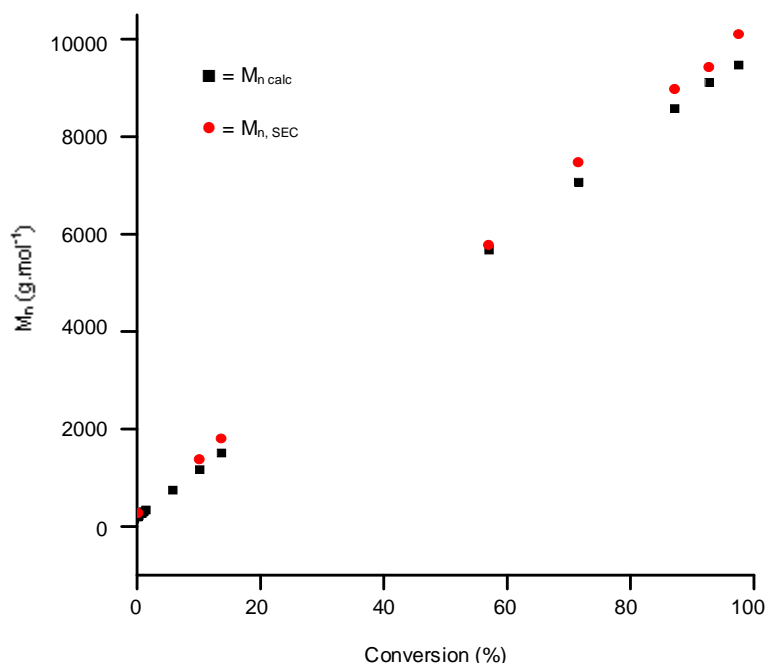


Figure 4.7: Plot of M_n versus conversion for PBA (run 2a Table 4.2) synthesised via RITP at 70 °C for 24 hours: (■) = $M_{n,calc}$ and (●) = $M_{n,SEC}$.

Figure 4.8 shows the molar mass distributions from SEC of two PBA homopolymers (run 3 and 4 Table 4.2). It is evident that there are two unimodal distributions that shift towards higher molar masses, with some tailing at lower molar masses.

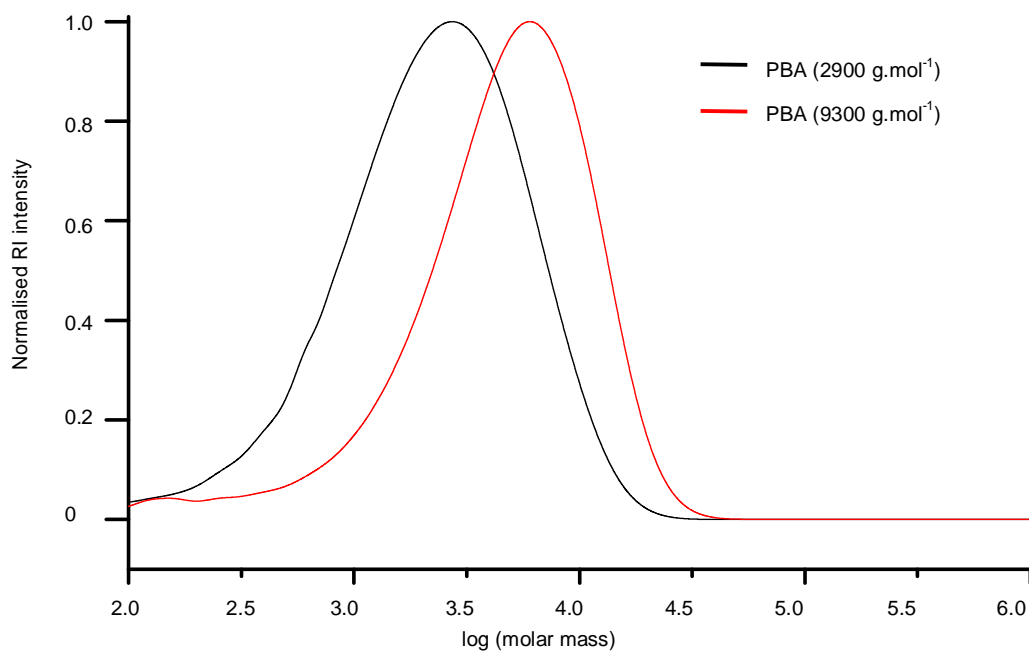


Figure 4.8: Molar mass distributions from SEC (RI traces) of PBA (run 3 and 4 Table 4.2) synthesised via RITP for 24 hours at 70 °C.

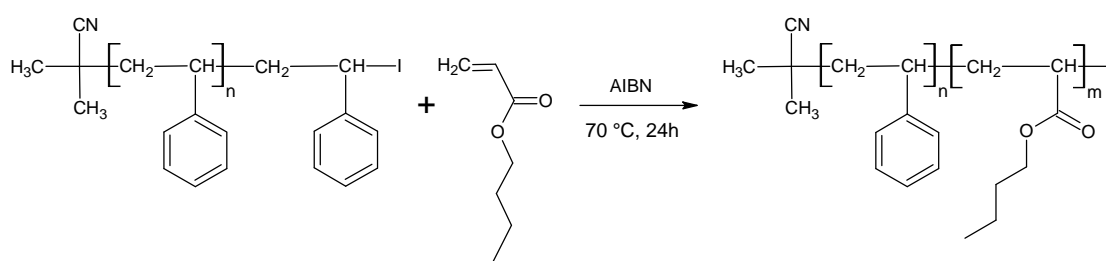
4.4.5 Synthesis of polystyrene-*b*-poly(*n*-butyl acrylate) block copolymers

There are a few factors to consider before preparing block copolymers. These factors include:¹

- the stability of the macro-radical
- the reactivity ratios of the respective monomers
- the stability of the dormant chains

The cross-propagation rate constant between PS radicals and *n*-butyl acrylate is fairly low ($k_{p,S}=498 \text{ M}^{-1} \cdot \text{s}^{-1}$ at 70 °C¹⁸ and $r_S=0.70$,¹⁹ giving $k_{p,S,BA}=711 \text{ M}^{-1} \cdot \text{s}^{-1}$).

This low cross-propagation rate constant results in the homopolymerisation of n-butyl acrylate ($k_{p,BA}=40400 \text{ M}^{-1} \cdot \text{s}^{-1}$ at $70 \text{ }^\circ\text{C}$ ¹⁸ and $r_{BA}=0.16$,¹⁹ giving $k_{p,BA,S}=252500 \text{ M}^{-1} \cdot \text{s}^{-1}$) being favoured over the block copolymerisation reaction. Therefore, the best strategy for preparing well controlled PS-*b*-PBA block copolymers is to add multiple injections of n-butyl acrylate to a low molar mass PS-I macro-initiator.¹ The block copolymerisation in this study was performed using PS-I homopolymer as a macro-initiator, followed by the addition of n-butyl acrylate in multiple injections. A basic representation of the block copolymerisation of PS-*b*-PBA *via* RITP is shown in Scheme 4.3.



Scheme 4.3: Basic representation of the block copolymerisation of PS-*b*-PBA *via* RITP.

4.4.6 Characterisation of polystyrene-*b*-poly(*n*-butyl acrylate) block copolymers

A typical ¹H NMR spectrum of PS-*b*-PBA is shown in Figure 4.9. The signal at 0.9 ppm is attributed to the methyl protons of the PBA segment. The signal at 1.4 ppm corresponds to the -CH₂- protons (**h** in Figure 4.9) of the PBA segment. The signal at 1.6 ppm is attributed to the -CH₂- protons (**g** in Figure 4.9) of the PBA segment. At 4.1 ppm (**f** in Figure 4.9) there is a signal attributed to the -OCH₂- protons. Aromatic proton signals at 6.4–7.3 ppm (**c** in Figure 4.9) belong to the PS segment of the copolymer. The molar mass of the block copolymers were calculated using Equation 4.5

$$M_{n,calc} = \frac{(m_{mon} \times X_{mon})}{n_{macro}} + M_{macro} \quad (4.5)$$

where m_{mon} is the mass of monomer used for the second block (n-butyl acrylate), X_{mon} is the conversion of n-butyl acrylate, n_{macro} is the number of moles of the macro-initiator

(PS-I) and M_{macro} is the molar mass of the macro-initiator.^{2,4,20} The results of the block copolymerisation reactions are shown in Table 4.3.

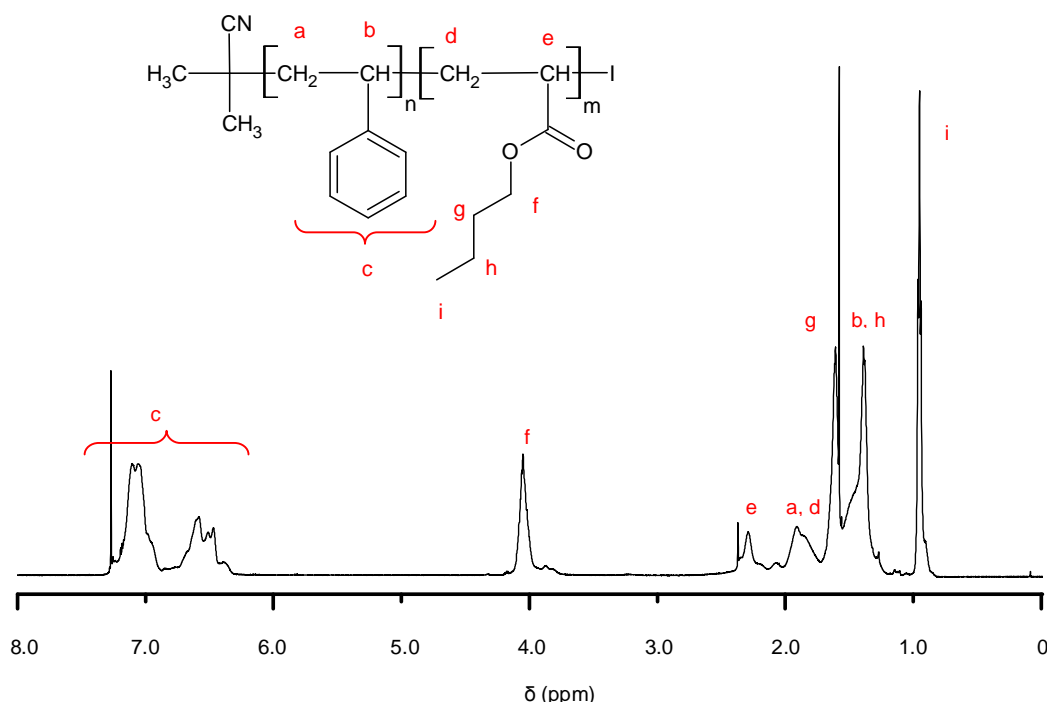


Figure 4.9: Typical ^1H NMR spectrum in CDCl_3 of PS-*b*-PBA (run 2) synthesised *via* RITP for 24 hours at 70 °C.

Table 4.3: Results of block copolymerisation of PS-*b*-PBA *via* RITP at 70 °C for 24 hours.

Run	$M_{n, \text{SEC, PS}}$ ($\text{g}\cdot\text{mol}^{-1}$) ^a	\bar{D} (PS)	Conv (%) ^b	$M_{n, \text{calc}}$ ($\text{g}\cdot\text{mol}^{-1}$) ^c	$M_{n, \text{SEC, PS-}b\text{-PBA}}$ ($\text{g}\cdot\text{mol}^{-1}$) ^a	\bar{D} (PS- <i>b</i> -PBA)	%PS : %PBA (SEC) ^d
1*	1600	1.67	81	2700	2900	1.46	57:43
2	5700	1.72	97	6800	7000	1.48	81:19
3	5700	1.72	70	9900	9600	1.63	59:41
4	5700	1.72	85	10900	11200	1.56	51:49

* Run using *in situ* ^1H NMR.

^a Calibrated using PS standards.

^b Determined from ^1H NMR of crude sample in CDCl_3 .

^c Calculated by $M_{n, \text{calc}} = (m_{\text{mon}} \times X_{\text{mon}}) / n_{\text{macro}} + M_{\text{macro}}$

^d Calculated using $\%PS = (M_{n, \text{PS}} / M_{n, \text{block}}) \times 100$

In run 1 (Table 4.3), one shot of n-butyl acrylate was added to a low molar mass PS-I macro-initiator and the final block copolymer showed a decrease in dispersity. In Run 2 (Table 4.3), three shots of n-butyl acrylate were added over the course of 6 hours. In run 3 (Table 4.3), the full amount of n-butyl acrylate was added at the start of the reaction. Runs 2 and 3 showed that the block copolymerisation reaction was controlled to almost the same extent, regardless of whether several shots or the full amount were added. This was presumably due to the fact that the PS-I macro-initiator had a fairly low molar mass.

The relative amounts of the respective monomer units incorporated into the block copolymer could be determined in two ways, using either integration from NMR or molar masses determined from SEC. In the first approach, the integrals from the ^1H NMR spectrum of the block copolymer were used in Equation 4.6

$$\%PS = \left(\frac{\int PS_{Ar} / 5}{(\int PS_{Ar} / 5) + (\int PBA_{CH_3} / 3)} \right) \times 100 \quad (4.6)$$

where $\int PS_{Ar}$ is the integral of the aromatic protons (**c** in Figure 4.9) attributed to polystyrene (first block) and $\int PBA_{CH_3}$ is the integral of the methyl protons (**i** in Figure 4.9) of the poly(n-butyl acrylate) segment (second block) of the copolymer. In the second approach, the SEC data obtained for the macro-initiator and that of the block copolymer were used in Equation 4.7

$$\%PS = \left(\frac{M_{n,PS}}{M_{n,block}} \right) \times 100 \quad (4.7)$$

where $M_{n,PS}$ is the molar mass of the first block (PS) as determined by SEC and $M_{n,block}$ is the molar mass of the block copolymer (PS-*b*-PBA) as determined by SEC. Table 4.4 shows a comparison of the results from NMR and SEC respectively. There was a reasonable agreement between the weight percentages determined from NMR and those determined from SEC.

Table 4.4: Comparison of the weight percentages of the monomer units incorporated into the block copolymers prepared *via* RITP.

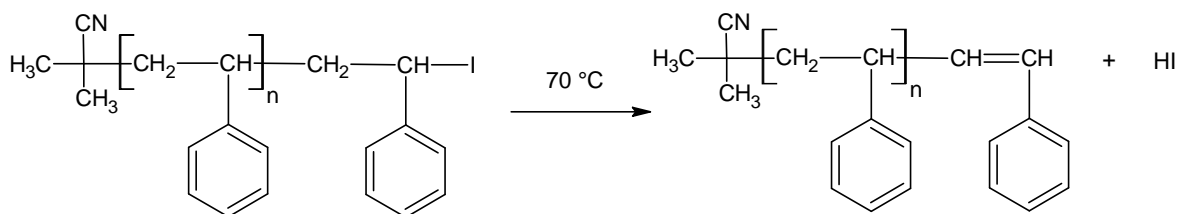
Run	$M_{n, SEC}^{PS-b-PBA}$ ($g \cdot mol^{-1}$) ^a	%PS : % PBA (NMR) ^b	%PS : %PBA (SEC) ^c
1	2900	51:49	57:43
2	7000	79:21	81:19
3	9600	57:43	59:41
4	11200	53:47	51:49

^a Calibrated using PS standards.

^b Calculated by $\%PS = (\int PS_{Ar} / 5) / ((\int PS_{Ar} / 5) + (\int PBA_{CH_3} / 3)) \times 100$

^c Calculated using $\%PS = (M_{n,PS} / M_{n,block}) \times 100$

Figure 4.10 shows an enlarged portion of the *in situ* 1H NMR spectra of PS-*b*-PBA at 4.2–4.9 ppm. This array of spectra shows that the methine proton from PS-I was not present at the end of the block copolymerisation reaction. In fact, the labile iodine end group of PS-I had almost completely disappeared after only 135 minutes. When the PS-I macro-initiator is heated, as is the case during the chain extension reaction, the labile iodine chain ends are liberated in the form of hydrogen iodide (HI) (Scheme 4.4).²¹

**Scheme 4.4: Degradation of PS-I macro-initiator during block copolymerisation.**

This iodine liberation results in a loss of functionality of the macro-initiator to some extent. Nevertheless, a proton signal at ~4.35 ppm (Figure 4.10) was indicative of the incorporation of the *n*-butyl acrylate unit adjacent to the iodine atom into the block copolymer.

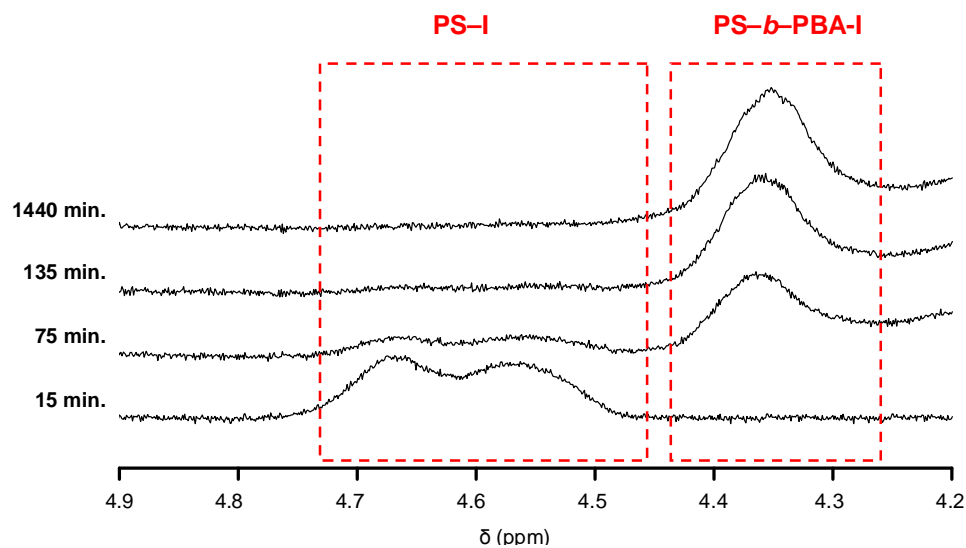


Figure 4.10: Enlarged portion (4.2–4.9 ppm) of the *in situ* ^1H NMR spectra of PS-*b*-PBA (run 1 Table 4.3) synthesised *via* RITP for 24 hours at 70 °C.

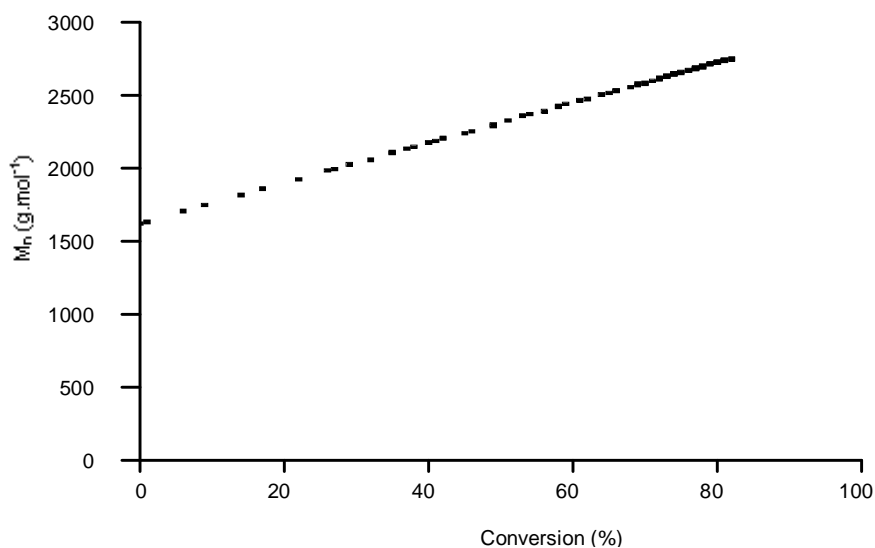


Figure 4.11: Plot of $M_{n, \text{calc}}$ versus conversion for the block copolymerisation of PS-*b*-PBA (run 1 Table 4.3) ($M_{n, \text{SEC}}$ of PS-I = 1600 g.mol^{-1} , $\mathcal{D} = 1.67$ and $M_{n, \text{SEC}}$ of PS-*b*-PBA = 2900 g.mol^{-1} , $\mathcal{D} = 1.46$).

Figure 4.11 shows a plot of $M_{n, calc}$ versus conversion for PS-*b*-PBA (run 1 Table 4.3) synthesised *via* RITP in an *in situ* ^1H NMR experiment. As would be expected, the conversion increases linearly with molar mass, while the dispersity decreased. The molar mass distributions from SEC (RI and UV) of the PS-I macro-initiator and PS-*b*-PBA block copolymer respectively are shown in Figure 4.12. Incidentally, the UV detector was set at 254 nm. There was a clear shift of the PS-I trace in the direction of increasing molar masses, indicating that there was in fact chain extension to form a block copolymer. In addition to this, the RI and UV traces overlapped, indicating that *n*-butyl acrylate was incorporated into the PS chains.

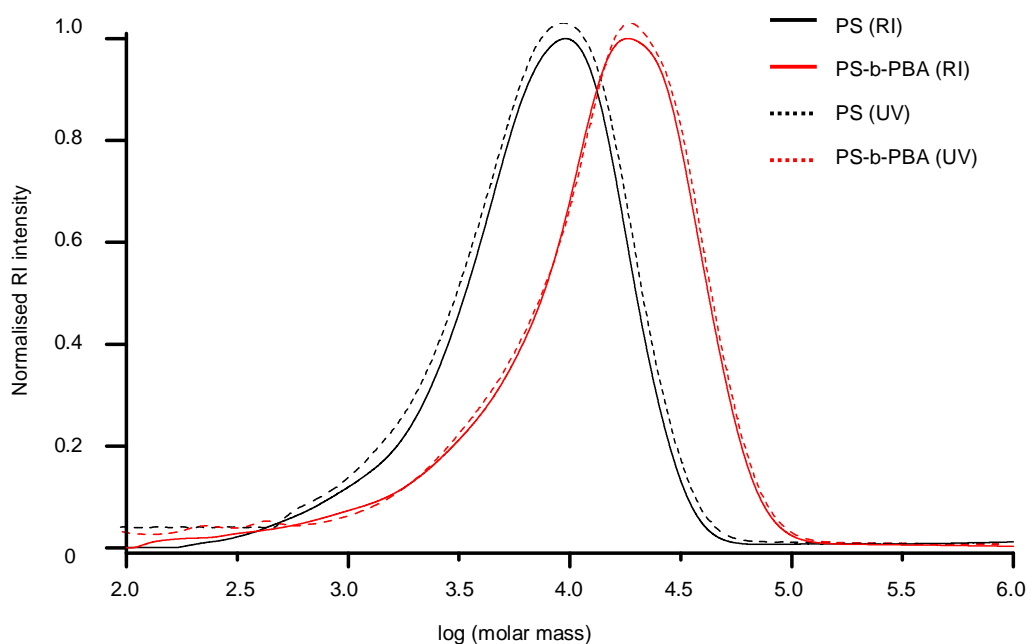


Figure 4.12: Molar mass distributions from SEC (RI and UV) of PS-I (run 4 Table 4.3) and PS-*b*-PBA (run 4 Table 4.3) synthesised *via* RITP for 24 hours at 70 °C.

4.4.7 Analysis of PS-*b*-PBA block copolymers by HPLC

4.4.7.1 Separation of PS-*b*-PBA block copolymers using gradient elution HPLC

Often block copolymers prepared by LRP show evidence of heterogeneity with respect to molar mass and chemical composition.^{22,23} It is therefore plausible for a block copolymer to contain homopolymer, unreacted macro-initiator and copolymer. In order to characterise block copolymers more completely, it is necessary to use more than one analytical technique.^{24,25} For this reason, HPLC analyses were performed to complement the results obtained from ¹H NMR and SEC. It should be emphasised that very little literature can be found regarding HPLC of polymers prepared *via* RITP, and therefore this work is of significant importance to progress the understanding of RITP.

A heptane/DCM binary system was used to achieve a separation of the PS-*b*-PBA block copolymer on a bare silica column. As suggested by Snyder *et al.*,²⁶ a small percentage of methanol was added to DCM to improve the eluting strength of the system. Although the methanol content can improve the eluting strength, the methanol content in the strong solvent should be as low as possible. For the separation of PS-*b*-PBA on a silica column, Sparidans *et al.*²⁷ found that a methanol content of 1.2% in DCM gave optimum separation efficiency. Table 4.5 shows the average molar masses, as determined from SEC, of the polymers used in this gradient HPLC study.

Table 4.5: Polymers synthesised *via* RITP that were used in the HPLC study.

Homopolymer	Abbreviation	$M_{n, SEC}$ ($\text{g}\cdot\text{mol}^{-1}$) ^a	\bar{D}
Polystyrene	PS	5700	1.72
Poly(<i>n</i> -butyl acrylate)	PBA	6100	2.02
Polystyrene- <i>b</i> -poly(<i>n</i> -butyl acrylate)	PS- <i>b</i> -PBA	9600	1.63

^a Calibrated using PS standards.

The linear gradient elution profile used for the separation is shown in Figure 4.13. Figure 4.14 shows the chromatograms of the PS and PBA homopolymers (Table 4.5) respectively, using the heptane/(DCM+1.2% methanol) gradient on a silica column.

The samples were dissolved in DCM and injected into the column that had been preconditioned with 100% heptane. Neither PS nor PBA is soluble in heptane and consequently both homopolymers precipitate and are retained on the column. As the overall solvent composition of DCM+1.2% methanol increases, the homopolymers redissolve and elute accordingly. PS dissolves more readily in DCM and therefore elutes first (~8.2 mL). PBA is soluble in DCM to a lesser extent than PS and consequently elutes at a later stage (~11.4 mL).

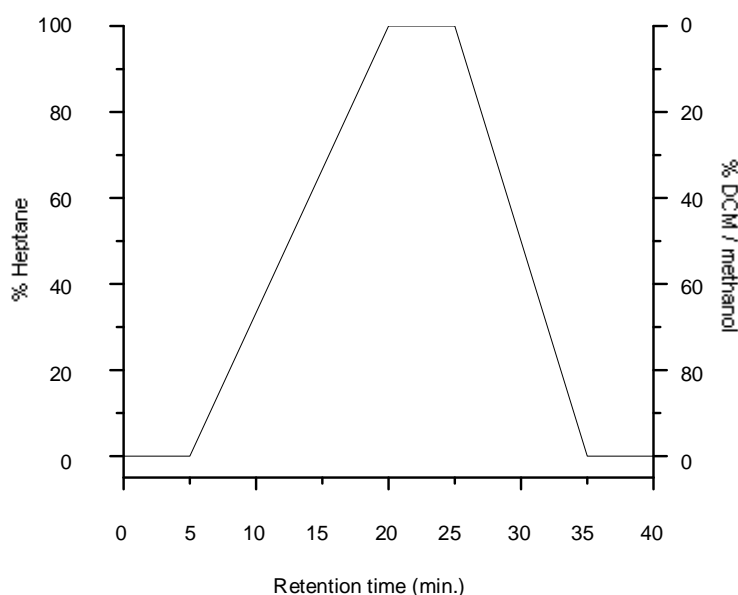


Figure 4.13: Gradient elution profile used to separate PS-*b*-PBA block copolymer (run 3 Table 4.3); stationary phase: Nucleosil silica 300 Å – 5 µm, mobile phase: heptane/(DCM+1.2%methanol).

It is apparent from the chromatograms of the respective homopolymers (Figure 4.14) that their elution volumes are fairly similar. This small difference in elution volume is due to the fact that these two homopolymers have a small difference in polarity.²⁷ The block copolymer was then analysed using the same gradient HPLC conditions. Figure 4.15 shows the chromatogram of the block copolymer. The PS-*b*-PBA block copolymer shows a separation with two signals. Referring to the chromatograms of the homopolymers (Figure 4.14), the signals in the chromatogram of the block copolymer can be assigned.

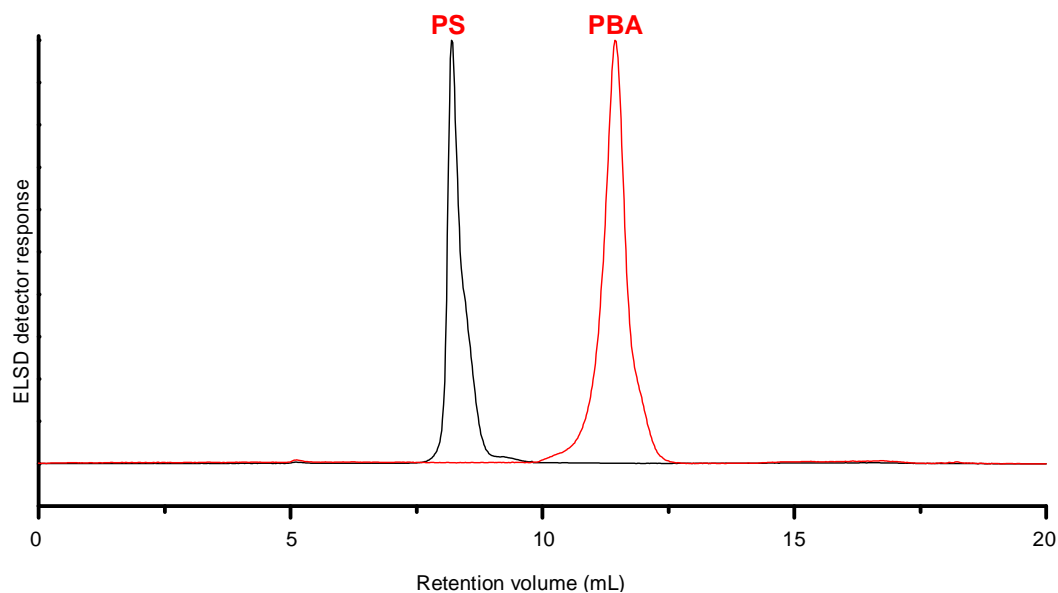


Figure 4.14: HPLC chromatogram of PS and PBA homopolymers respectively (Table 4.5); stationary phase: Nucleosil silica 300 Å – 5 µm, mobile phase: heptane/(DCM+1.2%methanol).

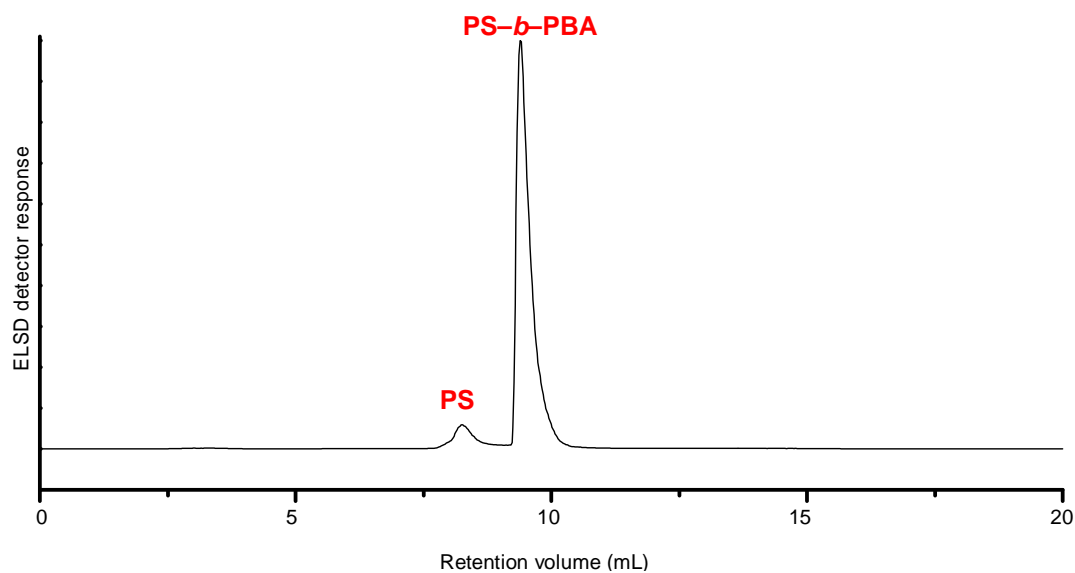


Figure 4.15: Gradient HPLC chromatogram of a PS-*b*-PBA block copolymer (run 3 Table 4.3); stationary phase: Nucleosil silica 300 Å – 5 µm, mobile phase: heptane/(DCM+1.2%methanol).

The first signal corresponds to unreacted PS-I macro-initiator, while the second signal corresponds to the PS-*b*-PBA block copolymer. Polymers synthesised by a LRP technique usually contain less than 10% dead chains.^{28,29} Consequently, a small amount of PS is incapable of participating in the chain extension during block copolymerisation due to the lack of a labile iodine end group. Therefore, a signal corresponding to the PS homopolymer was observed in the HPLC chromatogram of PS-*b*-PBA. The amount of PS was estimated by relating the percentage area of the two peaks. It was found that the PS peak constituted 1.6% of the total peak area, with the other 98.4% corresponding to the PS-*b*-PBA block copolymer.

4.4.7.2 Two-dimensional liquid chromatography of PS-*b*-PBA

In 2D-LC, separation in the first dimension is according to chemical composition, whilst separation in the second dimension is according to molar mass. A drawback associated with 2D-LC is the fact that the sample becomes less concentrated as fractions from the first dimension are injected into the second dimension. As a consequence of this decrease in sample concentration throughout the analysis, more highly concentrated samples must be prepared when running 2D-LC. The concentration of the samples analysed in 2D-LC were increased from 1 mg/mL (first dimension) to 5mg/mL with an injection volume of 50 μ L. Figure 4.16 and Figure 4.17 show the contour plot of the two-dimensional separation of PS-*b*-PBA (run 3 Table 4.3).

In Figure 4.16, the colour distribution is based on a linear scale and therefore the signal attributed to the unreacted PS-I can barely be seen at all. As it was, the signal intensity of the PS-I peak in the first dimension was already quite low. This low intensity was accentuated further in the second dimension as the fractions passed from the first dimension into the second dimension.

However, when the contour plot was set to use a logarithmic scale (Figure 4.17), the signal intensities were increased. The peak attributed to PS-I became visible and there was a clear separation due to chemical composition. The PS precursor had a molar mass of 5700 g/mol, while the PS-*b*-PBA block copolymer had a molar mass of 9600 g/mol. Therefore, the difference in molar mass was too small to see any sort of separation in SEC.

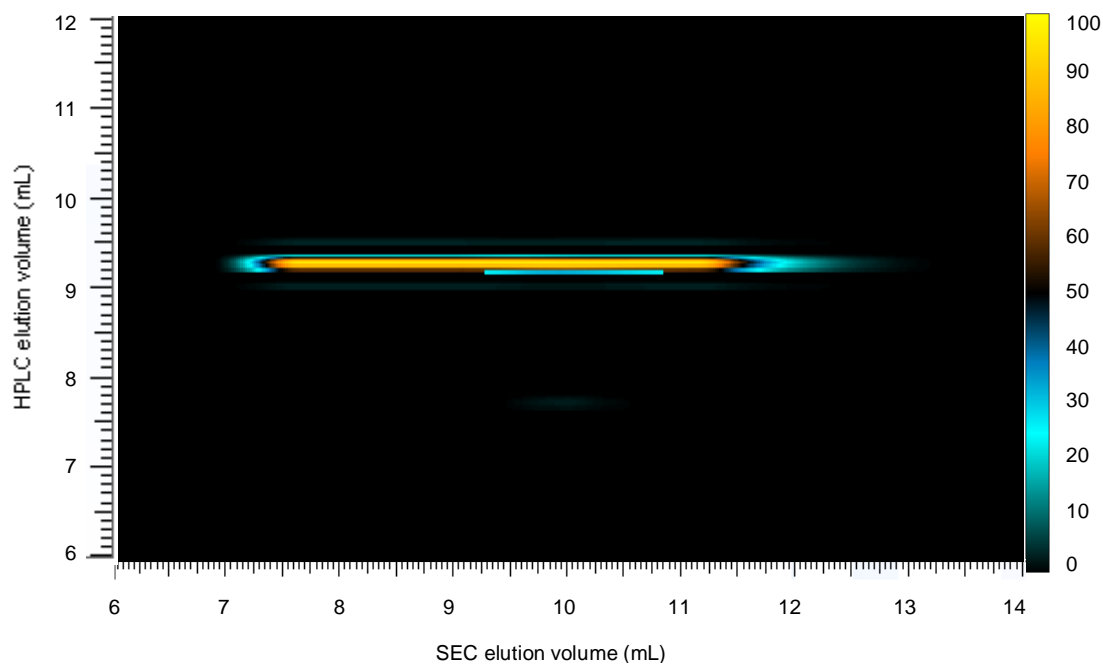


Figure 4.16: Contour plot (linear scale) of the two-dimensional separation of PS-*b*-PBA (run 3 Table 4.3) using a heptane/(DCM+1.2% methanol) gradient.

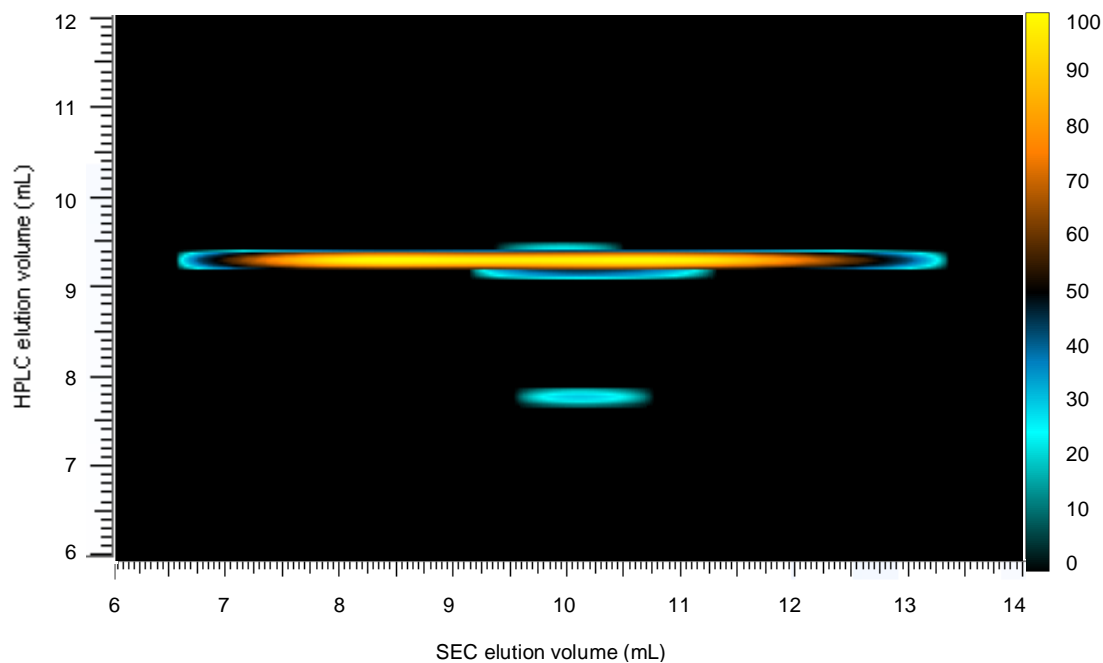


Figure 4.17: Contour plot (logarithmic scale) of the two-dimensional separation of PS-*b*-PBA (run 3 Table 4.3) using a heptane/(DCM+1.2% methanol) gradient.

4.5 Conclusions

RITP was used to prepare polystyrene and poly(n-butyl acrylate). Two [initiator]/[iodine] ratios were used to prepare polystyrene. It was found that the end group functionality of the polystyrene was highest when an [initiator]/[iodine] ratio of 1.7 was used. The two polymers exhibit different reaction kinetics. Polystyrene has a shorter inhibition time than poly(n-butyl acrylate), but the polymerisation time of poly(n-butyl acrylate) is much faster than that of polystyrene. ^1H NMR was used to confirm the structure of the two homopolymers. Polystyrene was used as a macro-initiator to prepare polystyrene-*b*-poly(n-butyl acrylate). The block copolymerisation reaction was followed by *in situ* ^1H NMR. An array of the ^1H NMR spectra showed that the methine proton signal intensity of the macro-initiator decreased quite rapidly. The subsequent methine proton signal of the block copolymer also increased quite rapidly. However, there was a loss of end group functionality when the macro-initiator was heated. The formation of a block copolymer was confirmed by SEC and HPLC. In the molar mass distributions from SEC, the RI and UV signals overlapped, thus indicating that butyl acrylate was incorporated into the polystyrene chains. HPLC analyses were run using a solvent gradient of heptane/(DCM+1.2% methanol). The chromatogram of the block copolymer shows two peaks corresponding to unreacted polystyrene and polystyrene-*b*-poly(n-butyl acrylate). Two-dimensional HPLC confirmed that the separation was based on chemical composition.

References

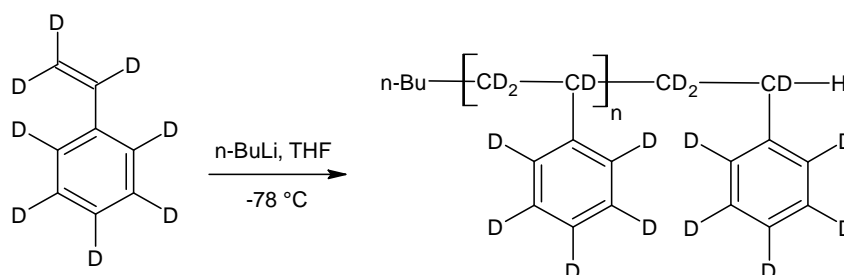
- 1 Enríquez-Medrano, F. J.; Guerrero-Santos, R.; Hernandez-Valdez, M.; Lacroix-Desmazes, P. *Journal of Applied Polymer Science* 2011, 119, 2476–2484.
- 2 Greesh, N.; Sanderson, R.; Hartmann, P. *Journal of Applied Polymer Science* 2012, 126, 1773–1783.
- 3 Lacroix-Desmazes, P.; Severac, R.; Boutevin, B. *Macromolecules* 2005, 38, 6299–6309.
- 4 Patra, B. N.; Rayeroux, D.; Lacroix-Desmazes, P. *Reactive & Functional Polymers* 2010, 70, 408–413.
- 5 Nottelet, B.; Lacroix-Desmazes, P.; Boutevin, B. *Polymer* 2007, 48, 50–57.
- 6 Tonnar, J.; Severac, R.; Lacroix-Desmazes, P.; Boutevin, B. *Polymer Preprints* 2008, 49, 68–69.
- 7 Wright, T.; Chirowodza, H.; Pasch, H. *Macromolecules* 2012, 45, 2995–3003.
- 8 Matyjaszewski, M. *Progress in Controlled Radical Polymerization: Mechanisms and Techniques*, American Chemical Society: Washington DC 2012, 1100, 1–13.
- 9 Jakubowski, W.; Kirci-Denizli, B.; Gil, R. R.; Matyjaszewski, K. *Macromolecular Chemistry and Physics* 2008, 209, 32–39.
- 10 Rayeroux, D.; Lapinte, V.; Lacroix-Desmazes, P. *Journal of Polymer Science: Part A: Polymer Chemistry* 2012, 50, 4589–4593.
- 11 Gaynor, S. G.; Wang, J.-S.; Matyjaszewski, K. *Macromolecules* 1995, 28, 8051–8056.
- 12 Valade, D.; Boyer, C.; Ameduri, B.; Boutevin, B. *Macromolecules* 2006, 39, 8639–8651.
- 13 Boyer, C.; Lacroix-Desmazes, P.; Robin, J.-J.; Boutevin, B. *Macromolecules* 2006, 39, 4044–4053.
- 14 Shiman, D. I.; Kostyuk, S. V.; Gaponik, L. V.; Kaputskii, F. N. *Russian Journal of Applied Chemistry* 2010, 83, 2028–2034.
- 15 Goto, A.; Fukuda, T. *Progress in Polymer Science* 2004, 29, 329–385.
- 16 Mueller, A. H. E.; Zhuang, R.; Yan, D.; Litvinenko, G. *Macromolecules* 1995, 28, 4326–4333.
- 17 Patra, B. N. *Polymer Preprints* 2008, 49, 345–346.
- 18 van Herk, A. M. *Journal of Macromolecular Science, Part C: Polymer Reviews* 1997, 37, 633–648.
- 19 Kaszás, G.; Földes-Bereznich, T.; Tüdös, F. *European Polymer Journal* 1984, 20, 395–398.
- 20 Tonnar, J.; Lacroix-Desmazes, P.; Boutevin, B. *Macromolecules* 2007, 40, 6076–6081.

- 21 Pouget, E.; Tonnar, J.; Eloy, C.; Lacroix-Desmazes, P.; Boutevin, B. *Macromolecules* 2006, 39, 6009–6016.
- 22 Mortensen, K.; Gasser, U.; Gürsel, S. A.; Scherer, G. G. *Journal of Polymer Science: Part B* 2008, 46, 1660–1668.
- 23 Suggs, L. J.; Payne, R. G.; Yaszemski, M. J.; Alemany, L. B.; Mikos, A. G. *Macromolecules* 1997, 30, 4318–4323.
- 24 Falkenhagen, J.; Much, H.; Stauf, W.; Müller, A. H. E. *Macromolecules* 2000, 33, 3687–3693.
- 25 Murgasova, R.; Hercules, D. M. *Analytical and Bioanalytical Chemistry* 2002, 373, 481–489.
- 26 Snyder, L. R. *Journal of Chromatographic Science* 1978, 16, 223–234.
- 27 Sparidans, R. W.; Claessens, H. A.; van Doremale, G. H. J.; van Herk, A. M. *Journal of Chromatography* 1990, 508, 319–331.
- 28 Braunecker, W. A.; Matyjaszewski, K. *Progress in Polymer Science* 2007, 32, 93–146.
- 29 Tonnar, J.; Severac, R.; Lacroix-Desmazes, P.; Boutevin, B. *Polymer Preprints* 2008, 49, 187–188.

5 SYNTHESIS OF DEUTERATED POLYSTYRENE AND BLOCK COPOLYMERS BY RITP

5.1 Introduction

Deuterium is an isotope of hydrogen that contains one proton and one neutron. The chemical symbol of deuterium is D. Deuterated compounds are typically quite expensive, but these compounds do have some useful applications. For example, deuterated compounds are used in pharmacology to follow metabolism,¹⁻⁶ deuterated compounds can be used to trace biodegradation of hydrocarbons in water⁷ and deuterated compounds are used in nuclear fusion experiments.⁸⁻¹⁰ Deuterated polystyrene (d-PS) is usually synthesised using living anionic polymerisation (Scheme 5.1).^{11,12}



Scheme 5.1: Typical anionic polymerisation of d-PS.

In living anionic polymerisation, the reaction typically involves the use of n-butyl lithium as an initiator at a temperature of $-78\text{ }^{\circ}\text{C}$. Hydrogenous PS (h-PS) has also been grafted with d-PS using living anionic polymerisation.¹³ It has also been reported that deuterated star polymers have been synthesised *via* RAFT polymerisation at a temperature of $80\text{ }^{\circ}\text{C}$.¹⁴ To the best of our knowledge, the use of RITP to synthesise deuterated polymers has not yet been reported in literature.

In this section the main objectives were to synthesise, for the first time, d-PS and block copolymers of hydrogenous polystyrene-*b*-deuterated polystyrene (hPS-*b*-dPS) *via* RITP. SEC and HPLC were used to confirm the formation of block copolymers.

5.2 Experimental section

5.2.1 Chemicals

Styrene ($\geq 99\%$ Sigma-Aldrich) was washed three times with a 0.3 M aqueous solution of sodium hydroxide followed by three washes with distilled de-ionised water. The washed styrene was left to dry overnight using anhydrous magnesium sulphate. The magnesium sulphate was filtered off and the styrene was distilled under vacuum and stored in a refrigerator at $-5\text{ }^{\circ}\text{C}$. Azobis(isobutyronitrile) (AIBN, Riedel de Haën) was recrystallised from methanol, dried under vacuum and stored in a refrigerator at $-5\text{ }^{\circ}\text{C}$. Deuterated styrene (styrene- d_8 , Sigma-Aldrich 98%) was passed through a column of alumina to remove inhibitor. Deuterated chloroform (CDCl_3 , Sigma-Aldrich 99%), deuterated benzene (C_6D_6 , Sigma-Aldrich 99%) and iodine (I_2 , ACROS Organics) were used as received.

5.2.2 Homopolymerisation of styrene and styrene- d_8

The homopolymerisation of styrene (hydrogenous) was performed by adding styrene (4.00 g, 3.84×10^{-2} mol), toluene (4.00g, 4.34×10^{-2} mol), AIBN (63.6 mg, 3.88×10^{-4} mol) and iodine (51.8 mg, 2.04×10^{-4} mol) into a Schlenk flask. A magnetic stirrer bar was added to the flask to ensure that the reaction mixture was stirred during polymerisation. The Schlenk flask was degassed by three successive freeze-pump-thaw cycles and back filled with UHP argon gas. To commence polymerisation, the flask was submerged in silicone oil heated to $70\text{ }^{\circ}\text{C}$. The polymerisation reaction proceeded in the dark for 24 hours before halting the reaction by placing the flask on ice. Finally, the polymer was precipitated in cold methanol and left to dry overnight in a vacuum oven.

For the homopolymerisation of styrene- d_8 , the same reaction conditions were used. However, due to the high cost of deuterated styrene, lower quantities of reagents were used for these reactions. In a typical reaction, styrene- d_8 (1.00 g, 8.91×10^{-3} mol), toluene (1.00g, 1.09×10^{-2} mol), AIBN (3.9 mg, 2.39×10^{-5} mol) and iodine (3.2 mg, 1.26×10^{-5} mol) were added to a Schlenk flask.

The homopolymerisations of styrene and styrene- d_8 were also analysed using *in situ* ^1H NMR. For hydrogenous styrene polymerisation, styrene (2.00 g, 19.2×10^{-2} mol), AIBN (31.8 mg, 1.94×10^{-4} mol) and iodine (25.9 mg, 1.02×10^{-4} mol) were mixed in a glass vial. A small amount (0.15 g) of this stock solution was injected into a J Young NMR tube and 0.15 g of benzene- d_6 was added. The NMR tube was degassed by three successive freeze-thaw pump cycles and filled with UHP argon gas. For styrene- d_8 polymerisation, styrene- d_8 (0.30 g, 2.67×10^{-3} mol), AIBN (4.80 mg, 2.91×10^{-5} mol) and iodine (3.90 mg, 1.53×10^{-5} mol) were added to the J Young NMR tube.

Before starting the *in situ* ^1H NMR experiment, a pre-polymerisation spectrum was recorded at 25 °C to be used as a reference. The NMR tube was removed from the NMR magnet and the temperature of the magnet was elevated to 70 °C. After the temperature was stable at 70 °C, the NMR tube was inserted again the magnet was shimmed at the elevated temperature. Each spectrum was recorded with 15 scans every 15 minutes for 24 hours with a pulse width of 3 μs (40°) and a 4 second acquisition time.

ACD Labs 10.0 ^1H NMR processor[®] was used to process the NMR data. All spectra were phased with automatic phase correction, whilst performing manual baseline correction and integration of proton signals.

5.2.3 Block copolymerisation of styrene and styrene- d_8

The precipitated h-PS was dried in a vacuum oven overnight to ensure no unreacted monomer was present. H-PS was used as a macro-initiator and typical copolymerisation reaction conditions are as follows; PS-I (1.0 g, 2.78×10^{-5} mol) was mixed with styrene- d_8 (1.0 g, 8.91×10^{-3} mol), AIBN (1.37 mg, 8.33×10^{-6} mol) and toluene (2.0 g, 2.17×10^{-2} mol) in a Schlenk flask. The flask was degassed by three successive freeze-pump-thaw cycles and then back filled with UHP argon gas. The flask was then submerged in silicone oil heated to 70 °C and the reaction was run for 24 hours in the dark. The resulting copolymer was precipitated in cold methanol and left to dry in a vacuum oven overnight.

5.3 Characterisation of polymers

5.3.1 SEC analysis

An SEC instrument equipped with a Waters 717plus Autosampler, Waters 600E system controller and a Waters 610 fluid unit were used to perform SEC analyses. A Waters 2414 differential refractometer was used for detection. Two PLgel 5 μm Mixed-C columns and a PLgel 5 μm guard column were used. The oven temperature was maintained at 30 °C and 100 μL of 2mg/mL sample was injected into the column set. THF (HPLC grade, BHT stabilised) was used as the eluent for the analyses at a flow rate of 1mL/min. Narrow polystyrene standards with molar masses ranging from 800– 2×10^6 g/mol were used to calibrate the instrument. Data obtained from SEC is reported as polystyrene equivalents.

5.3.2 NMR analysis

^1H NMR spectra were recorded on a Varian Unity INOVA 400 MHz spectrometer. Deuterated chloroform (CDCl_3) was used to dissolve polymer samples (crude and precipitated). For *in situ* ^1H NMR experiments of hydrogenous styrene, the samples were run in deuterated benzene (C_6D_6).

5.3.3 HPLC analysis

For the HPLC analyses, an Agilent 1200 series (Agilent Technologies, Boblingen, Germany) comprising an auto sampler, vacuum degasser, quaternary pump, column oven, variable wavelength UV detector and Agilent 1260 infinity ELSD was used. The data was recorded and processed using WinGPC Unity (version 7). Critical conditions were established for h-PS using a Phenomenex C_{18} 300 Å (250 x 4.6 mm) with 5 μm particle size. THF and acetonitrile (ACN) (HPLC grade) were used as the mobile phase and premixed by volume. Samples were dissolved in the premixed solvent with a concentration of 0.5 mg/mL. The mobile phase was set for a flow rate of 0.5 mL/min and sample injection volume was 10 μL . The column oven temperature was kept constant at 35 °C. Conditions where one PS species eluted in SEC mode while the other eluted in LAC mode were established at a mobile phase composition of THF/ACN 48:52 (v/v). The column oven temperature was kept constant at 46 °C. Samples were dissolved in the premixed solvent with a concentration of 0.5 mg/mL.

5.3.4 Two-dimensional liquid chromatography

The first dimension separated according to chemical composition on a C₁₈ column, whilst the second dimension separated according to molar mass. Samples were dissolved in THF with concentrations of 1 mg/mL and 50 µL injected in the first dimension with a flow rate of 0.02 mL/min. In the two-dimensional liquid chromatography analysis, sample fractions from the first dimension were injected into the second dimension column *via* an electronically controlled eight port transfer valve (VICI Valco instruments, Texas, USA) consisting of two 50 µL storage loops. The apparatus used in the second dimension consisted of an Agilent 1200 isocratic pump and a 50 mm x 20 mm PSS Linear M 5 µm styrene-divinylbenzene (SDV) column. THF was the solvent used for analyses in the second dimension, with a flow rate of 3 mL/min. Detection in the second dimension was done using an ELSD detector. The nebuliser temperature was set to 90 °C and nitrogen gas was used as the carrier gas in the ELSD. The data was recorded and processed using WinGPC Unity (version 7).

5.4 Results and discussion

5.4.1 Homopolymerisation of styrene

Since h-PS was to be used as a macro-initiator in the synthesis of block copolymers, the end group functionality was an important factor. In Section 4.4.2, the highest functionality of the PS samples was achieved when an [initiator]/[iodine] ratio of 1.7 was used. In the present case, h-PS samples were prepared using an [initiator]/[iodine] ratio of 1.7 and targeting molar masses from 10000–100000 g.mol⁻¹. The conversion of h-PS could be determined using the ¹H NMR spectrum of crude samples. The conversion was determined using Equation 5.1

$$X_{mon} = \left(1 - \frac{\int CH_2}{\int C_6H_5} \right) \times 100 \quad (5.1)$$

where $\int CH_2$ is the integral of the vinylic protons of residual styrene (5.1 – 5.7 ppm) and $\int C_6H_5$ is the integral of the aromatic protons of PS.¹⁵ The conversion was then substituted into Equation 5.2 to determine the molar mass

$$M_{n, calc} = \frac{(m_{mon} \times X_{mon})}{(2 \times n_{iodine})} + M_{chain\ ends} \quad (5.2)$$

where m_{mon} is the mass of the monomer, X_{mon} is the monomer conversion determined from ^1H NMR, n_{iodine} is the number of moles of iodine and $M_{\text{chain ends}}$ is the combined molar mass of the cyanoisopropyl and iodinated chain ends ($195 \text{ g}\cdot\text{mol}^{-1}$).¹⁶⁻¹⁸ The results obtained from the abovementioned calculations are tabulated in Table 5.1.

Table 5.1: Results of styrene homopolymerisation via RITP for 24 hours at 70 °C.

Run	[AIBN]/[I ₂]	$M_{n, \text{target}}$ ($\text{g}\cdot\text{mol}^{-1}$)	Conv (%) ^a	$M_{n, \text{calc}}$ ($\text{g}\cdot\text{mol}^{-1}$) ^b	$M_{n, \text{SEC}}$ ($\text{g}\cdot\text{mol}^{-1}$) ^c	\bar{D}
1	1.7	10000	59	6000	6200	1.65
2	1.7	30000	60	17900	18400	1.77
3	1.7	40000	62	25200	24700	1.77
4	1.7	60000	58	34600	35200	1.73
5	1.7	70000	64	44700	43100	1.70
6	1.7	100000	60	59800	55300	1.68

^a Determined by ^1H NMR of crude sample in CDCl_3 by $X_{\text{mon}} = (1 - ([\text{CH}_2]/[\text{C}_6\text{H}_5])) \times 100$ where $[\text{CH}_2]$ is the integral of the vinylic protons of residual styrene at 5.1 – 5.7 ppm, and $[\text{C}_6\text{H}_5]$ is the integral of the aromatic protons PS.

^b Calculated by $M_{n, \text{calc}} = ((m_{\text{mon}} \times X_{\text{mon}})/(2 \times n_{\text{iodine}})) + M_{\text{chain ends}}$.

^c Calibrated using polystyrene standard.

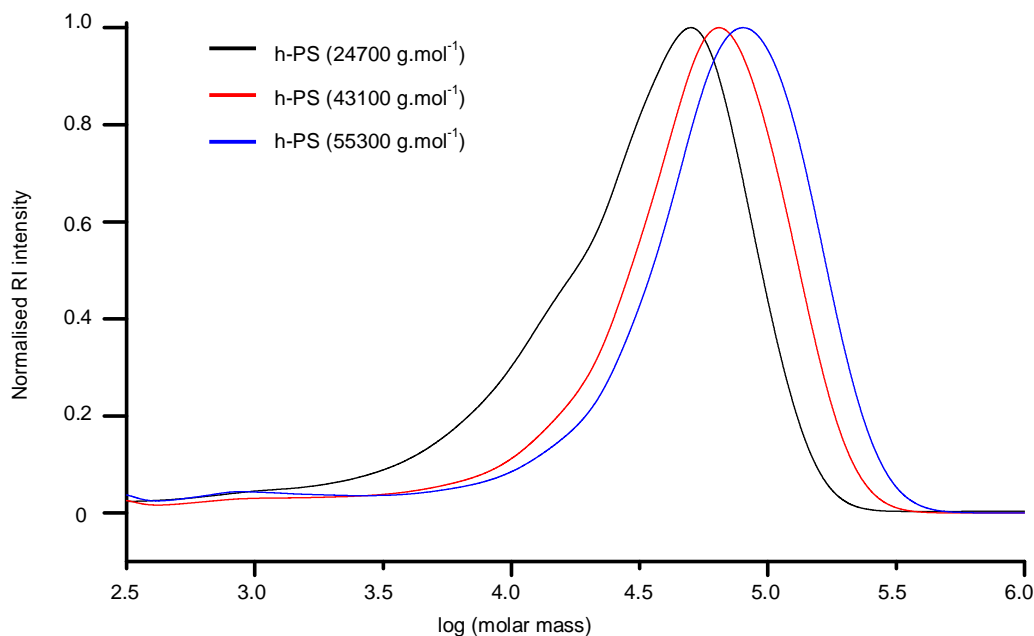
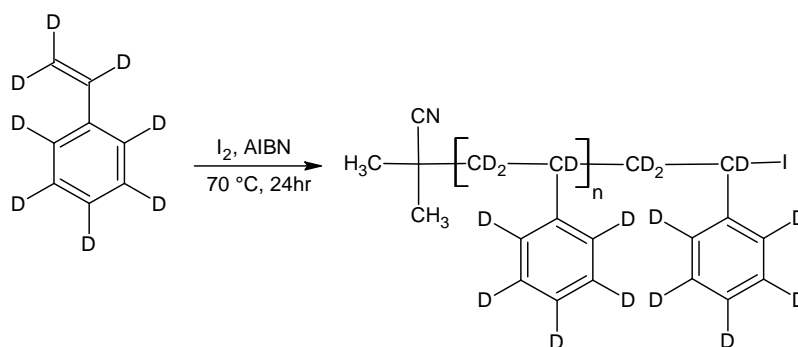


Figure 5.1: Molar mass distributions from SEC (RI traces) of h-PS (run 3, 5 and 6 Table 5.1) synthesised via RITP at 70 °C for 24 hours.

As was seen in Section 4.4.2, the monomer conversion for styrene polymerisation is ~60%. Also, the dispersity values of the h-PS samples were in a typical range for styrene polymerised *via* iodine mediated polymerisation.¹⁸⁻²² The molar mass distributions from SEC of three h-PS samples (run 3, 5 and 6 Table 5.1) are shown in Figure 5.1. There was a clear shift towards higher molar masses with tailing at lower molar masses.

5.4.2 Homopolymerisation of styrene-d₈

Although the synthesis of d-PS *via* RITP has not been reported in literature, it was expected to follow the same reaction mechanism as h-PS. A schematic of the expected polymerisation pathway of styrene-d₈ *via* RITP is shown in Scheme 5.2.



Scheme 5.2: Basic representation of the homopolymerisation of styrene-d₈ by RITP.

The results of polymerisation reactions performed at 70 °C for 24 hours using styrene-d₈ are shown in Table 5.2. At a glance it is apparent that the monomer conversion for styrene-d₈ polymerisation is < 50%. Regardless of this fact, the dispersity values are between 1.6–1.8, which is typical of styrene polymerised *via* RITP.¹⁸⁻²² The molar mass distributions from SEC of three d-PS samples (run 2, 3 and 4 Table 5.2) are shown in Figure 5.2. There is a clear shift towards higher molar masses with tailing at lower molar masses. In RITP there are two stages, an inhibition period and a polymerisation period. In the inhibition period, CTAs are generated *in situ*. These CTAs (A-I) are formed by the reaction between initiator radicals (A) and molecular iodine (I). The evolution of this CTA has been reported for hydrogenous styrene polymerisation. In the *in situ* ¹H NMR spectrum of styrene polymerised *via* RITP, the proton signal for A-I was observed at δ=1.65 ppm.²² An overlay of the evolution of this A-I transfer agent is shown in Figure

5.3 for h-PS and d-PS. Clearly the two PS species exhibited similar behaviour with respect to the formation of the transfer agent A-I. The concentration of the A-I transfer agent increased during the inhibition period until it reached a maximum. The drop in concentration signified the start of the polymerisation period. Figure 5.4 shows the evolution of the AIBN concentration for h-PS and d-PS. Again, similar behaviour was observed for the two PS species.

Table 5.2: Results of styrene-d₈ homopolymerisation via RITP for 24 hours at 70 °C.

Run	[AIBN]/[I ₂]	M _{n, target} (g.mol ⁻¹)	Conv (%) ^a	M _{n, calc} (g.mol ⁻¹) ^b	M _{n, SEC} (g.mol ⁻¹) ^c	<i>D</i>
1	1.7	10000	48	4800	4900	1.63
2	1.7	25000	47	11700	12100	1.72
3	1.7	40000	47	18800	19000	1.79
4	1.7	60000	49	29600	30100	1.83
5	1.7	100000	48	48200	45500	1.77

^a Determined using gravimetry.

^b Calculated by $M_{n, calc} = ((m_{mon} \times X_{mon}) / (2 \times n_{iodine})) + M_{chain ends}$.

^c Calibrated using polystyrene standard.

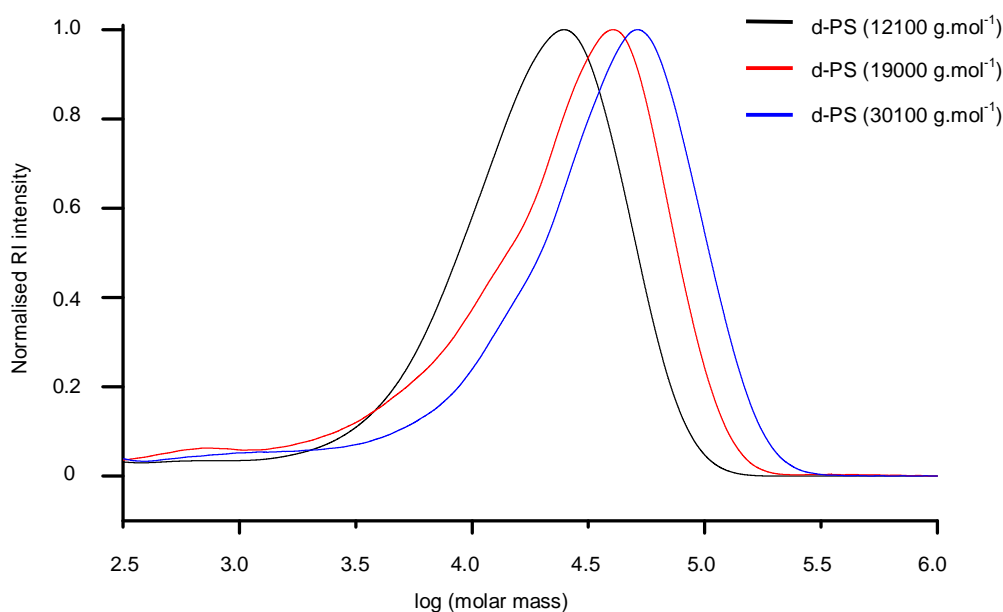


Figure 5.2: Molar mass distributions from SEC (RI traces) of d-PS (run 2, 3 and 4) synthesised via RITP at 70 °C for 24 hours.

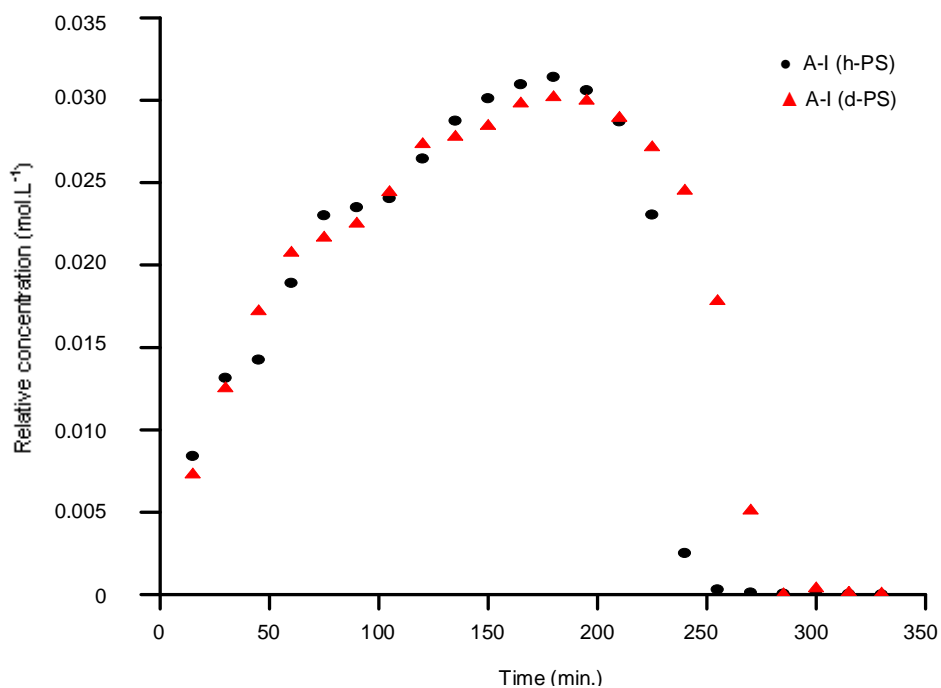


Figure 5.3: Evolution of the A-I transfer agent for the polymerisation of h-PS (●) and d-PS (▲) at 70 °C for 24 hours.

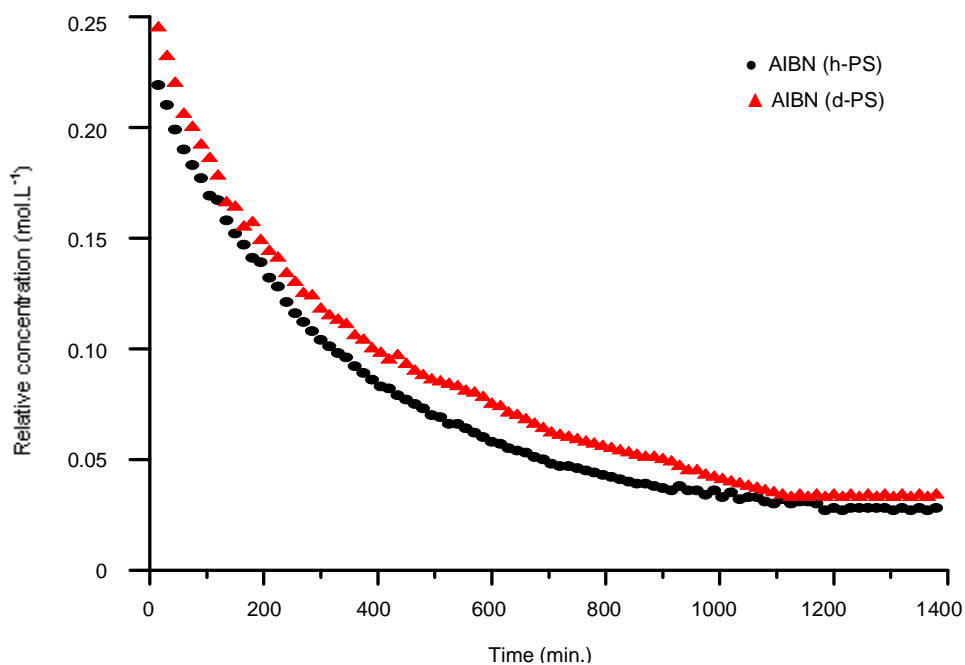
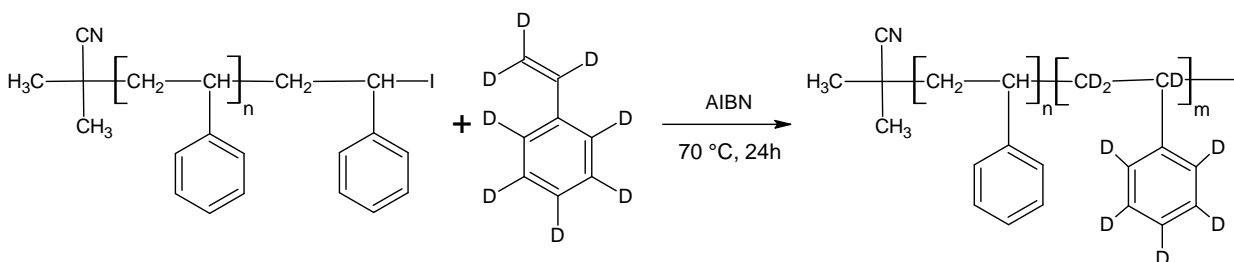


Figure 5.4: Evolution of the AIBN concentration h-PS (●) and d-PS (▲) during polymerisation at 70 °C for 24 hours.

5.4.3 Synthesis of hPS-*b*-dPS block copolymers

The synthesis of hPS-*b*-dPS block copolymers using anionic polymerisation has been reported in literature.²³ Withstanding this fact, hPS-*b*-dPS block copolymers have not, to the best of our knowledge, been prepared *via* RITP. Due to the high cost of deuterated monomers, RITP offers a relatively cheap and simple method of preparing these rather expensive compounds. It is, therefore, important to understand the mechanism of RITP of deuterated compounds by using a combination of advanced analytical methods.

When synthesising the PS homopolymers, it was necessary to add iodine and AIBN to the reaction mixture in order to form chain transfer agents *in situ*. These homopolymers could then be used as a macro-initiator (PS-I) to synthesise block copolymers. The hPS-*b*-dPS block copolymers were synthesised using hydrogenous PS-I as a macro-initiator together with styrene-*d*₈. Toluene was added to the mixture to ensure that all PS-I dissolved. Scheme 5.3 shows a basic representation of the copolymerisation mechanism of hydrogenous PS with styrene-*d*₈.



Scheme 5.3: Simplified schematic of the copolymerisation of h-PS with styrene-*d*₈ via RITP.

5.4.4 Characterisation of hPS-*b*-dPS block copolymers

Block copolymers of different molar masses were prepared and analysed by SEC and HPLC. The results for the block copolymerisation reactions are shown in Table 5.3. The weight percentage of the respective monomer units could be determined by using the molar masses from SEC. This was done by substituting the molar mass values from SEC into Equation 5.3

$$\% d - PS = \left(\frac{M_{block} - M_{h-PS}}{M_{block}} \right) \times 100 \quad (5.3)$$

where M_{block} is the molar mass of the block copolymer and M_{h-PS} is the molar mass of the precursor h-PS. The molar mass of the d-PS block ($M_{n, d-PS}$) was estimated from the percentage (using Equation 5.3) of the total molar mass of the block copolymer (see Table 5.3).

Table 5.3: Results of hPS-*b*-dPS polymerisation via RITP for 24 hours at 70 °C.

Run	$M_{n, SEC, h-PS}$ ($g \cdot mol^{-1}$) ^a	\bar{D} (PS)	$M_{n, SEC, hPS-b-dPS}$ ($g \cdot mol^{-1}$) ^a	\bar{D} (hPS- <i>b</i> -dPS)	%h-PS : %d-PS (SEC) ^b	$M_{n, d-PS}$
1	18400	1.77	31100	1.68	59:41	12700
2	18400	1.77	47600	1.63	39:61	29200
3	35200	1.73	77900	1.65	45:55	42700

^a Calibrated using PS standards.

^b Weight percentage calculated using %d-PS = $((M_{block} - M_{h-PS}) / M_{block}) \times 100$.

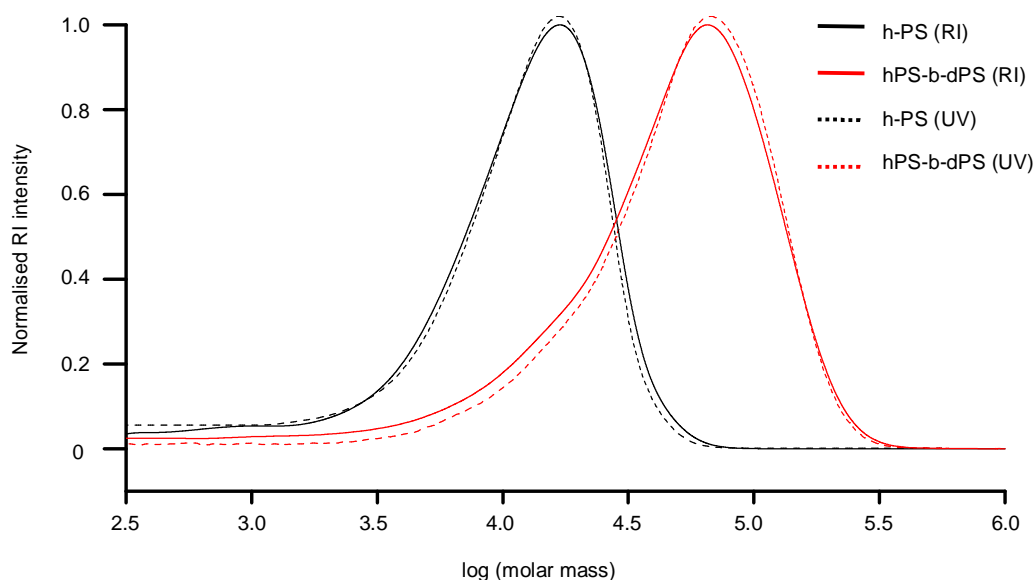


Figure 5.5: Molar mass distributions from SEC (RI and UV) of h-PS precursor and hPS-*b*-dPS block copolymer (run 2 Table 5.3) synthesised via RITP for 24 hours at 70 °C.

Figure 5.5 shows an overlay of the RI and UV (set to 254 nm) traces for h-PS precursor and hPS-*b*-dPS block copolymer. There is a clear shift in molar mass of the h-PS precursor to the hPS-*b*-dPS block copolymer. The overlay of the RI and UV traces also shows that the majority of styrene- d_8 was incorporated into the h-PS chains. Also, there is no indication that there is any residual PS precursor at lower molar masses.

5.4.5 Analysis of hPS-*b*-dPS block copolymers by HPLC

5.4.5.1 Separation of hPS-*b*-dPS at critical conditions of h-PS

It has been reported that deuterated polystyrene (d-PS) is more polar than hydrogenous polystyrene (h-PS), due to an enhanced electron donating ability.²⁴ It has also been reported in literature that isotopes display chromatographic selectivity in reversed phase liquid chromatography (RPLC).²⁵⁻²⁷ That is, d-PS interacts less strongly with RP columns than h-PS. This was the basis for selecting a C_{18} (non-polar) column to analyse the hPS-*b*-dPS block copolymers. LCCC was used in this study in order to be as selective as possible with respect to isotopic effects. A Phenomenex C_{18} 300 Å – 5 μ m stationary phase was used to establish critical conditions at a temperature of 35 °C while varying the composition of the THF/ACN mobile phase. The h-PS (Section 5.4.1) and d-PS (Section 5.4.2) samples that were prepared *via* RITP were used to study the hPS-*b*-dPS block copolymers by LCCC. These samples are listed in Table 5.4.

Table 5.4: Molar masses of the h-PS and d-PS samples used in the HPLC analyses.

h-PS	$M_{n, SEC}$ (g.mol ⁻¹) ^a	d-PS	$M_{n, SEC}$ (g.mol ⁻¹) ^a
Sample 1	6200	Sample 1	4900
Sample 2	15600	Sample 2	12100
Sample 3	21600	Sample 3	19000
Sample 4	43100	Sample 4	30100
Sample 5	55300	Sample 5	45500

^a Calibrated using PS standards.

The critical diagram for the h-PS samples prepared *via* RITP is shown in Figure 5.6. At a mobile phase composition of THF/ACN 55:45 (v/v), h-PS elutes in SEC mode. H-PS eluted in LAC mode when the mobile phase composition was THF/ACN 48:52 (v/v).

The critical point, where all h-PS samples elute at the same retention volume regardless of their molar mass, was found at a solvent composition of THF/ACN 50:50 (v/v). The critical conditions for h-PS were used to establish where d-PS samples would elute. At the critical conditions of h-PS, the d-PS samples elute in SEC mode, as seen in Figure 5.7. Under critical conditions for h-PS, the hPS-*b*-dPS block copolymers were expected to behave in the same mode as d-PS homopolymers.

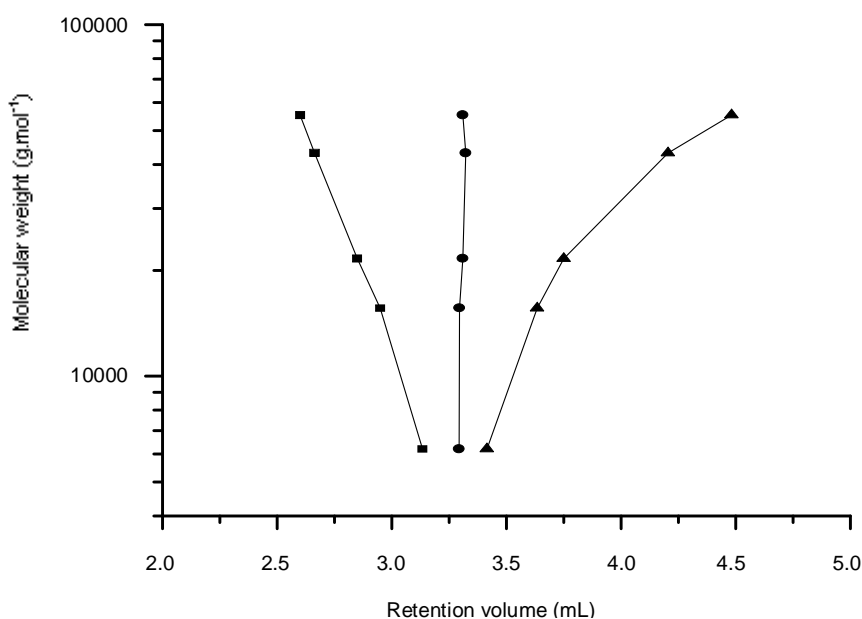


Figure 5.6: Critical diagram of molar mass *versus* retention volume for h-PS synthesised via RITP; stationary phase: Phenomenex C₁₈ 300 Å – 5 µm; mobile phase: THF/ACN; (■) = 55:45 (SEC), (●) = 50:50 (LCCC) and (▲) = 48:52 (LAC) (v/v).

Figure 5.8 shows an overlay of the chromatograms of the h-PS precursor and respective block copolymers (run 1 and 2 Table 5.3). The hPS-*b*-dPS block copolymers eluted in SEC mode, as was expected. This type of isotopic separation has been reported in literature before.^{11,23} It was clear that a higher d-PS content in the block copolymers resulted in the block copolymer eluting earlier. Therefore, an hPS-*b*-dPS block copolymer of higher molar mass was prepared (run 3 in Table 5.3).

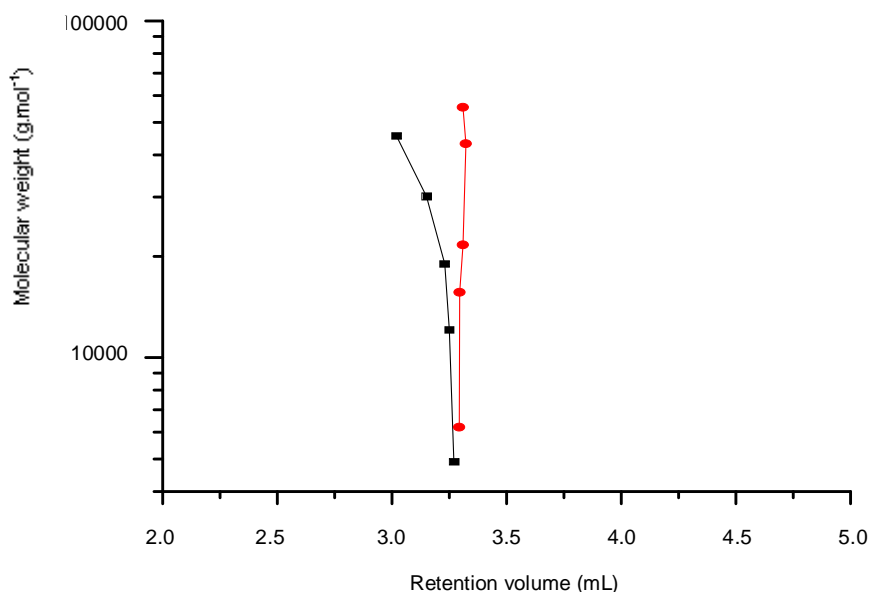


Figure 5.7: Plot of molar mass *versus* retention volume for h-PS and d-PS samples prepared *via* RITP at the critical conditions of h-PS; stationary phase: Phenomenex C₁₈ 300 Å – 5 µm; mobile phase: THF/ACN 50:50; (■) = d-PS (SEC) and (●) = h-PS (LCCC) (v/v).

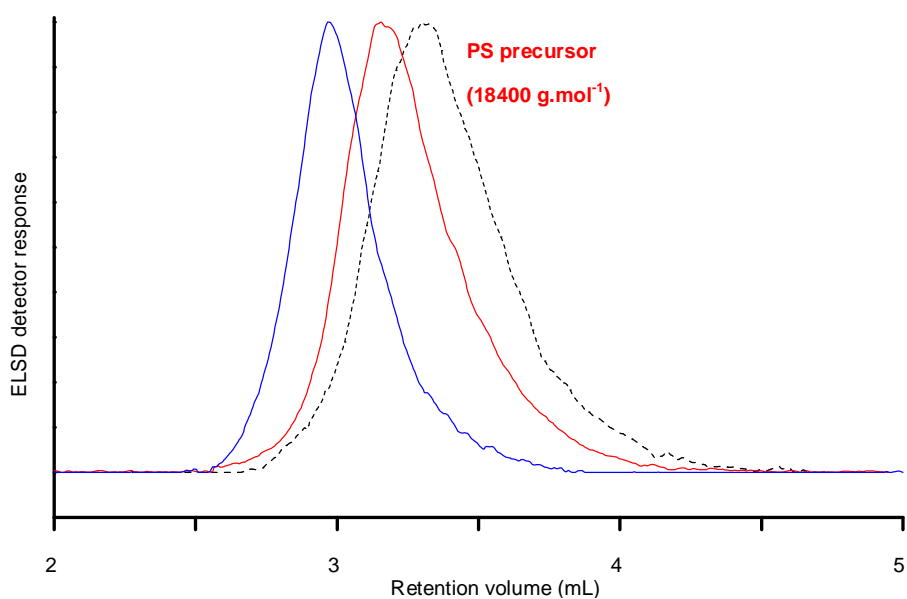


Figure 5.8: Superimposed chromatograms of the hPS-*b*-dPS copolymers (solid lines) and the h-PS precursor at the critical conditions of h-PS; stationary phase: Phenomenex C₁₈ 300 Å 5 µm; mobile phase: THF/ACN (50:50). Run 1 (red) and run 2 (blue) from Table 5.3.

For the high molar mass hPS-*b*-dPS block copolymer, new separation conditions were established where one PS species eluted in SEC mode while the other eluted in LAC mode. This was done using a solvent composition of THF/ACN 48:52 (v/v). The temperature where the two PS species are separated in different elution mode was found to be at 46 °C. Figure 5.9 shows the plot of molar mass *versus* retention volume for the h-PS and d-PS samples prepared *via* RITP. The plot shows that the d-PS samples eluted in SEC mode, while the h-PS samples eluted in LAC mode.

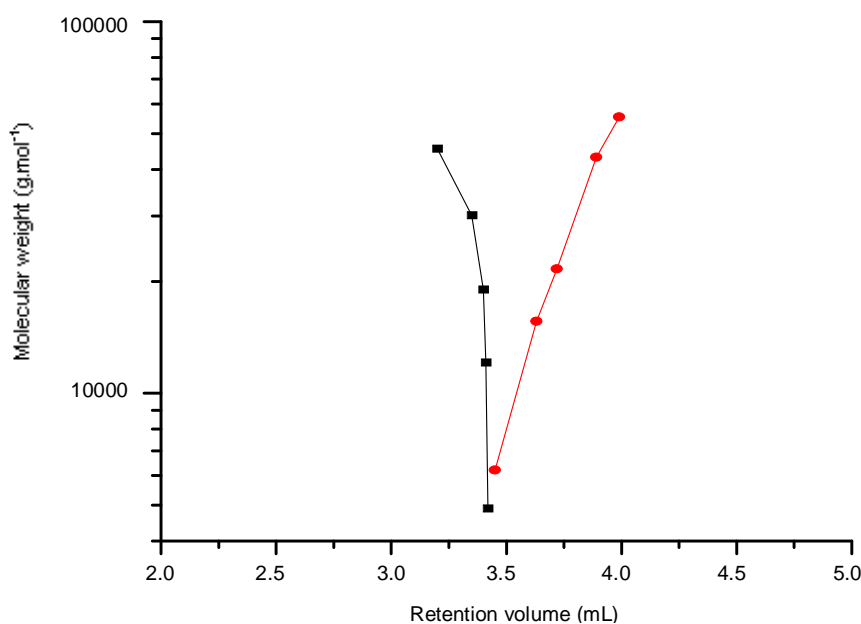


Figure 5.9: Plot of molar mass *versus* retention volume for h-PS and d-PS samples prepared *via* RITP at the LAC conditions of h-PS and SEC conditions of d-PS ; stationary phase: Phenomenex C₁₈ 300 Å – 5 μm; mobile phase: THF/ACN (48:52); (■) = d-PS (SEC) and (●) = h-PS (LCCC).

The chromatogram of the hPS-*b*-dPS block copolymer (run 3), analysed at 46 °C and THF/ACN 48:52 (v/v), is shown in Figure 5.10. The chromatogram shows a separation of the hPS-*b*-dPS block copolymer from the corresponding precursor block. The d-PS portion of the block copolymer shifts the block copolymer to SEC elution mode, while the h-PS portion of the block shifts the block copolymer to LAC elution mode.

Such a separation has been reported in literature for a blend of d-PS and h-PS prepared *via* living anionic polymerisation.¹¹ No baseline separation for the block copolymer could be achieved, as seen in Figure 5.10. This was expected, due to the fact that the polarity of two components is so similar. Also, the block copolymer eluted with respect to the component of the block copolymer with the higher molar mass. In the present case, the d-PS component had a molar mass of 42700 g/mol, while the h-PS component had a molar mass of 35200 g/mol. Therefore, the hPS-*b*-dPS block copolymer was inclined to follow the elution behaviour of d-PS component more so than the h-PS component.

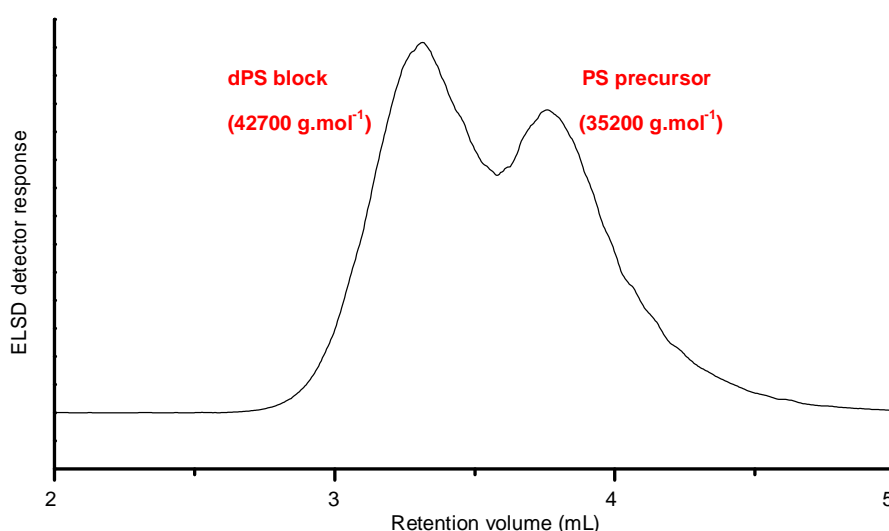


Figure 5.10: HPLC chromatogram of the hPS-*b*-dPS block copolymer (run 3 Table 5.3) at 46 °C and THF/ACN (48:52) (v/v); stationary phase: Phenomenex C₁₈ 300 Å 5 µm.

5.4.5.2 Two-dimensional liquid chromatography of hPS-*b*-dPS

The conditions used to separate the two components of the hPS-*b*-dPS block copolymer (run 3) were used in 2D-LC. Figure 5.11 shows the contour plot of the two-dimensional separation of the hPS-*b*-dPS block copolymer. The separation in the first dimension was based on a separation due to isotopic effect, while the second dimension separated according to molar mass. The 2D contour plot shows a separation due to isotopic effects, while there is no obvious separation due to molar mass in the second dimension. It is interesting to note that the 2D contour plot is different to the chromatogram from the one-dimensional analysis, in that there appears to be three components.

In the 2D contour plot, component **1** and component **3** can be assigned as the hPS-*b*-dPS block copolymer and the PS precursor respectively. This assignment is in line with what was observed for the one-dimensional analysis. However, component **2** was not observed in the one-dimensional analysis and this component could tentatively be assigned as d-PS homopolymer. Of course this assignment is just speculation and further investigations would be required to be entirely sure of this assignment.

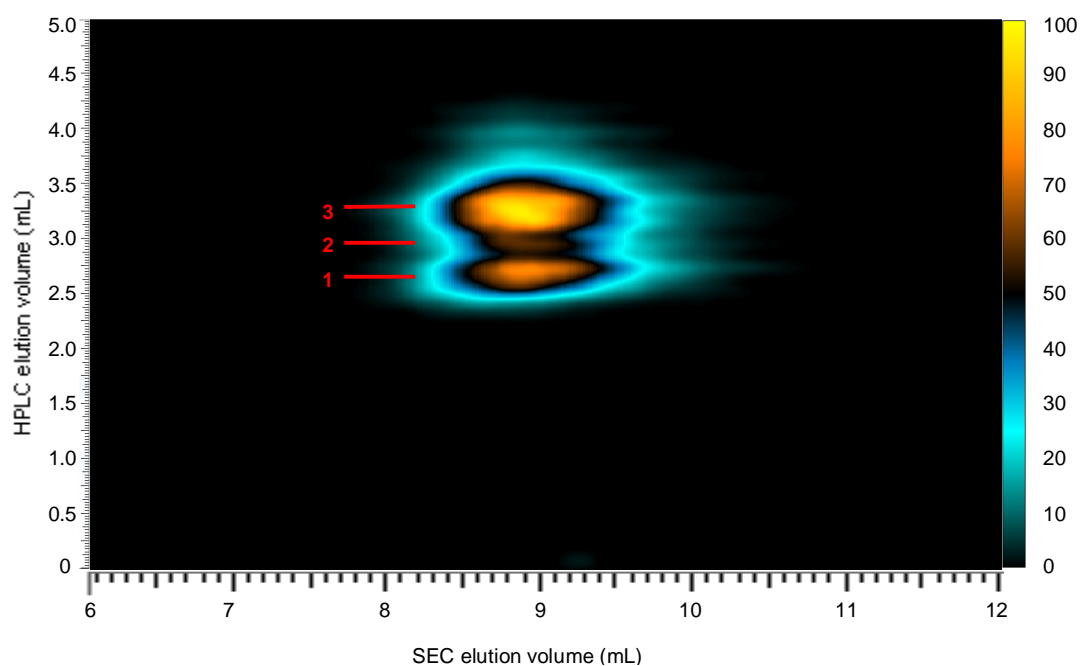


Figure 5.11: Contour plot of the two-dimensional separation of the hPS-*b*-dPS block copolymer (run 3) measured at a THF/ACN composition of 48:52 (v/v) and column oven temperature of 46 °C.

5.5 Conclusions

Hydrogenous polystyrene was synthesised *via* RITP to be used as a macro-initiator in the block copolymerisation of hPS-*b*-dPS. Similarly, deuterated polystyrene was successfully prepared *via* RITP for the first time. The livingness of the h-PS precursors was demonstrated by the successful synthesis, for the first time, of hydrogenous-polystyrene-block-deuterated-polystyrene (hPS-*b*-dPS) *via* RITP. Liquid chromatography at critical conditions was used to confirm that d-PS was in fact incorporated into the copolymer. At critical conditions for the h-PS block, the hPS-*b*-dPS block copolymers eluted in SEC mode. That is, the block copolymer eluted with respect to the d-PS block. A separation was also achieved where one component shifted the elution behaviour of the block copolymer to SEC mode, while the other component shifted the elution behaviour of the block copolymer to LAC mode. The overall elution behaviour was influenced more by the higher molar mass component. Two-dimensional liquid chromatography also showed that this separation was due to isotopic effects.

References

- 1 Baker, M. T.; Ronnenberg, W. C.; Ruzicka, J. A.; Chiang, C. K.; Tinker, J. H. *Drug Metabolism & Disposition* 1993, 21, 1170–1171.
- 2 Costanzo, L. D.; Moulin, M.; Haertlein, M.; Meilleur, F.; Christianson, D. W. *Archives of Biochemistry and Biophysics* 2007, 465, 82–89.
- 3 Modutlwa, N.; Maegawa, T.; Monguchi, Y.; Sajiki, H. *Journal of Labelled Compounds and Radiopharmaceuticals* 2010, 53, 686–692.
- 4 Nelson, S. D.; Trager, W. F. *Drug Metabolism & Disposition* 2003, 31, 1481–1497.
- 5 Pons, G.; Rey, E. *Pediatrics* 1999, 104, 633–639.
- 6 Sharma, R.; Strelevitz, T. J.; Gao, H.; Clark, A. J.; Schildknecht, K.; Obach, R. S.; Ripp, S. L.; Spracklin, D. K.; Tremaine, L. M.; Vaz, A. D. N. *Drug Metabolism & Disposition* 2012, 40, 625–634.
- 7 Thierrin, J.; Davis, G. B.; Barber, C. *Groundwater* 1995, 33, 469–475.
- 8 Gillich, D. J.; Kovanen, A.; Danon, Y. *Journal of Nuclear Materials* 2010, 405, 181–185.
- 9 Lin, Z.; Yongjian, T.; Chifeng, Z.; Xuan, L.; Houqiong, Z. *Nuclear Instruments and Methods in Physics Research Section A: Accelerators, Spectrometers, Detectors and Associated Equipment* 2002, 480, 242–245.
- 10 Nemoto, K.; Maksimchuk, A.; Banerjee, S.; Flippo, K.; Mourou, G.; Umstadter, D.; Bychenkov, V. Y. *Applied Physics Letter* 2001, 78, 595–597.
- 11 Sinha, P.; Harding, G. W.; Maiko, K.; Hiller, W.; Pasch, H. *Journal of Chromatography A* 2012, 1265, 95–104.
- 12 Wang, X.; Xu, Z.; Wan, Y.; Huang, T.; Pispas, S.; Mays, J. W.; Wu, C. *Macromolecules* 1997, 30, 7202–7205.
- 13 Ahn, S.; Im, K.; Chang, T.; Chambon, P.; Fernyhough, C. M. *Analytical Chemistry* 2011, 83, 4237–4242.
- 14 Boschmann, D.; Mänz, M.; Pöpller, A.-C.; Sörensen, N.; Vana, P. *Journal of Polymer Science: Part A: Polymer Chemistry* 2008, 46, 7280–7286.
- 15 Valade, D.; Boyer, C.; Ameduri, B.; Boutevin, B. *Macromolecules* 2006, 39, 8639–8651.
- 16 Boyer, C.; Lacroix-Desmazes, P.; Robin, J.-J.; Boutevin, B. *Macromolecules* 2006, 39, 4044–4053.
- 17 Lacroix-Desmazes, P.; Severac, R.; Boutevin, B. *Macromolecules* 2005, 38, 6299–6309.
- 18 Tonnar, J.; Severac, R.; Lacroix-Desmazes, P.; Boutevin, B. *Polymer Preprints* 2008, 49, 68–69.

-
- 19 Enríquez-Medrano, F. J.; Guerrero-Santos, R.; Hernandez-Valdez, M.; Lacroix-Desmazes, P. *Journal of Applied Polymer Science* 2011, *119*, 2476–2484.
 - 20 Greesh, N.; Sanderson, R.; Hartmann, P. *Journal of Applied Polymer Science* 2012, *126*, 1773–1783.
 - 21 Shiman, D. I.; Kostyuk, S. V.; Gaponik, L. V.; Kaputskii, F. N. *Russian Journal of Applied Chemistry* 2010, *83*, 2028–2034.
 - 22 Wright, T.; Chirowodza, H.; Pasch, H. *Macromolecules* 2012, *45*, 2995–3003.
 - 23 Lee, S.; Lee, H.; Thieu, L.; Jeong, Y.; Chang, T. *Macromolecules* 2013, *46*, 9114–9121.
 - 24 Bates, F. S.; Wignall, G. D. *Physical Review Letters* 1986, *57*, 1429–1432.
 - 25 Kayillo, S.; Gray, M. J.; Shalliker, R. A.; Dennis, G. R. *Journal of Chromatography A* 2005, *1073*, 83–86.
 - 26 Kim, Y.; Ahn, S.; Chang, T. *Analytical Chemistry* 2010, *82*, 1509–1514.
 - 27 Perny, S.; Allgaier, J.; Cho, D.; Lee, W.; Chang, T. *Macromolecules* 2001, *34*, 5408–5415.

6 SUMMARY, CONCLUSIONS AND FUTURE WORK

6.1 Summary and conclusions

Over the last two decades, various living radical polymerisation techniques have been developed that allow control over the macromolecular heterogeneity, including the molar mass and chemical composition distributions. Among them, RAFT and RITP are interesting due to the fact that they allow polymerisation of a wide variety of different monomers and copolymers. However, as in every polymerisation technique, secondary reactions take place and the formation of unwanted by-products cannot be avoided. In order to understand the respective polymerisation mechanisms, it is necessary to trace such reactions and to detect and quantify any by-products.

It was the aim of the present study to prepare complex polymer architectures by RAFT and RITP and to develop advanced analytical methods to follow the reactions. The focus was on proving the livingness of the polymerisation technique and on the comprehensive analysis of the reaction products. To this aim, advanced separation methods were to be used and combined with detailed spectroscopic studies.

In the first part of this work, a specific RAFT polymerisation was investigated. Styrene was polymerised *via* RAFT polymerisation using a tetrafunctional RAFT agent. This tetrafunctional RAFT agent has a benzyl leaving group that follows a Z-RAFT star polymerisation mechanism. The main objectives were to determine the topology of the resultant PS using *in situ* ^1H NMR and SEC and compare SEC results before and after aminolysis. After polymerisation of styrene in the presence of the tetrafunctional RAFT agent, the monomer conversion was usually 35–40%. The low monomer conversion was attributed to the inefficient pre-equilibrium of Z-star RAFT agents containing a benzyl leaving group.¹ The polymerisation was followed using *in situ* ^1H NMR, where deuterated styrene was used instead of hydrogenous styrene. The spectra showed a proton signal (~2.5 ppm) corresponding to the CH_2 protons of the RAFT agent being incorporated into the polymer as a terminal group. The intensity of this signal increased as the polymerisation proceeded, while the signal intensity corresponding to the CH_2 of the RAFT agent (~4.2 ppm) decreased. SEC was performed on the star-shaped PS to determine the molar masses of the polymers.

The molar masses determined by SEC, with linear PS calibration, were found to be lower than the theoretical molar masses. This was due to the fact that a linear PS calibration was used for branched polymers.² Therefore, to determine the molar masses of the PS prepared by RAFT, the polymers were cleaved using an amine. The cleaved linear arms were analysed by SEC. By multiplying the molar mass of the cleaved linear arms by the number of arms, the calculated molar mass was found to be in reasonable agreement with the theoretical molar mass determined for the star-shaped PS.

In the next part of this work, PS, PBA and PS-*b*-PBA block copolymers were prepared *via* RITP. The aims of this work were to determine whether the homopolymers were synthesised in a controlled manner and to characterise the block copolymers, synthesised from PS precursor, using SEC and HPLC. First, PS was prepared and characterised by SEC and ¹H NMR. It was found that the [initiator]/[iodine] ratio affected the end group functionality. It was essential to use conditions where PS had the highest functionality, since it was to be used as a macro-initiator in the preparation of block copolymers. PBA was prepared to determine whether the polymerisation of n-butyl acrylate proceeded in a controlled manner. The PBA polymers were characterised by SEC and ¹H NMR. PS-*b*-PBA block copolymers were prepared using PS-I as a macro-initiator. The resultant polymers were analysed using SEC and ¹H NMR. The successful formation of the PS-*b*-PBA block copolymer was determined using gradient HPLC. A solvent gradient of heptane/DCM(1.2% methanol) was used to perform the separation on a silica column. The solvent gradient was applied to both homopolymers (PS and PBA) to establish where the two would elute. It was found that PS eluted before PBA. The PS-*b*-PBA block copolymers eluted between the two homopolymers. Two peaks were detected where the first peak corresponded to unreacted PS macro-initiator, while the more substantial second peak was attributed to the block copolymer. 2D-LC was performed on the block copolymer. In 2D-LC, the first dimension separation is based on chemical composition, while the second dimension separation is based on molar mass. Running the same solvent gradient in 2D-LC, the two peaks could be seen more clearly when the colour distribution was set to a logarithmic scale.

In the concluding part of this work, h-PS, d-PS and hPS-*b*-dPS were prepared *via* RITP. The aims of this work were to analyse the deuterated polymers using NMR and SEC and to characterise the block copolymers using SEC and HPLC.

H-PS and d-PS were expected to show similar reaction kinetics, since they only differ in their isotopic composition. The h-PS and d-PS were characterised by SEC and *in situ* ^1H NMR. The monomer conversion of the deuterated styrene was found to be slightly lower (<50%) than that of its hydrogenous counterparts (~60%). The dispersity of the d-PS samples was in an acceptable range for styrene polymerised *via* RITP.³⁻⁶ H-PS was used as a macro-initiator to form block copolymers of hPS-*b*-dPS. The incorporation of deuterated styrene onto the h-PS chains was determined using SEC. The successful formation of the block copolymers as was determined using HPLC on a C_{18} column. Isotopes exhibit chromatographic selectivity in reversed phase liquid chromatography.⁷⁻⁹ That is, on a C_{18} column, the d-PS interacts less strongly than h-PS. Critical conditions were established for h-PS where all h-PS samples eluted at the same elution volume regardless of molar mass. At the critical conditions of h-PS, d-PS eluted in SEC mode. Two hPS-*b*-dPS samples of different molar mass were investigated at the critical conditions of h-PS. The two eluted in SEC mode as expected, with the block copolymer with higher d-PS content eluting earlier. This separation is due to isotopic effect. New separation conditions were established where d-PS eluted in SEC mode and h-PS eluted in LAC mode. A block copolymer was analysed at these new conditions, showing a separation of the block copolymer due to isotopic effects. The peaks in the chromatogram corresponding to the h-PS precursor block and the block copolymer were not baseline separated. This was due to the small difference in polarity between the d-PS and h-PS components of the block copolymer. The overall elution behaviour was influenced mainly by the higher molar mass component of the block copolymer, d-PS in this instance.

6.2 Future work

Synthesise an analogous tetrafunctional RAFT agent containing a phenylethyl leaving group instead of the benzyl leaving group. Star RAFT agents containing phenylethyl leaving groups have been found to be much more efficient than those containing benzyl leaving groups.^{2,10}

Investigate the livingness of the star-shaped PS by synthesising block copolymers.

Fractionate the PS and PS-*b*-PBA and analyse them using ^1H and ^{13}C NMR. The NMR spectrum of PS can then be compared to that of PS-I precursor.

Use the gradient HPLC conditions established in this work to separate other acrylate block copolymers prepared *via* RITP.

References

- 1 Barner-Kowollik, C.; Quinn, J. F.; Nguyen, T. L. U.; Heuts, J. P. A.; Davis, T. P. *Macromolecules* 2001, 34, 7849–7857.
- 2 Boschmann, D.; Edam, R.; Schoenmakers, P. J.; Vana, P. *Polymer* 2008, 49, 5199–5208.
- 3 Enríquez-Medrano, F. J.; Guerrero-Santos, R.; Hernandez-Valdez, M.; Lacroix-Desmazes, P. *Journal of Applied Polymer Science* 2011, 119, 2476–2484.
- 4 Greesh, N.; Sanderson, R.; Hartmann, P. *Journal of Applied Polymer Science* 2012, 126, 1773–1783.
- 5 Shiman, D. I.; Kostyuk, S. V.; Gaponik, L. V.; Kaputskii, F. N. *Russian Journal of Applied Chemistry* 2010, 83, 2028–2034.
- 6 Tonnar, J.; Severac, R.; Lacroix-Desmazes, P.; Boutevin, B. *Polymer Preprints* 2008, 49, 68–69.
- 7 Kayillo, S.; Gray, M. J.; Shalliker, R. A.; Dennis, G. R. *Journal of Chromatography A* 2005, 1073, 83–86.
- 8 Kim, Y.; Ahn, S.; Chang, T. *Analytical Chemistry* 2010, 82, 1509–1514.
- 9 Perny, S.; Allgaier, J.; Cho, D.; Lee, W.; Chang, T. *Macromolecules* 2001, 34, 5408–5415.
- 10 Boschmann, D.; Mänz, M.; Pöppler, A.-C.; Sörensen, N.; Vana, P. *Journal of Polymer Science: Part A: Polymer Chemistry* 2008, 46, 7280–7286.